NOTICE

AVIS

Canada

The author has granted an irrevocable non-exclusive licence allowing the National Library of Canada to reproduce, loan, distribute or sell copies of his/her thesis by any means and in any form or format, making this thesis available to interested persons.

The author retains ownership of the copyright in his/her thesis. Neither the thesis nor substantial extracts from it may be printed or otherwise reproduced without his/her permission.

L'auteur a accordé une licence irrévocable et non exclusive permettant à la Bibliothèque nationale du Canada de reproduire, prêter, distribuer ou vendre des copies de sa thèse de quelque manière et sous quelque forme que ce soit pour mettre des exemplaires de cette thèse à la disposition des personnes intéressées.

L'auteur conserve la propriété du droit d'auteur qui protège sa thèse. Ni la thèse ni des extraits substantiels de celle-ci ne doivent être imprimés ou autrement reproduits sans son autorisation.

Canada

THE UNIVERSITY OF ALBERTA

MINERALOGY OF THE LAKE ZONE DEPOSIT, THOR LAKE,
NORTHWEST TERRITORIES

BY

DANIEL ROBERT PINCKSTON

A THESIS

SUBMITTED TO THE FACULTY OF GRADUATE STUDIES AND RESEARCH

IN PARTIAL FULFILMENT OF THE REQUIREMENTS FOR THE DEGREE

OF MASTER OF SCIENCE

DEPARTMENT OF GEOLOGY

EDMONTON, ALBERTA

FALL, 1989

THE UNIVERSITY OF ALBERTA

RELEASE FORM

NAME OF AUTHOR: Daniel Robert Pinckston

TITLE OF THESIS: Mineralogy of the Lake Zone Deposit, Thor
Lake, Northwest Territories

DEGREE: Master of Science

YEAR THIS DEGREE GRANTED: Fall, 1989

Permission is hereby granted to THE UNIVERSITY OF
ALBERTA LIBRARY to reproduce single copies of this thesis
and to lend or sell such copies for private, scholarly or
scientific research purposes only.

The author reserves other publication rights, and
neither the thesis nor extensive extracts from it may be
printed or otherwise reproduced without the author's written
permission.

(SIGNED)...........................
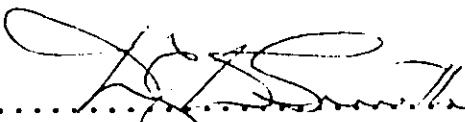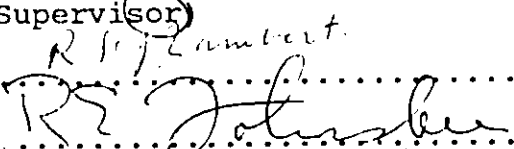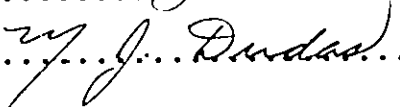
PERMANENT ADDRESS:

...14428-79th Ave...

...Edmonton Alberta...

...Canada...

Date: ...July 28, 1989.

THE UNIVERSITY OF ALBERTA

FACULTY OF GRADUATE STUDIES AND RESEARCH

The undersigned certify that they have read, and
recommend to the Faculty of Graduate Studies and Research
for acceptance, a thesis entitled MINERALOGY OF THE LAKE
ZONE DEPOSIT, THOR LAKE, NORTHWEST TERRITORIES submitted by
Daniel Robert Pinckston in partial fulfilment of the
requirements for the degree of Master of Science.

....
(Supervisor)

....

....

Date: ....

DEDICATION

To my parents

ABSTRACT

The Thor Lake rare-metal deposit is located 100 kilometres SE of Yellowknife along the north shore of Hearne Channel, Great Slave Lake, N.W.T. The deposits contain significant quantities of Be, Y, REEs, Zr, Nb, Ta, Li, Ga, U and Th situated within the peralkaline Thor Lake syenite of the Blachford Lake Intrusive Suite. Five mineralised zones have been identified, the largest of which, the Lake zone, contains Nb-, Zr-, Y- and REE-mineralisation associated with an altered, central region of the Thor Lake syenite. The ring-shaped appearance of the host Blachford Lake Intrusive Suite, plus the associated rock-types and styles of mineralisation draw parallels to the numerous anorogenic ring complexes of Nigeria.

In the Lake zone, Zr mineralisation is confined to zircon. Nb is found in a number of minerals including: aeschynite and pyrochlore group minerals, fergusonite-(Y), ferrocolumbite and samarskite-(Y)(?). Ferrocolumbite is the most common Nb-bearing mineral in the Lake zone. Because both Ta concentrations in the niobates and Hf values in zircons are minimal, rare-metal fractionation within the Lake zone, especially compared to rare-metal pegmatites, has been nonexistent. REE-bearing minerals include the bastnäsite group, monazite-(Ce) and allanite-(Ce). Fergusonite-(Y), zircon and infrequent xenotime-(Y) are the only Y-bearing minerals. All economically important minerals are found to have formed in two general stages; the

first features relatively well-formed grains and the second, more prevalent stage exhibits finer grained, poorly defined crystals.

Immediately underlying the Lake zone is a body of silica-undersaturated rocks believed to be, in part, responsible for rare-metal mineralisation in the Lake zone. Most of the rock is nepheline syenite although urtites, ijolites and sodalite syenite have been found. Rare-metal-bearing minerals such as zircon, cerianite-(Ce), britholite-(Ce), allanite-(Ce), thorite and other minerals, some of which appear to be new species, are found clustered into small clots scattered throughout. These pockets have formed at low temperatures in a highly oxidising environment and give evidence for late-stage metasomatism affecting both these silica-undersaturated rocks and the overlying Thor Lake syenite.

ACKNOWLEDGEMENTS

First of all I would like to thank my supervisor, Dr. Dorian G.W. Smith for instigating the project and being of helpful assistance throughout. Also, thanks go to my examining committee: Dr. R.St.J. Lambert, Dr. R.E. Folinsbee and Dr. M.J. Dudas. I would also like to acknowledge the generous help received from the numerous electron micropobe/SEM operators encountered over the past 2 years. Thanks go to Tina Barker, Maggie Piranian, Ed Zacharuk, Scott Ercit and most importantly, Dave Tomlinson.

Recognition must also go to Highwood Resources Ltd. for providing the financial and logistics support for such a project. A special thanks goes to Dave Trueman for being an unending source of information and encouragement.

I would also like to give my gratitude to family and friends who have provided me with unending support from beginning to end. Finally, many thanks to Beth Edmunds for being the light at the end of the tunnel.

TABLE OF CONTENTS

LIST OF TABLES

LIST OF FIGURES

LIST OF PLATES

LIST OF ABBREVIATIONS USED IN THE PLATES

aeschynite-(Nd) (AS)
aegirine (AE)
albite (AB)
allanite-(Ce) (A)
analcime (AN)
andradite (AD)
apatite (AP)
arfvedsonite (AF)
bastnäsite-(Ce) (B)
betafite (BE)
biotite (BT)
britholite-(Ce) (BR)
britholite-(La) (BR)
calcite (CC)
cerianite-(Ce) (CE)
chamosite (CH)
fayalite (FA)
fergusonite-(Y) (FG)
ferrocolumbite (FC)
fluorite (F)
galena (GA)
hedenbergite (HD)
hematite (HM)
ishikawaite (IS)
magnetite (MT)
microcline (M)
monazite-(Ce) (MZ)
nepheline (NE)
nioboaeschynite-(Nd) (NS)
'orange mineral' (OR)
pectolite (PC)
perthite (PR)
pyrochlore (PY)
quartz (Q)
samarskite-(Y) (SA)
sodalite (SD)
synchisite-(Ce) (S)
thorite (TH)
willemite (W)
wollastonite (WO)
xenotime-(Y) (X)
zircon (ZR)
plane polarised light   PPL
cross polarised light   XPL
not analysed   n.a.
not detected   n.d.

I INTRODUCTION

LOCATION AND ACCESS

An economically significant Be, Nb, Ta, REE, Y, Zr and Ga deposit known as the Thor Lake rare-metal deposit exists approximately 100 km southeast of Yellowknife, N.W.T. and 5 km north of the Hearne Channel, Great Slave Lake (fig. 1). The exact location in latitude and longitude is $62^{\circ}06'N$ and $112^{\circ}35'W$, respectively. Physiographically, the area exhibits minimal topographic relief and is covered by lakes, bogs and thickly wooded vegetation. Geologically, mineralisation is associated with the core of a Proterozoic (Aphebian) peralkaline granite-syenite system as five distinct zones: the R, S, T, Lake and Fluorite zones. Outcrop in this region is generally good although the zones of mineralisation are recessive and tend to be lake or bog-covered. Access to the property is obtained by airplane equipped with floats (summer) or skis (winter). In 1986, a road constructed from the shore of Great Slave Lake to the mine site has allowed year-round access via barge and truck or winter road.

EXPLORATION HISTORY

The rare-metal potential in the area has been known for almost 20 years, when, in 1970 the Odin 1-4 claims were staked and optioned to Giant Yellowknife Mines Ltd. At the time samples were assayed for REEs, Nb, Y, U and Th. Later in that year, the property was optioned to Bluemount
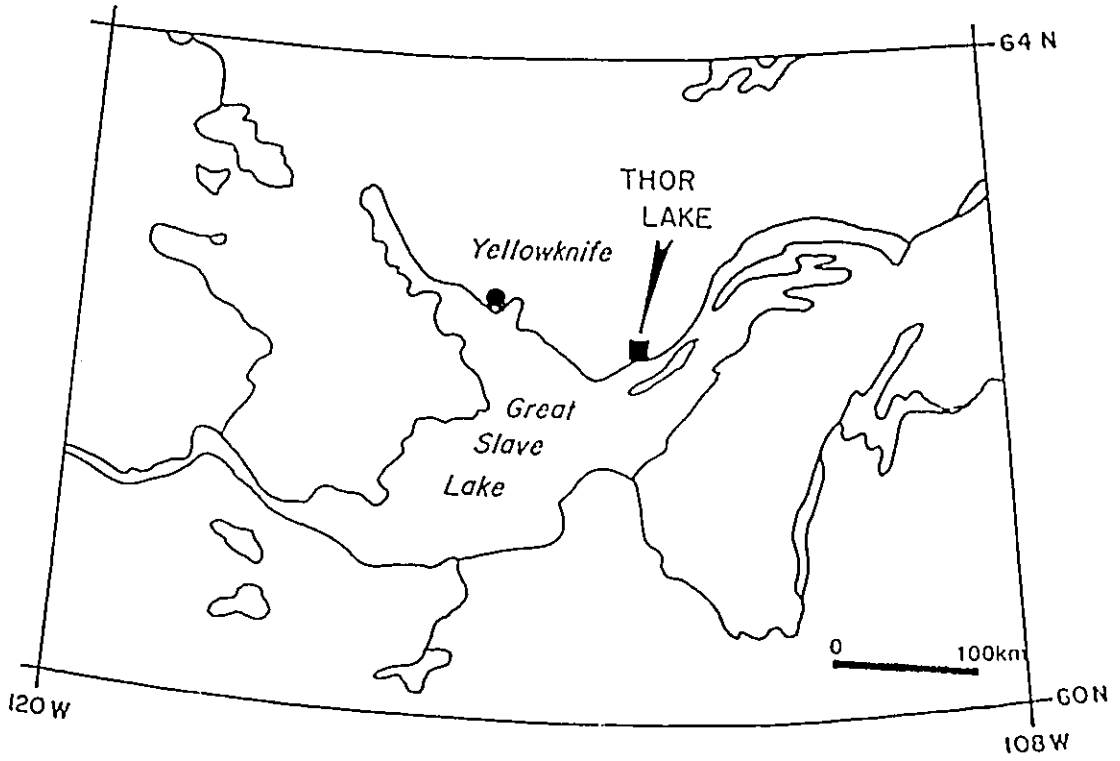
Figure 1   Location map for the Thor Lake rare-metal
deposits. After de St. Jorre (1986).

Minerals Ltd. but the option was subsequently allowed to lapse. Realising the area's potential, in 1977, Highwood Resources Ltd. restaked the area and within the next 2 years completed diamond drilling, prospecting, mapping and surveying. Magnetometer, airborne spectrometer and radon surveys were all performed within this period of time. By 1978, other companies became interested and one of them, Calabras Ltd. acquired a 30% interest in the property.

In 1979 the potential of the Lake zone was realised when test drilling was first begun. In March of 1980, Placer Development Ltd. optioned the property and, in the two years they carried that option, completed metallurgical studies and conducted a drilling program within the Lake zone. Drilling delineated 70 million tons combined Ta and Nb grading 0.06% Ta_2O_5 and 0.6% Nb_2O_5. In addition approximately 2.0% REE_2O_3 and 4.5% ZrO_2 had been found.

In 1983, a gravity survey over the Lake zone was completed. Also in that year resampling for Be in the R, S, and T zones began. A berylometer survey delineated significant Be enrichment in the T zone (461,000 tons grading 1% BeO in the north T zone and 1.31 million tons grading 0.66% BeO in the south T zone) thus instigating bulk sampling and metallurgical work in 1984/85. Hecla Mining Co. optioned the property in 1986 and have since engaged in a feasibility study to make a decision about Be production from the T zone. In addition, they have financed a Lake

zone drill program in early 1988 to help in outlining Y_2O_3 reserves.

PURPOSE OF STUDY

By 1986, both Highwood Resources Ltd. and Placer Development Ltd. had drilled 32 holes within the Lake zone for a combined total of almost 5000 m of core. At the time, it was realised that a detailed mineralogical study of this zone was needed. This thesis is therefore the study of all minerals which contain the elements of economic interest (REEs, Zr, Nb, Ta and Y) within the Lake zone. Also included is a glimpse of the rock-forming and accessory minerals found within the mineralised zone.

The following will be investigated: the identification of all minerals including the numerous minor or accessory phases; observations of textures including grain sizes, replacement features, intergrowths and paragenetic relationships and finally determination of the distribution of rare-metal-bearing minerals with particular emphasis on REE, Y and Nb-bearing phases. To carry out the research, a number of analytical and observational techniques were employed. This includes optical petrography, cathodoluminescence microscopy and a heavy reliance on electron microprobe analysis, both semi-quantitative (EDA) and quantitative (WDA).

With the subsequent discovery of silica-undersaturated rocks closely associated with the Lake zone, a thorough

discussion of these rocks was also undertaken. It is hoped that this information will assist in determining whether these underlying rocks are economically viable and/or responsible for Lake zone mineralisation. This study will also assist in determining whether beneficiation and economic exploitation of REEs, Nb and Y-bearing minerals is viable within the Lake zone.

II REGIONAL GEOLOGY

SETTING

The Blachford Lake Intrusive Suite is located at the southern margin of the 3.2 Ga Slave Province of the Canadian Shield. In general terms, the province consists of granitic intrusions and batholiths within large-scale metasedimentary sequences (fig. 2). The metasediments, called the Yellowknife Supergroup, are for the most part turbiditic rocks that accumulated in an ancient marine basin approximately 2.5-3.0 Ga (Henderson, 1985). Obscuring many original depositional features is large-scale folding, faulting and a regional metamorphic event. Numerous Archean batholiths both post and predate these metasedimentary rocks.

At 2.1 Ga, the Blachford Lake complex intruded Yellowknife Supergroup sediments and older Archean granites. One of these granites, to the west, is a two mica granite known as the Morose Granite while to the northeast are two smaller plugs of granodioritic rock identified as the Defeat Plutonic Suite. Another sequence of plutonic rocks known as the Compton Intrusive Suite has also been recognized within the Blachford Lake complex. These dioritic to quartz monzonitic rocks have been found as small plugs within the alkaline sequence and according to Henderson (1985), are believed to be laccoliths intruded into nearby limestones and mudstones of the early Proterozoic Pethei Group (Great Slave Supergroup) to the south (fig. 2).

6
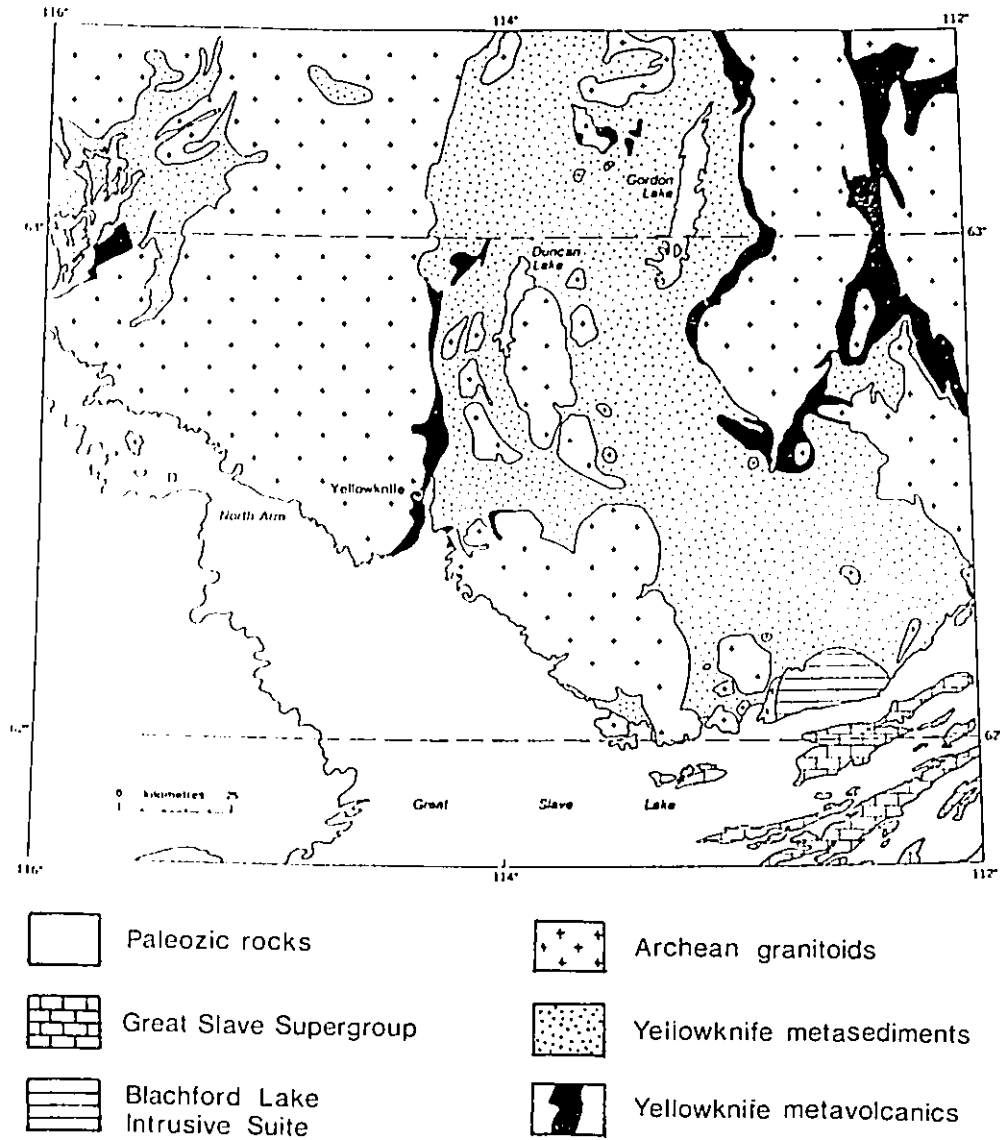
Figure 2   Generalised geological map of the southern Slave Province.
Modified after Henderson (1985).

To the northeast and, in places, within the Blachford
Lake Complex lie metasediments of the Burwash Formation.
These rocks, as part of the Yellowknife Supergroup, consist
of pelites, graphitic shales and quartzites which have
experienced lower greenschist to upper amphibolite grade
metamorphism. Adjacent to the Blachford Lake Suite all such
sedimentary rocks experienced amphibolite grade metamorphism
and as a result lie above the regionally common cordierite
isograd. Henderson (1985) has suggested that the
metamorphic affects are not due to the numerous intrusions
found in the area but to increased levels of heat flow in
the Yellowknife basin just prior to Archean magma
emplacement.

The Blachford Complex is one of the youngest igneous
complexes in the area and although a number of theories as
to the origin of its emplacement have been proposed, its
history is still unclear. Badham (1978) suggested that
compression between the Slave and Superior Cratons between
2.5 and 1.8 Ga resulted in deflection of sediments along the
rigid Slave craton. Deflection in these rocks, which is
part of the Taltson Block (Superior Province), caused
strike-slip faulting and graben formation resulting in the
present day East Arm of Great Slave Lake. Contemporaneous
with this was the intrusion of the Blachford Lake Complex.
Hoffman (1980) proposed the presence of two hot spots at 2.1
Ga under thick continental crust with subsequent rifting and
the intrusion of three alkaline-peralkaline magmatic bodies:

Bigspruce Lake, Blachford Lake and the Hearne Dykes. One arm of the Great Slave hot spot coalesced with an arm of the Coronation hot spot resulting in the Wopmay rift while a second arm failed thus creating the Athapuscow Aulacogen, seen today as the East Arm of Great Slave Lake. Hoffman (1981) refined the aulacogen theory and proposed a six stage model for its formation.

Bowring et al. (1984) also expound upon the aulacogen theory but they have suggested that the timing between alkaline-peralkaline magmatism and rifting does not correspond, and have therefore proposed anorogenic processes. Recently, Hoffman (1987) has modified his aulacogen theory to include large scale transform faulting, similar to those of Badham's model. Such large scale shearing did not begin before 2.0 Ga therefore implying anorogenic origins for the Blachford Lake Complex.

INTRUSIVE SUITE GEOLOGY

The Blachford Lake Intrusive Suite is a subalkaline to peralkaline body of rocks, circular in shape, with an areal extent of approximately 220 square kilometres. The complex can be divided into two portions, a western, less alkaline series of gabbros, anorthosites, granites and syenites and an eastern peralkaline granite-syenite system (fig. 3). The western rocks have been subdivided into the following: the Hearne Channel and Mad Lake granites, the Whiteman Lake quartz syenite and the Caribou Lake gabbro-diorite.
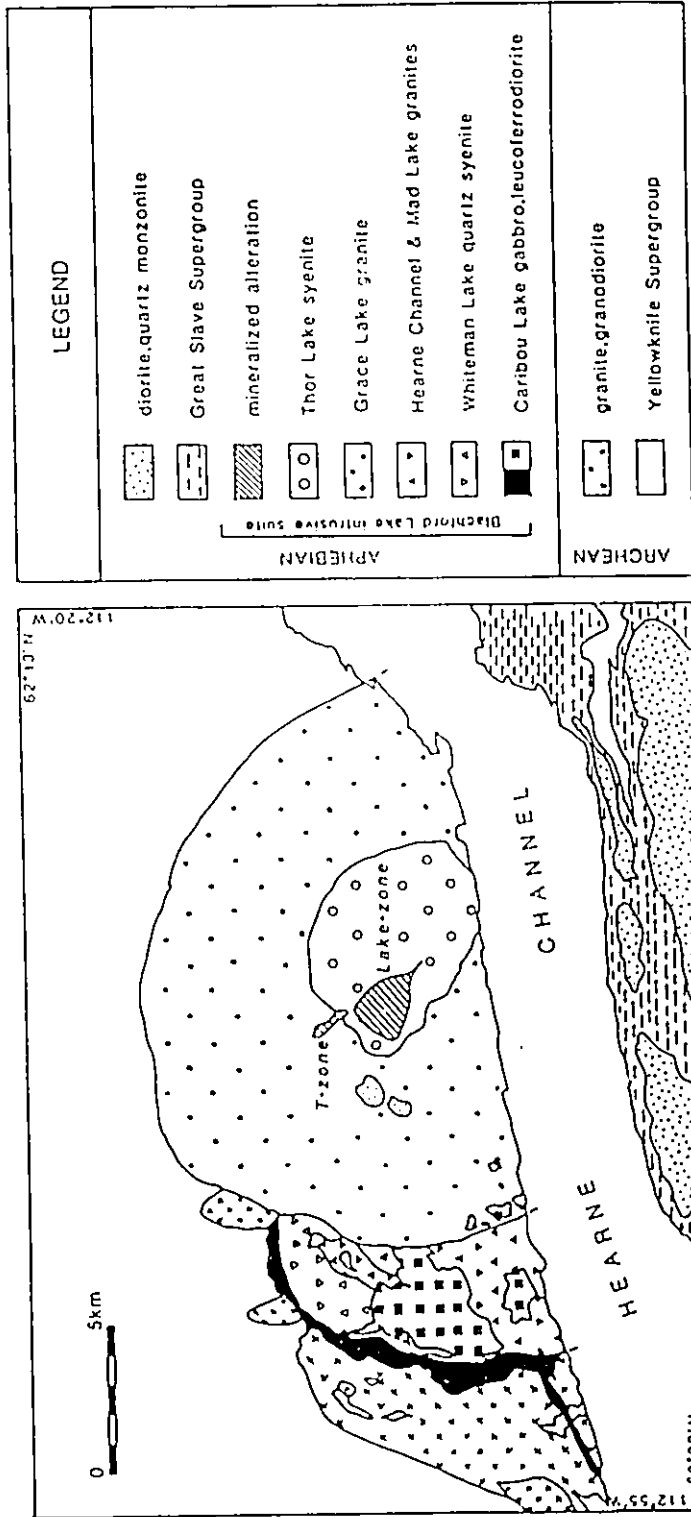
Figure 3   Generalised geological map of the Blachford Lake Complex.   After
          Davidson (1982).

Rimming the western edge of the complex at less than one kilometre in apparent thickness is the Caribou Lake gabbro which grades inward into diorite and leucodiorite. In the field, the rocks are very recessive and of variable compositions. Typically they are composed of olivine (olivine gabbro), pyroxenes (norites and pyroxenites) and lesser amounts of plagioclase, amphibole and sulphides. Some poorly defined plagioclase and pyroxene layering was also noted. Associated with the gabbro are large blocks of anorthosite, especially prevalent at the southeastern extremity of the gabbro-diorite system.

In the western subdivision Davidson (1978) identified two separate granite phases: the Mad Lake and Hearne Channel Granites. Both are very similar in texture and composition, the main difference being the presence of plagioclase xenocrysts and the intergrowth of quartz and feldspar in the matrix of the Hearne Channel Granite. Both granites contain feldspar with antiperthite cores and perthite rims and have identical mafic mineralogy.

The Whiteman Lake quartz syenite intrudes the Caribou Lake gabbro-anorthosite system and contains a number of gabbro and metasedimentary xenoliths. The rock is somewhat variable in appearance, changing from a brownish, rubbly perthite-rich syenite to a quartz-rich variety, rich enough to be a granite. The mafic mineralogy is variable with biotite, chlorite and hornblende noted along with minor olivine. Accessory minerals include hematite, carbonate,

zircon and minor apatite. Hudson (1987) has suggested a genetic link between this syenite and the Thor Lake syenite 8 km to the east. This does not appear to be possible as the Whiteman Lake quartz syenite contains no sodic minerals such as albite or arfvedsonite and hence cannot, unlike the Thor Lake syenite, be peralkaline. In addition, the overall textural and geochemical differences between these rocks, as noted by Davidson (1981, 1982), also suggest that the Thor Lake syenite and its associated mineralised sequences are unrelated.

All rocks in the western portion of the Complex show alkaline to subalkaline characteristics in contrast to the eastern lying Grace Lake granite and Thor Lake syenite which have peralkaline affinities (molecular $(Na_2O + K_2O) > Al_2O_3$). These last two rock bodies are richer in sodium-bearing minerals such as arfvedsonite, albite and aenigmatite and contain greater concentrations of accessory minerals such as zircon, monazite and apatite.

Dominating the Blachford Lake suite is the Grace Lake granite (fig. 3), a pink weathered rock of variable textures and striking appearance. Typically it is a coarse-grained granite abundant in pink perthite, quartz and riebeckite with accessory fluorite, zircon, apatite and monazite. Moving toward the centre of the granite body, the rock changes quite noticeably into the feldspar-rich Thor Lake syenite. One can detect a gradual change in the weathering characteristics of the rock; the quartz content decreases

and there is a concomitant change of the feldspar's
weathered surface colouration from pink to tan-brown. The
Thor Lake syenite is therefore, in general, browner in
colour and more rubbly than the Grace Lake granite.

The contact relationship between granite and syenite is
fairly clear. Most of the contact (north and east) is
demarcated by an abrupt change in lithology, although along
some portions of the western margin the contact becomes
gradational. This sharp distinction is denoted by a rim
shaped topographic high arcing around the Thor Lake syenite
for a distance of about 8 kilometres. This resistant rock
is called the Rim syenite and it is a fayalite-bearing
syenite devoid of quartz but with moderate amounts of
hedenbergite plus minor biotite and amphibole (plate 1). In
the field, the rock forms a rather prominent ridge with a
sharp, steeply dipping outer contact and a gradational inner
contact with the Thor Lake syenite. Weak lineation of the
feldspars (microcline) plus its sharp, circular orientation
suggests this to be a ring dyke emplaced into the
surrounding Grace Lake granite. Air photo interpretations
have shown that many circular ring-shaped fractures pervade
the complex, providing evidence for the emplacement of a
magma body characteristic of a geometrically simple
anorogenic ring complex.

To the west the ring dyke is not exposed, instead, the
contact between syenite and granite is gradational. In this
area the syenite has become porphyritic with phenocrysts,
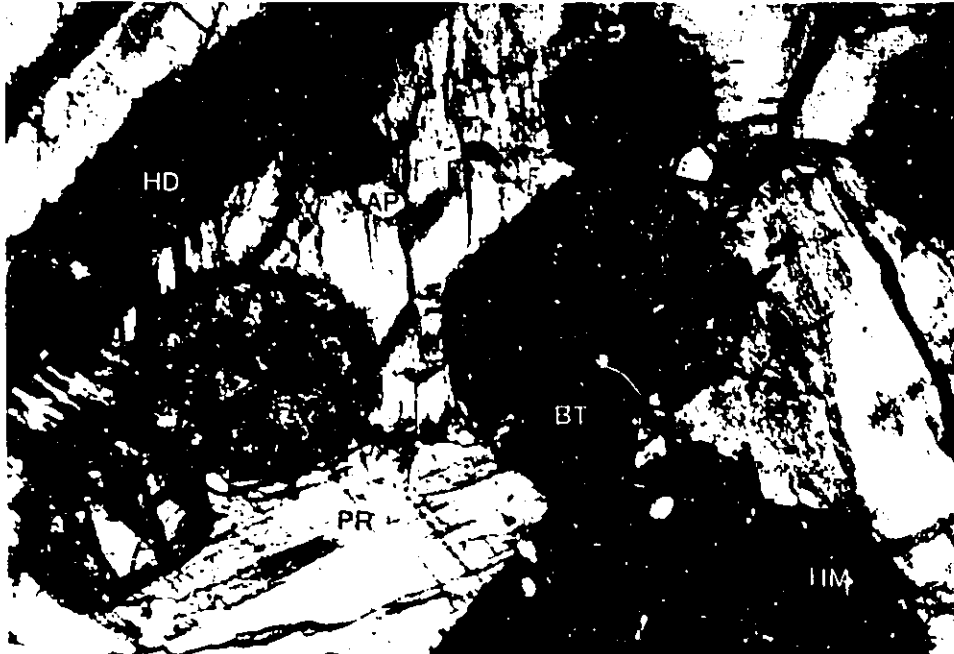
Plate 1. Photograph of the fayalite-bearing 'Rim' syenite. Magnification X50, PPL

Plate 2. Typical arfvedsonite-bearing Thor Lake syenite. Magnification X50, PPL

commonly of K-feldspar, up to one centimetre in length. Dykes of this porhyritic syenite were noted to intrude the granite proving without a doubt a younger age for the Thor Lake syenite.

The syenite is not as homogeneous as the Grace Lake granite and as such a number of varieties have been described. The first, as mentioned previously, is the rim syenite; the second is a porphyritic syenite prominent along the western margin; the third is an arfvedsonite syenite which contains well-aligned mafic minerals, while the fourth variety is also an arfvedsonite syenite but without the amphibole crystal alignment (plate 2). Davidson (1978) subdivided this final rock unit into a coarse grained variety and a poikilitic variety. Another type is an aegirine syenite found locally adjacent to the Lake zone. This rock contains abundant perthite and plagioclase with xenomorphic aegirine and biotite.

It should be noted that the primary mafic mineralogy within the Thor Lake syenite changes substantially. In the rim syenite the dominant mafic minerals are olivine and hedenbergite whilst surrounding the Lake zone aegirine dominates. Farther away from the zones of mineralisation arfvedsonite prevails. Biotite and chlorite are also very common but neither are believed to be primary.

THOR LAKE DEPOSIT

Situated almost entirely within the Thor Lake syenite
are five zones of mineralisation (fig. 4). These areas are
labelled as the R, S, T, Fluorite and Lake zones and are
host to the extensive rare-metal deposits. At present, this
deposit is known to contain approximately 85-90 recognised
mineral species (table 1). With time more may be identified
thus making it comparable to some of the more prolific
mineral localities of the world (i.e., Mount St. Hilare,
Quebec; Lovozero massif, USSR). Trueman et al. (1988) have
summarised the geology of the Thor Lake rare-metal deposits.

Of the five zones, the most studied and probably best
understood is the T zone. de St. Jorre (1986) recently
completed a mineralogical study of the T zone and found or
confirmed the existence of a number of unusual rare-metal-
bearing minerals. Be minerals include phenacite,
bertrandite, the gadolinite group and helvite group. Other
minerals of significance include the bastnäsite group,
thorite, ferrocolumbite and zircon. de St. Jorre (1986)
carried out work on the four known zones of alteration
within the T zone, (Wall, Lower Intermediate, Upper
Intermediate and Quartz zones) including an investigation of
mineralogical and textural relationships. It was found that
Be mineralisation is concentrated within the Upper and Lower
Intermediate zones, Y and REEs seem to pervade throughout
whilst Nb is concentrated in the Lower Intermediate and Wall
zones.
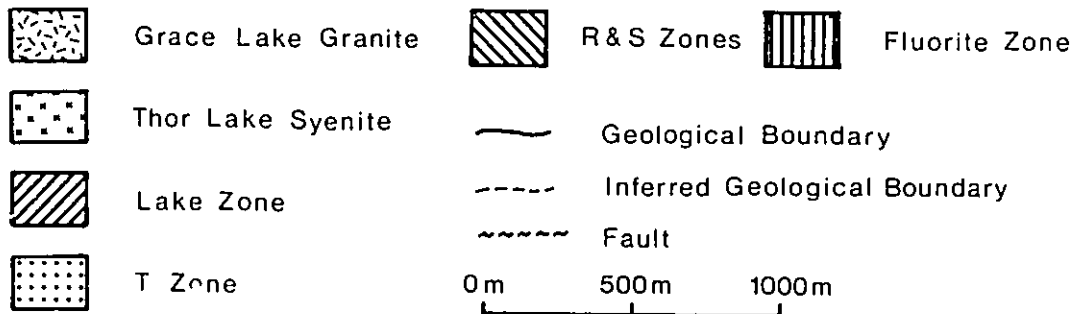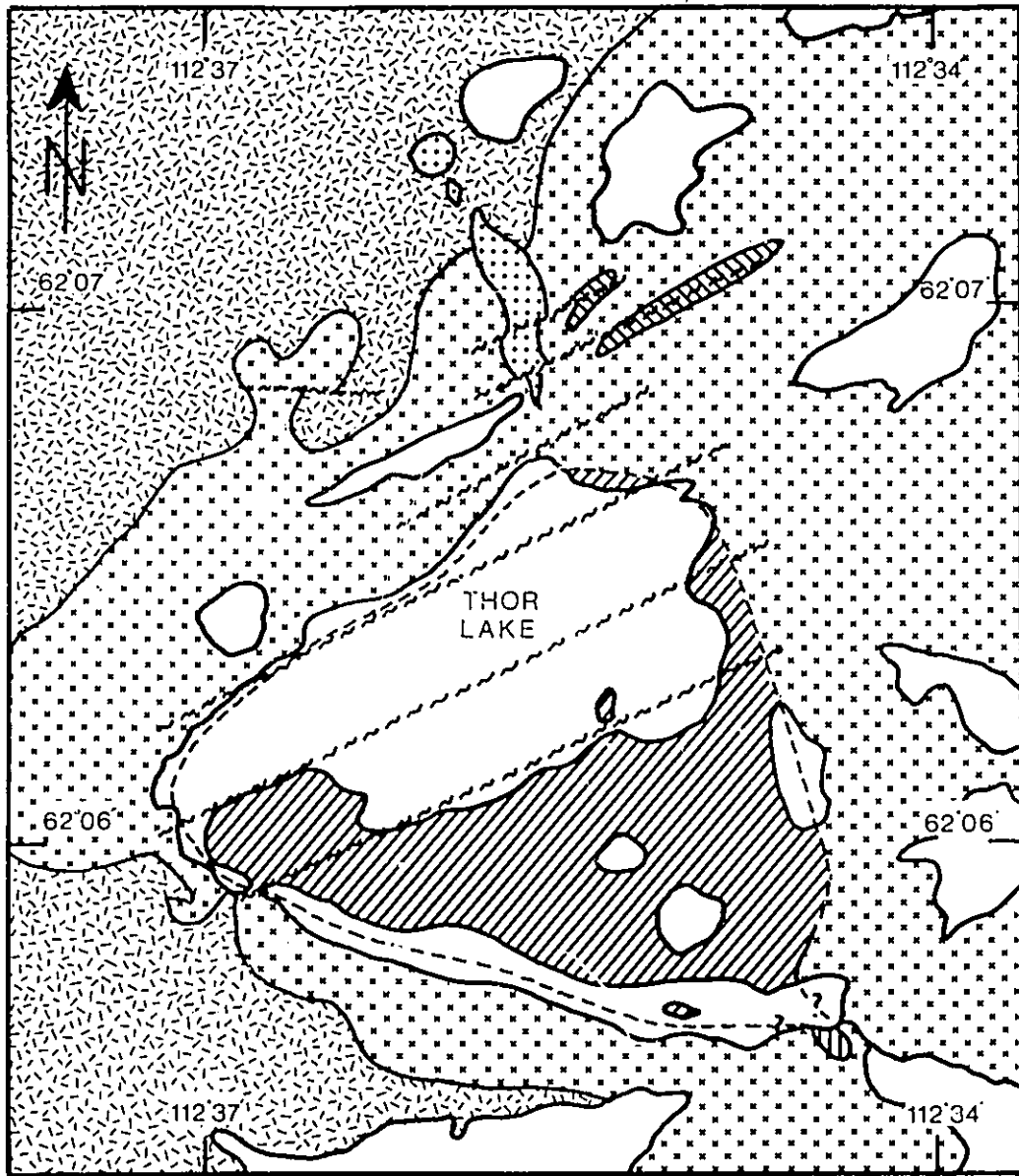
Figure 4   Geological map of the Thor Lake area. After Černý and Trueman(1985)
and Johnson(1977).

TABLE 1

LIST OF ALL KNOWN MINERAL SPECIES IN THE THOR LAKE
RARE-METAL DEPOSITS AND HOST PERALKALINE GRANITE-SYENITE

SILICATES

NAME	FORMULA[*]
aegirine	$NaFe^{3+}Si_2O_6$
aenigmatite	$Na_2Fe_5^{2+}TiSi_6O_{20}$
albite	$NaAlSi_3O_8$
allanite-(Ce)	$(Ce,Ca)_2(Al,Fe^{3+})_3(SiO_4)_3(OH)$
analcime	$NaAlSi_2O_6:H_2O$
andradite	$Ca_3Fe_2^{3+}(SiO_4)_3$
annite	$KFe_3^{2+}AlSi_3O_{10}(OH,F)_2$
arfvedsonite	$Na_3(Fe^{2+},Mg)_4Fe^{3+}Si_8O_{22}(OH)_2$
astrophyllite	$(K,Na)_3(Fe^{2+},Mn)_7Ti_2Si_8O_{24}(O,OH)_7$
bertrandite	$Be_4Si_2O_7(OH)_2$
biotite	$K(Mg,Fe^{2+})_3(Al,Fe^{3+})Si_3O_{10}(OH,F)_2$
britholite-(Ce)	$(Ce,Ca)_5(SiO_4,PO_4)_3(OH,F)$
britholite-(La)	$(La,Ca)_5(SiO_4,PO_4)_3(OH,F)$
chamosite	$(Fe^{2+},Mg,Fe^{3+})_5Al(Si_3Al)O_{10}(OH,O)_8$
clinochlore	$(Mg,Fe^{2+})_5Al(Si_3Al)O_{10}(OH)_8$
danalite	$Fe_4^{2+}Be_3(SiO_4)_3S$
fayalite	$Fe_2^{2+}SiO_4$
ferrobustamite	$Ca(Fe^{2+},Ca,Mn)Si_2O_6$
ferrorichterite	$Na_2Ca(Fe^{2+},Mg)_5Si_8O_{22}(OH)_2$
gadolinite-(Y)	$Y_2Fe^{2+}Be_2Si_2O_{10}$
helvite	$Mn_4Be_3(SiO_4)_3S$
lepidolite	$K(Li,Al)_3(Si,Al)_4O_{10}(F,OH)_2$
mesolite(?)	$Na_2Ca_2Al_6Si_9O_{30}:8H_2O$
microcline	$KAlSi_3O_8$
muscovite	$KAl_2(Si_3Al)O_{10}(OH,F)_2$
natrolite	$Na_2Al_2Si_3O_{10}:2H_2O$
nepheline	$NaAlSiO_4$
orthoclase	$KAlSi_3O_8$
pectolite	$NaCa_2Si_3O_8(OH)$
phenakite	Be_2SiO_4
polylithionite	$KLi_2AlSi_4O_{10}(F,OH)_2$
quartz	SiO_2
riebeckite	$Na_2(Fe^{2+},Mg)_3Fe_2^{3+}Si_8O_{22}(OH)_2$
sodalite	$Na_8Al_6Si_6O_{24}Cl_2$
thorite	$ThSiO_4$
topaz	$Al_2SiO_4(F,OH)_2$
willemite	Zn_2SiO_4
wollastonite	$CaSiO_3$
zinnwaldite	$KLiFe^{2+}Al(AlSi_3)O_{10}(F,OH)_2$
zircon	$ZrSiO_4$
Ca,Zr silicate	
hydrated Fe silicate	
Ca,Nb,Ti silicate	
Ca,Nb silicate	

TABLE 1 CONT.

SILICATES (CONT.)

NAME	FORMULA
Th,Fe silicate	
Nb,U,Ti silicate	

OXIDES

NAME	FORMULA
aeschynite-(Nd)	$(Nd,Ce,Ca)(Ti,Nb)_2(O,OH)_6$
anatase	TiO_2
ashanite(?)	$(Nb,Ta,U,Fe,Mn)_4O_8$
betafite	$(Ca,Na,U)_2(Ti,Nb)_2O_6(OH)$
cassiterite	SnO_2
cerianite-(Ce)	$(Ce^{4+},Th)O_2$
ceriopyrochlore-(Ce)	$(Ce,Ca,Y)_2(Nb,Ta)_2O_6(OH,F)$
fergusonite-(Y)	$YNbO_4$
ferrocolumbite	$Fe^{2+}Nb_2O_6$
fersmite(?)	$(Ca,Ce)(Nb,Ta,Ti)_2(O,OH,F)_6$
goethite	$Fe^{3+}O(OH)$
hematite	Fe_2O_3
hydrohetaerolite	$Zn_2Mn_4^{3+}O_8:H_2O$
ilmenite	$Fe^{2+}TiO_3$
ixiolite	$(Ta,Nb,Sn,Fe,Mn)_4O_8$
magnetite	$Fe^{2+}Fe_2^{3+}O_4$
nioboaeschynite-(Ce)	$(Ce,Nd)(Nb,Ti)_2(O,OH)_6$
nioboaeschynite-(Nd)	$(Nd,Ce)(Nb,Ti)_2(O,OH)_6$
pyrochlore	$(Ca,Na)_2Nb_2O_6(OH,F)$
rutile	TiO_2
samarskite-(Y)(?)	$(Y,Fe,U,Ce)(Nb,Ta,Ti)O_4$
uraninite(?)	UO_2
uranpyrochlore	$(U,Ca,Ce)_2(Nb,Ta)_2O_6(OH,F)$

SULPHIDES

NAME	FORMULA
arsenopyrite	$FeAsS$
chalcopyrite	$CuFeS_2$
galena	PbS
gersdorffite(?)	$NiAsS$
marcasite	FeS_2
molybdenite	MoS_2
pyrite	FeS_2
pyrrhotite	$Fe_{1-x}S$, $x=0-0.17$
sphalerite	$(Zn,Fe)S$

FLUORIDES

NAME	FORMULA
fluorite	CaF_2

TABLE 1 CONT.

CARBONATES

NAME	FORMULA
ankerite	$Ca(Fe^{2+},Mn)(CO_3)_2$
bastnäsite-(Ce)	$(Ce,La)(CO_3)F$
calcite	$CaCO_3$
dolomite	$CaMg(CO_3)_2$
malachite(?)	$Cu_2(CO_3)(OH)_2$
parisite-(Ce)	$Ca(Ce,La)_2(CO_3)_3F_2$
rhodocrosite	$MnCO_3$
röntgenite-(Ce)	$Ca_2(Ce,La)_3(CO_3)_5F_3$
siderite	$Fe^{2+}CO_3$
synchysite-(Ce)	$Ca(Ce,La)(CO_3)_2F$

PHOSPHATES

NAME	FORMULA
fluorapatite	$Ca_5(PO_4)_3F$
monazite-(Ce)	$(Ce,La,Nd,Th)PO_4$
xenotime-(Y)	YPO_4

*All chemical formulae both here and in the text are based on those given by Fleischer (1987).

The T zone is somewhat different from the other zones in that superimposed on earlier episodes of K and Na metasomatism is late-stage greisenisation and silicification (Quartz and Upper Intermediate zones). Greisenisation is the hydrothermal alteration of granitoids resulting in a rock rich in quartz and micas plus variable amounts of, among others, B-, F- and Be-bearing minerals. In the T zone, the occurrence of minor topaz, extensive polylithionite, late-stage Be mineralisation and numerous fluid inclusions abundant in complex daughter salts, (R.D. Morton, pers. comm.) all seem to indicate high degrees of acidity (μ_{HF}) and salinity (μ_{KF}) necessary for greisen formation. Burt (1981) found that when both μ_{HF} and μ_{KF} are high, beryl, normally stable over a wide range of P-T conditions, breaks down to phenakite plus quartz and K-feldspar or topaz. Other Al-free Be minerals such as bertrandite and the helvite group are also stable under such conditions thereby providing good indicators of high μ_{HF} and μ_{KF} (greisenisation).

As shown by figure 4, offsetting the southern terminus of the south T zone are two ENE trending faults. The northern most fault offsets the next zone of mineralisation to be discussed, the S zone. The S zone is a roughly elliptical-shaped area of intense alteration measuring approximately 300 m in length by 10 m in width. Alteration sequences are crudely zoned and include albite-polylithionite and albite assemblages. Important elements

include Be, Y, REEs (bastnäsite group), Nb (ferro-columbite), Th and U therefore in order to define this zone better, extensive trenching has been completed. In general though, little is known about this zone. Subparallel to the S zone and to the south some 200 m is the R zone. Even less is known about this zone except that it closely parallels the second ENE trending fault mentioned above and measures about 1 km in length by 10 m in width. The zone is not readily apparent in the field but contains patches of albitisation in foliated and, in part, pegmatitic syenite. This zone is enriched in Th, REEs, Be, Nb and Y but not to the extent of the S zone.

Moving southward again, one arrives at the next zone of alteration, the Lake zone. It is by far the largest zone with the greatest potential for Nb, Zr, Y and REEs. Mineralogically, it is not as complex as the T zone yet an added complication was the recent discovery of an underlying body of silica-undersaturated rocks which may bear some significance with respect to the mineralisation. The Lake zone will be discussed further in the following chapter.

The final zone is the Fluorite zone. It is located at the southern tip of the Lake zone possibly as a small-scale appendage (fig. 4). It sits entirely within the well aligned arfvedsonite syenite described earlier and is obviously an altered region of that rock. In hand specimen it is dense (enriched in Zr, U, Th and REEs) with 30-40 modal % dark purple fluorite in a tan-brown matrix. The

fluorite is generally late-stage and commonly displays zoning from colourless cores to dark purple rims. Minor sulphides such as pyrite and chalcopyrite are also present. The tan-brown regions are a combination of quartz, biotite, carbonate, zircon and bastnäsite. The most common of these minerals, zircon, occurs as small, zoned bipyramids enriched in Y, U and Th, and found not infrequently overgrowing small hematite grains. The rock is very similar to those seen in the southern regions of the Lake zone and although drilling found no subsurface connection between the two, the Fluorite zone is thought to be a F-rich appendage to the Lake zone. This seems likely as similar massive, fluorite-rich appendages are found in mineralised granites of the Arabian Shield (Jackson, 1986). The Fluorite zone is mildly radioactive due, in part, to moderate concentrations of U and Th in the zircons.

III GEOLOGY OF THE LAKE ZONE

GENERAL FEATURES

Of the five zones of mineralisation, the Lake zone is by far the largest in areal extent. It is approximately triangular in shape and covers about 1.8 square km in area. Figure 5 shows, in addition to drill hole locations, the general shape of the Lake zone. Topographically, it is, because of its altered nature, recessive and flat lying with half of the zone submerged under Thor Lake and the other half as swamp and bog-covered ground (< 5% outcrop).

In general, the Lake zone contains altered and brecciated syenite which has been affected by late-stage magmatic to post-magmatic (subsolidus) alteration. The surrounding peralkaline syenite contains, as mentioned earlier, one feldspar (perthite) and thus represents a hypersolvus (dry magma) system. The Lake zone and the underlying nepheline syenite both contain two feldspars (albite and microcline) and therefore represent a subsolvus (wet magma) system. It is likely that some degree of late-stage retrograde boiling of the more fluid-rich (H_2O, CO_2, P, F, Cl) magma may have concentrated dissolved Na, K, Zr, REEs, Nb, Y and other incompatible elements. Best (1982) notes that with retrograde boiling mineralogical changes such as microclinisation and albitisation are actively promoted. In essence, then, the Lake zone may be the result of late-stage to post-magmatic alteration as witnessed by albitisation, microclinisation and associated rare-metal

24

Figure 5   Drill hole locations within the Lake Zone

enrichment (implications for the nepheline syenite will be discussed later). This type of alteration is common with late-stage plutons of highly fractionated granitoid suites (Pollard, 1986). Commonly, zonation in this type of alteration can be delineated, such that early K and Na metasomatism may be followed by later Fe metasomatism, greisenisation and silicification (T zone). In the Lake zone, alteration sequences did not progress as far as those in the T zone, although rare-metal mineralisation was very extensive.

Due to the lack of outcrop and the large spacing between holes, only two broad subdivisions can presently be made. First, there is an outer Wall zone composed essentially of quartz, albite and microcline and second an inner Core zone rich in biotite and host to most of the mineralisation. Plates 3 and 4 display typical Wall and Core zone rocks, respectively.

In general, the Wall zone contains abundant K-feldspar, albite and quartz along with minor biotite, magnetite, hematite, calcite, fluorite, sulphides, monazite-(Ce) and ferrocolumbite. Early phases of K and then Na metasomatism resulted in a very felsic rock which is, in many places, mono- or dimineralic. Magnetite and hematite, either in the form of large, independent grains or as fine-grained crystals dusting feldspar, are the dominant oxide minerals. Late-stage biotite, calcite, fluorite and minor monazite-(Ce) and ferrocolumbite are present although uncommon.
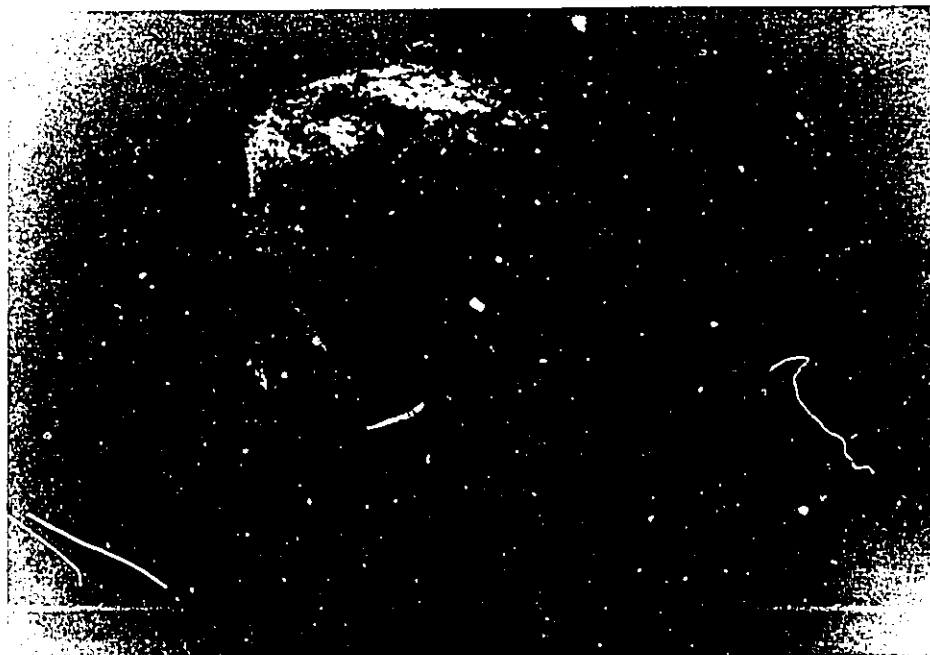
Plate 3. Typical Wall zone rock composed of albite, microcline and minor biotite.

Plate 4. Typical Core zone rock composed of biotite, feldspars, quartz and minor carbonate, zircon and allanite-(Ce).

Table 2 displays a paragenetic scheme for all minerals in the Wall zone.

The Core zone shows the same types of alteration sequences but, in addition, continued post-magmatic alteration in the form of extensive biotite flooding and significantly greater quantities of rare metal-bearing minerals such as zircon, monazite-(Ce), fergusonite-(Y) and allanite-(Ce). Table 2 also gives a generalised paragenetic sequence for the Core zone.

It should be noted that from this point onward, all rare-earth-bearing mineral species will have element suffixes as suggested by the IMA Commission on New Minerals and Mineral Names (Nickel and Mandarino, 1987; Bayliss and Levinson, 1988). The suffix is applied to denote the dominant REE in a mineral species and is used only if chemical information about the mineral is known.

ROCK-FORMING MINERALS

In essence, only four rock-forming minerals have been observed: microcline, albite, quartz and biotite. The following section describes each of these and includes discussions of their chemistry, textures and paragenetic relationships. Before discussing them, one other common mineral of note, arfvedsonite, should be mentioned. It probably existed at some point but has since experienced complete replacement to siderite, quartz and hematite. With

TABLE 2

PARAGENESIS OF THE ROCK-FORMING AND
ACCESSORY MINERALS IN THE WALL AND CORE ZONES

WALL ZONE

```
quartz                                  ---
microcline        ----
albite              -----
green biotite                             ---
magnetite              ---
hematite                  ---------
sulphides                          ---
calcite                               ---
fluorite                              ---
monazite-(Ce)         --
ferrocolumbite        --
```

CORE ZONE

```
quartz                            ---------------           --
microcline        ----
albite              -----
brown biotite                          -----
green biotite                               ----------
chamosite                                             ---
muscovite                                           ---
magnetite              ---
hematite                  -------------------
ilmenite              ?--?
cassiterite           ?-?
sulphides                                    ?--?
calcite                                          -----
siderite                        --              --
ankerite                                      ----
fluorite                                           -----
apatite               --
rare-metal
 minerals*            ------------------

             TIME    --------->
```
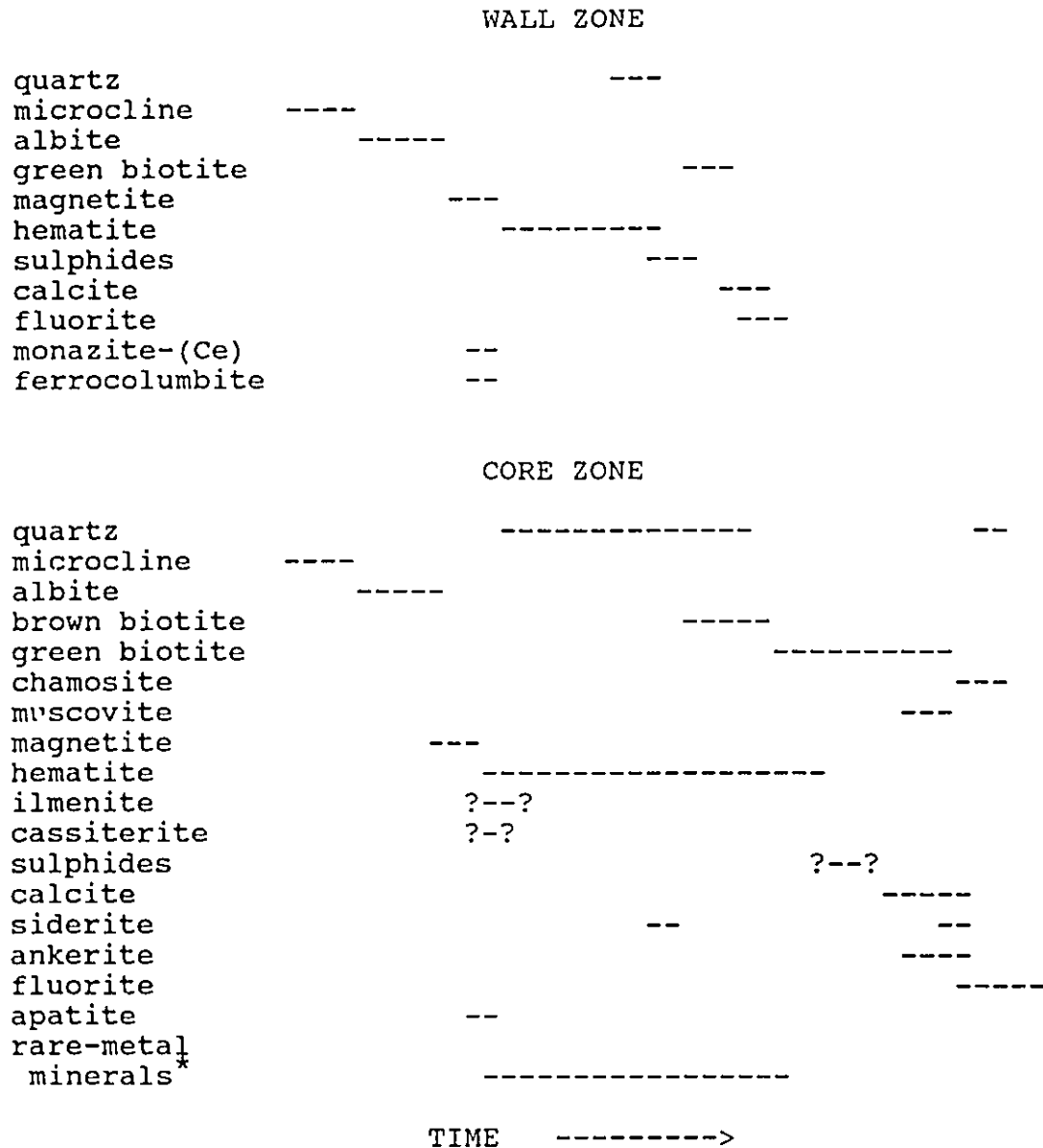
*see table 3

an influx of carbonate ions, the following reaction may result:

$$CO_3{}^{2-} + Na_3Fe^{2+}{}_4Fe^{3+}Si_8O_{22}(OH)_2 \rightarrow 2Fe_2O_3 + FeCO_3 + 8SiO_2 + H_2O + 3Na^{+2}$$
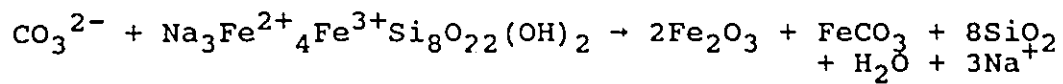
Such a mineralogical change is also noted in the aegirine crystals of the nepheline syenite.

All the feldspars formed as a result of pervasive microclinisation (K metasomatism) and albitisation (Na metasomatism). As an example, consider the very felsic Wall zone rocks typified by large (>1 cm) phenocrysts of microcline in a matrix of finer grained (100-200 μm) albite laths. According to Hudson (pers. comm.), all alkali feldspars are microcline as determined by X-ray work. This agrees with optical observations as all grains are found to have 2V(gamma)>90° (microcline only) even though characteristic 'tartan' twinning is absent. The familiar cross-hatched twinning results from the inversion of disordered monoclinic precursors to the more ordered lower temperature triclinic forms. In this situation, the ordering of Al and Si into the various nonequivalent sites within the feldspar must then be due to either one of two processes: ion-exchange of feldspar precusors (metasomatic replacement) or a primary growth feature (Smith, 1974). Ribbe (1983) has suggested that the lack of twinning must be a result of low temperature (<450°C) crystallisation (primary growth).

Untwinned microcline is not the only highly ordered feldspar in the Lake zone; the other is low albite (var.

cleavelandite). At least two generations of albite have been noted, the first is a coarser grained variety (0.5-2 mm) followed by a fine grained, subhedral type (75-200 μm) typically found embaying or intruding the earlier formed crystals. Plate 5 is a fine example of both generations of albite. Note in plate 5 the yellow colour of albite. The higher interference colours are due to the thicker and hence greater retarding effect of polished slides versus the standard thickness (30 μm) of thin sections. Commonly, the albite displays crystal distortion and milling due to subsequent fluid movement and later crystal development.

Appendix 1 is a summary of typical analyses performed on both common and accessory minerals. Only the better analyses of each mineral were included and they are meant to show some of the more subtle and salient features in each mineral. For albite, analyses 1 and 2 display the typical minor element-free chemistry of these plagioclases and of the low mole. % An and Or, typical of highly ordered, low temperature albite (Smith, 1974). A peculiar feature is the occurrence of `chessboard' feldspar (plate 6). Starkey (1959) and Callegari and De Pieri (1967) both suggested that this phenomenon is due to Na metasomatic replacement of original K-feldspar (microcline and/or orthoclase). In some instances, the replacement of K-feldspar by albite is incomplete, the result being micro-domains of albite in a matrix of untwinned microcline as shown in the photomicrograph.
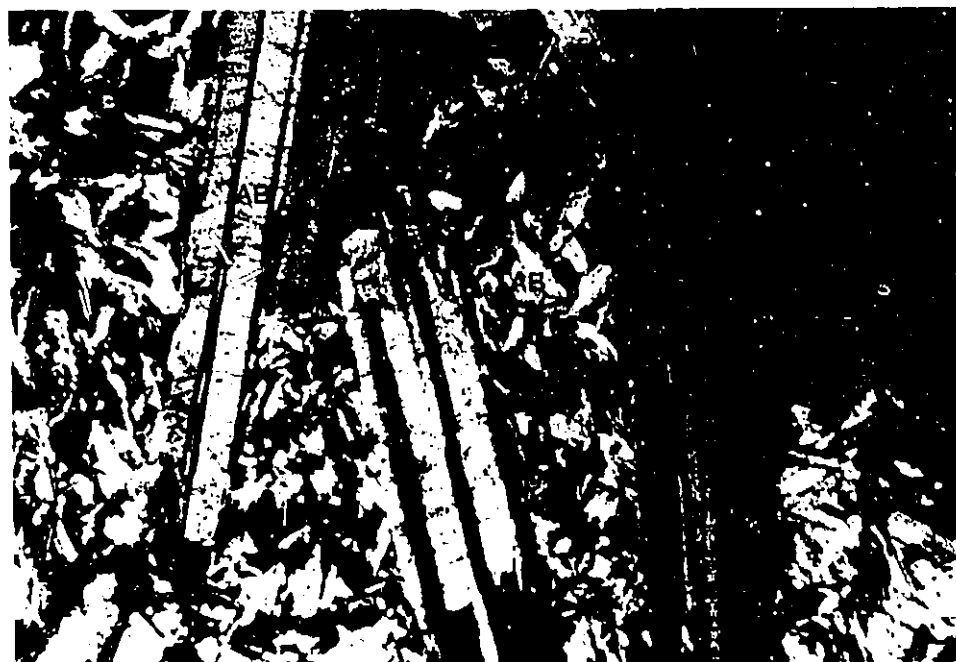
Plate 5. Photograph showing large laths of first
stage albite with smaller second stage
albite. Magnification X50, XPL
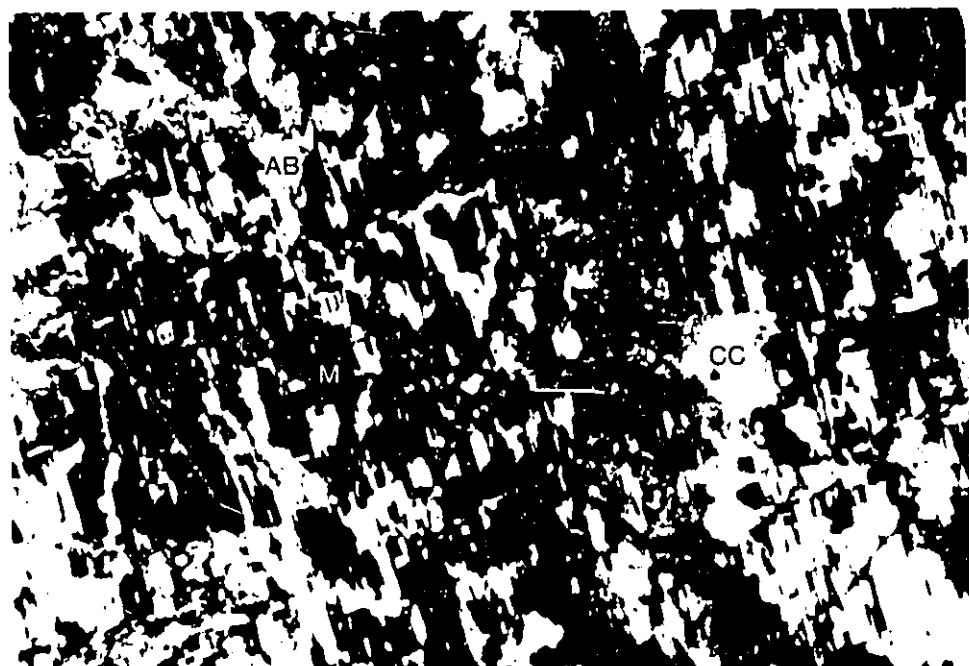
Plate 6. The effects of albitisation as shown in
'checkerboard' albite. Light areas are
the regions of albite-replaced microcline.
Magnification X62, XPL

Most but not all albite grains display some degree of polysynthetic twinning. Callegari and De Pieri (1967) have attributed the lack of ubiquitous twinning to result from the Na metasomatic replacement of previously existing more calcic-plagioclase. The epitaxial replacement of calcic-plagioclase by sodic-plagioclase apparently does not promote twinning. Alternatively, it is likely that the processes responsible for untwinned microcline (low temperatures) is also causing the paucity of twinning especially within second stage albite.

As an aid to mineral identification, limited cathodo-luminescence studies were performed. Minerals that were observed to cathodoluminesce include the feldspars, zircon, fluorite and carbonates in addition to numerous minerals found within the silica-undersaturated rocks. The feldspars show a number of different features. K-feldspar displays weak yellow to orangy-red luminescence due to Fe^{3+} activators within the Al^{3+} sites (Mariano and Birkett, 1988). Albite generally luminescesces orangy-red to dark red, also believed to be in response to Fe^{3+}. Other albite grains are mildly emissive (yellowish) to non-emissive indicating variability of Fe^{3+} concentrations. Some albite displays blue luminescent rims which, as discussed by de. St. Jorre and Smith (1988), is due to late-stage Ga enrichment.

Quartz is very common in the Lake zone. The introduction of quartz either as a result of fenitisation by

the underlying nepheline syenite or from remobilisation of
previously existing quartz, has meant the persistence of
this mineral over a long period of time and of at least
three generations (table 2). One noteworthy phase of quartz
crystallisation is that associated with arfvedsonite
replacement. In this situation the quartz is anhedral, of
variable grain size and occurs interstitially to the coeval
magnetite and hematite. A very late-stage quartz veining
event has also been observed.

Two main quartz generations have been noted: a lesser
euhedral, inclusion-free type and a more common anhedral,
inclusion-rich variety. The inclusion-rich type is
typically matrix material found in all rock types, from the
feldspathic Wall zone to the melanocratic zircon-rich
regions found at various depths within the Core zone. The
inclusions are various and include fluids, gases and
dustings of hematite, aegirine, biotite and other
unidentified minerals. This inclusion-rich generation of
quartz inundates many areas such as that seen in plate 7.
In this photograph, small cleavage-controlled inclusions of
Fe-oxides outline previously existing minerals (micas?).

In drill core, quartz is conspicuously absent below a
depth of 100-120 m. This means that there is a zone
approximately 30-60 m thick immediately overlying the
nepheline syenite that is devoid of both excess silica and
nepheline. Adjacent to the rock causing fenitisation,
fenites commonly have a zone where quartz has been removed
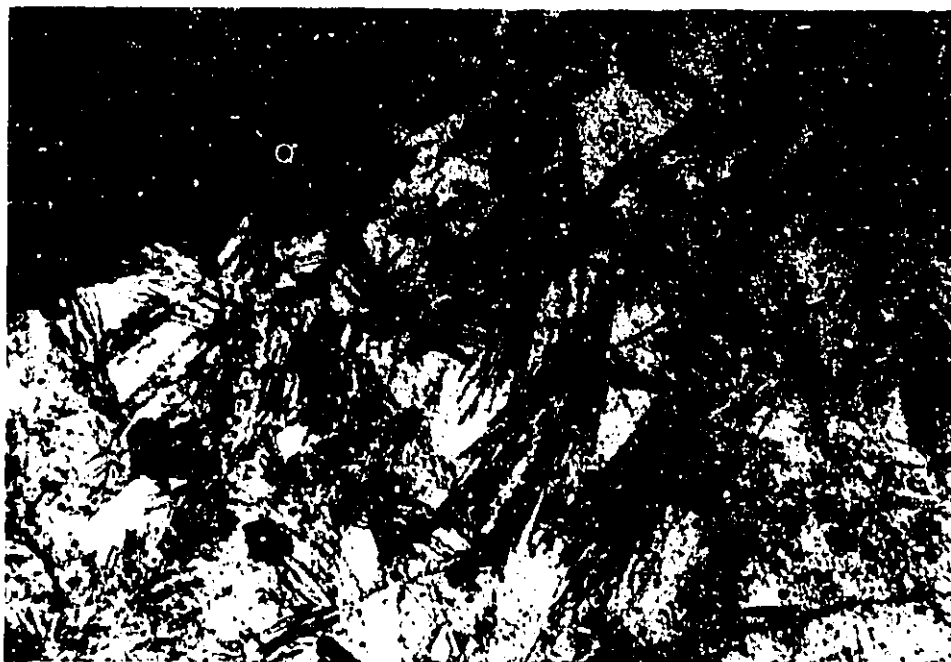
Plate 7. An example of quartz flooding leaving
behind Fe-oxide inclusions originally in
micas(?). Magnification X75, XPL
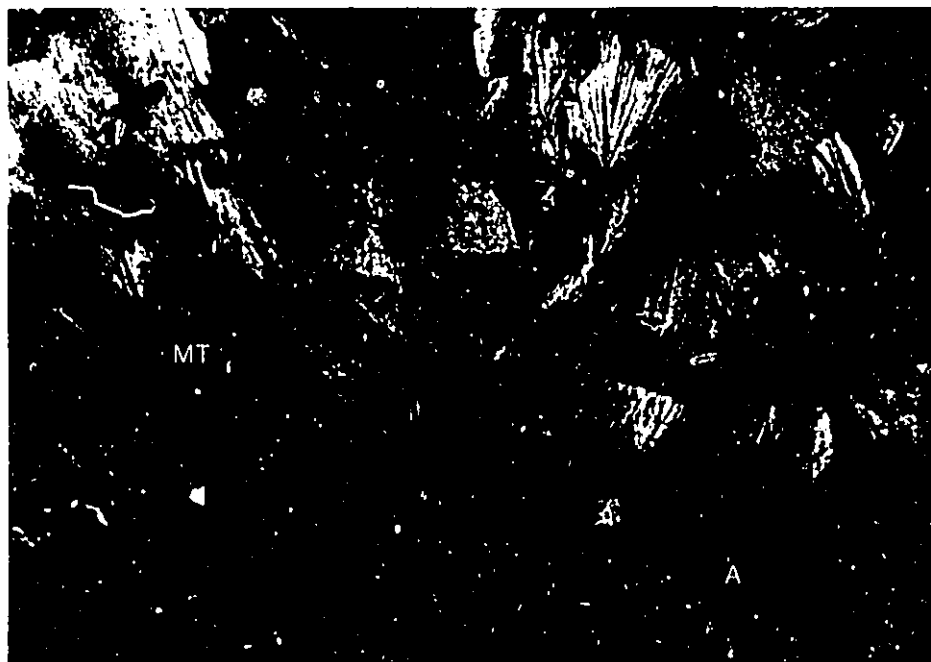
Plate 8. Photograph showing the pleochroic scheme
of green biotite. Note the grain of
allanite-(Ce) in the lower right. Mag-
nification X75, PPL

and subsequently deposited at some distance from the contact (in this instance >60 m).

The most common type of mica is biotite. The first to form is a brown variety which, according to chemical information (appendix 1, anal. 16), is annitic in nature. The second, and by far the most common, is a green variety which by nature of its pleochroic scheme (n_a = light yellow-brown, n_b = dark green, n_c = dark green) must contain low Ti and high ferric iron (Deer et al., 1962). Plate 8 shows the pleochroic nature of this variety of biotite while analyses 13 and 14 display the typical compositions. Certain green biotites have cation deficiencies in both the tetrahedral and octahedral sites (i.e., anal. 15). The deficiency of Al in this particular sample can be compensated by the existence of Fe^{3+} in the tetrahedral sites (Miyano and Miyano, 1982) whereas the deficiency of elements in the octahedral sites may be compensated by minor amounts of Li. By stoichiometric considerations, the mineral should contain approximately 1 wt% Li_2O which, in addition to H_2O and presumably F, would provide reasonable totals for all biotite analyses.

In thin section, the brown biotite is of variable grain sizes, generally from 50-200 μm. It is typically found surrounding or invading previously formed feldspar crystals. Finer grained varieties tend to form as matrix material away from the larger grain boundaries provided by feldspars, allanite-(Ce) or bastnäsite-(Ce). The green biotite

displays similar petrographic features to the brown variety
and as such represents the continued formation of annitic
biotite, albeit with higher concentrations of Fe^{3+}. The
widespread formation of biotite has caused the embayment,
replacement and milling in earlier formed feldspar, quartz
and some rare-metal-bearing minerals leading one to suggest
the importance of biotite in Lake zone brecciation.
Numerous pleochroic haloes due to nearby zircon,
ferrocolumbite and xenotime-(Y) have been noted especially
in the later-forming green variety.

After the formation of green biotite, more Li-rich
micas such as lithian muscovite and polylithionite formed.
The lithian muscovite (appendix 1, anal. 19) has
considerably more Si and less Al than does the muscovite
from the silica undersaturated rocks (anal. 20). This
feature is a result of Li substitution and becomes more
pronounced as the Li content increases (Foster, 1959). The
low total in analysis 19 can then be ascribed to Li^{+}
substitution of Al^{3+} in the octahedral sites in the range of
1-1.5 wt%. Also note the low alkali element total probably
due to electron beam damage in this particular sample.
Finally, in the later stages of crystallisation, Li becomes
even more enriched and polylithionite formation is favoured
although in small quantities.

Another late-stage mineral is chamosite (appendix 1,
anal. 17 and 18). Chamosite, an Fe-rich member of the
chlorite group, is found as radiating bundles in-filling

voids left by feldspar or quartz. Brown biotite formation was likely gradational into green biotite and finally chamosite. Thus, chamosite represents the end product of phyllosilicate formation (table 2) which implies that with time residual liquids contained higher Fe/Mg ratios and lower concentrations of alkalis. Optically, chamosite has a pleochroic scheme that mimics green biotite although it displays typical anomalous first order blue-green birefringence. No Li chlorites (cookeite, manandonite) were noted although their existence here seems likely.

ACCESSORY MINERALS

The term 'accessory' is, in this situation, applied to any mineral which is present in quantities of 5-10 modal % or less. Minerals such as magnetite, hematite, ankerite and fluorite fit this criterion in most situations but in some instances, a particular rock may become enriched in an 'accessory' mineral. For example, ankerite, a carbonate that is found in most samples to approach 5 modal % is found in other samples to comprise >50% of the rock. In general though, the important accessory minerals discussed include ilmenite, magnetite, hematite, fluorite, carbonates, apatite and sulphides. All minerals containing elements of economic interest are treated separately in the next chapter.

The deposit contains a number of Fe-bearing minerals, the most obvious and ubiquitous being the oxides, magnetite and hematite. Magnetite is found as idiomorphic grains,

usually as octahedra, 30-300 μm in size scattered throughout
or associated with the quartz-carbonate assemblages of
replaced arfvedsonite. Chemically, magnetite does not
contain any appreciable trace elements including Ti or Nb
(appendix 1, anal. 38).

Intimately associated with several magnetite crystals
is an isotropic, orange coloured material (plate 9).
Analysis 39 indicates the mineral to be a highly hydrated
Fe-silicate. This apparently amorphous material might
possibly have been fayalite that has since undergone
alteration, in an oxidising environment, into magnetite plus
an orange-coloured, hydrated Fe-silicate. According to
Champness (1970), the alteration of fayalite to magnetite-
like precipitates plus an amorphous silica similar to the
one seen here occurs at temperatures ranging from 500° to
800°C. However scant, this material provides the only
evidence for previously existing olivines and as such may
represent remnants of the ring dyke separating the Grace
Lake granite from the Thor Lake syenite.

More widespread than magnetite is the other major oxide
mineral, hematite. Generally, hematite is rare in igneous
rocks except under those conditions in which the fO_2 is
sufficient and abundant earlier formed Fe-bearing minerals
exist. In the Lake zone, hematite is present in many
different forms: first it is found as small, euhedral
plates associated with the quartz-carbonate replacement of
arfvedsonite (plate 10); second it occurs as undefined,
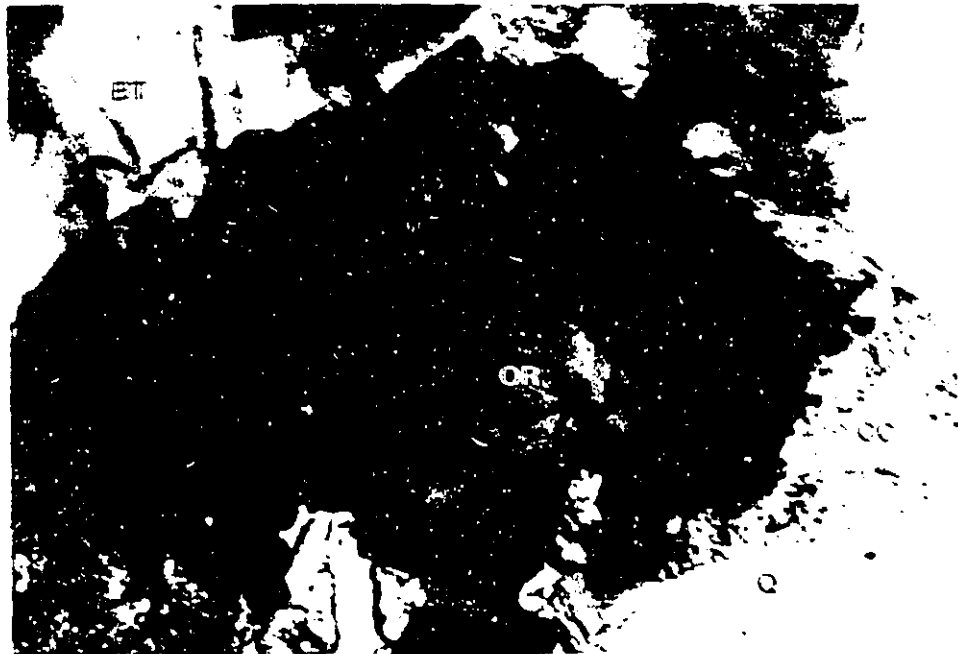
Plate 9. Photograph showing the association of magnetite with the 'orange mineral' surrounded by biotite. Magnification X300, PPL

Plate 10. Secondary electron image of hematite in a quartz-biotite matrix. Note at the centre of the photo the platelet-like nature of the hematite. Scale bar represents 5% µm.

anhedral masses interstitial to albite and microcline; and third, it commonly dusts grains of microcline as very small (<2 μm) crystals. In microcline, the hematite crystals are believed to nucleate after feldspar growth (subsolidus decomposition) and are strongly controlled by {001} cleavage planes. The resulting inclusions are responsible for the red colouration commonly seen in Lake zone feldspars. Analysis 37 indicates the chemical composition of some later-forming hematite. Note the rather substantial Nb content, possibly significant to overall Nb values in the Lake zone. The substantial Si present in this analysis is probably due to the inadvertent excitation of Si from nearby minerals.

Even though it occurs in limited quantities, ilmenite was one of the few Ti minerals found within the Lake zone. It never occurs larger than 50 μm and always displays well formed crystal habits. Generally though, the overall lack of Ti-rich minerals such as ilmenite, chevkinite-(Ce) [$(Ca,Ce)_4(Fe^{2+},Mg)_2(Ti,Fe^{3+})_3Si_4O_{22}$] and more noticeably rutile, suggests a minor influence of Ti in the Lake zone (see also biotite analyses in appendix 1) contrary to the findings of Hylands and Campbell (1980).

Pyrite, chalcopyrite, sphalerite and galena are all found in very minor quantities most often in the felsic rocks of the Wall zone. Galena, 5-10 μm in size, has been noted intimately associated with ferrocolumbite and pyrochlore in the zircon-rich rocks. Pyrite is found

throughout as small, euhedral tetrahedra whilst sphalerite and chalcopyrite both generally occur as ill-defined crystal shapes. Overall, sulphide minerals are not as common as they are in the T zone.

Fluorite is a very common accessory mineral. It is the last mineral formed in the Lake zone (table 2) and as such fills in pre-existing voids left between other minerals. Unlike the T zone, no large dodecahedra of green fluorite were found. Instead, only purple or colourless anhedral crystals exist. In thin section the fluorite is commonly colourless but adjacent to mildly or strongly metamict minerals, such as ferrocolumbite or zircon, the mineral turns purple in response to alpha and/or beta particle bombardment. The colourless fluorite cathodoluminesces light blue in response to Eu^{2+} activators (Nickel, 1978) while radiation damaged (purple) fluorite does not luminesce.

In mineralised peralkaline granites, the HREEs and Y are commonly found within fluorite (Jackson, 1986) or they may form other REE fluorides such as gagarinite-(Y) [$NaCaYF_6$]. This is not the case at Thor Lake. Numerous WDS crystal scans with the electron microprobe for the HREEs on various fluorite grains detected nothing and only very minor amounts of Y thereby suggesting the incorporation of most if not all REEs and Y into earlier formed oxides. The detection limits of WDS scans will vary with the element investigated and upon the instrument and its operating

conditions. Theoretically, detection limits can approach 50 ppm (D.G.W. Smith, pers. comm.) but in this case detection is on the order of 10X this theoretical limit.

Another common late-stage mineral is calcite (plus ankerite). The abundance of carbonates and hence of CO_3^{2-} ions mean that any available LREEs in the system will be favourably complexed, along with fluorine, to form the bastnäsite group minerals. The only mineral with substantial Ca is calcite whose formation may be explained by CO_3^{2-} ions combining with Ca released from plagioclase during albitisation. Alternatively, the abundance of carbonates may be explained by the existence of a carbonatite at depth.

The carbonates are generally anhedral and of variable grain size. Calcite is colourless whereas ankerite, because of substantial Fe, is yellow to orange. Ankerite does not cathodoluminesce (Fe^{2+} quenchers) whereas calcite generally displays orange to dark red colours (Mn^{2+} or Ce^{3+} activators). Chemically, the carbonates were not found to contain any LREEs (WDS element scans) as all available REEs were apparently incorporated into earlier formed bastnäsite group minerals.

Apatite is rare, being found only within large crystals of allanite-(Ce). Typically they are small (5-20 μm) euhedral crystals probably formed early in the crystallisation sequence (table 2). Later, all available

phosphorous was incorporated into monazite-(Ce) and xenotime-(Y).

The last group of accessory minerals are the rare-metal-bearing species. These minerals are of considerable importance and as such will be treated separately in the next chapter. In general, though, two discrete time frames have been noted, the first is a subordinate phase formed shortly after K and Na metasomatism and features, typically, well-formed, euhedral crystals. The second phase is somewhat later and is responsible for the large scale enrichment of REEs, Nb, Y and Zr in the Lake zone. This second enrichment features fine grained, poorly developed crystals. The identification of, and specific relationships between, these minerals will be explored in detail in the next chapter.

IV ELEMENTS OF ECONOMIC INTEREST

INTRODUCTION

Because the Lake zone is North America's largest deposit of Nb and Zr (D.L. Trueman, pers. comm.), a thorough examination of the minerals containing these elements is necessary. Supplemental to the Nb and Zr are large quantities of REEs and Y along with lesser amounts of Ga, Ta, U and Th. Thus, the following chapter describes, in separate sections, Zr, Nb, REE and Y-bearing minerals. Be and Li, present in economic quantities within the T zone are not common in the Lake zone and are therefore not discussed. The following is a description of the minerals, both common and uncommon, that contain the elements of economic interest.

ZIRCONIUM

Probably most widespread of the above mentioned elements is Zr, all of which is found in zircon. Complex zircono-silicates, such as eudialyte or rosenbuschite, only crystallise in hyperalkaline, silica-undersaturated rocks rich in incompatible elements (Ilimaussaq, Greenland, Khibina, USSR). At Thor Lake, three general phases of zircon formation have been noted (table 3). The first is a relatively early, well-zoned form which would correspond to the 'zonally metamictised' type noted by de St. Jorre (1986). The second is a late-forming, subhedral to anhedral

TABLE 3
PARAGENESIS OF THE RARE METAL-BEARING MINERALS

```
quartz                                    -------
albite                      ---
green biotite                                            -------
zircon                        ---              -----            --
xenotime-(Y)                  ----
allanite-(Ce)                         ---            ---
monazite-(Ce)                 ---                          ---
bastnäsite-(Ce)                          ---    ---
parisite-(Ce)                            ---    ---
synchisite-(Ce)                          ---
ferrocolumbite              ---                 ---
fersmite(?)                 --
uranpyrochlore                                 --
ceriopyrochlore-(Ce)                             ---
pyrochlore                                           --
betafite                                         ---
fergusonite-(Y)                                     --------
samarskite-(Y)                                            --
aeschynite-(Nd)                        ----
nioboaeschynite-(Ce)                   ----
nioboaeschynite-(Nd)                   ----

            TIME      --------->
```

type of zircon called the 'bipyramidal' type by de St. Jorre while the third is a minor 'hydrothermal' phase.

Compared with the more common later-forming zircons, the zonally metamictised grains are bigger (100-200 μm), are relatively clear, have better defined crystal shapes usually with better development of the {010} faces and are often more fragmented usually as a result of late stage biotite flooding.

Zonation within these types of zircons was studied by de St. Jorre (1986). She found that most contain minor differences in U, Hf and Y concentrations from zone to zone thus indicating crystal formation not at one specific time, such as early in the crystallisation sequence, but as continual crystal growth. The zones therefore reflect changes in the activities of U, Hf and Y within the melt as the zircons grew. Because the radioactive elements (U, Th) vary in concentration from zone to zone, variations in the degree of metamictisation are noticeable. Metamictisation also affects neighbouring crystals, resulting in synuresis cracks in minerals such as feldspars and commonly seen pleochroic haloes in green biotite. These particular zircons show zonal cathodoluminesence varying from a dull orange-yellow to bright orange. The luminescence is due mainly to the presence of Dy^{3+} activators (Mariano and Birkett, 1988). Of all the minerals containing elements of economic interest, zircon is the only one that cathodoluminesces.

Some zircons contain clouded cores which, in many cases, do not appear to result from metamictisation but from inclusions of other minerals. One such example has small hematite crystals acting as nucleation sites for zircon overgrowths. Other minerals such as xenotime-(Y) and older generation, metamict zircons also contain overgrowths of clear zircon.

More important than the earlier formed, zonally metamict crystals are the smaller bipyramidal and associated anhedral zircons. These small grains are commonly found within 5-10 m thick bands of zircon-rich rock at various depths in the Lake zone. These zones can be roughly correlated and appear to form tabular bodies of rock which have been termed the upper, intermediate and lower zones (J.C. Pedersen, pers. comm.). In these zones the rock is fine grained, melanocratic and, on average, contains 60-80 modal% zircon with the remainder composed of quartz, biotite, magnetite, carbonate, allanite-(Ce), fergusonite-(Y) and ferrocolumbite.

In general, these zircons are severely metamict, bipyramidal crystals of about 10-50 μm in diameter. Plate 11 illustrates the maximum size noted for these unzoned zircons. These crystals contain minor amounts of water, inferred from the 'light' area seen in plate 11 (the square in which 'ZR' is placed). This square represents an area of electron beam bombardment, and as a result of high energy electron impingement, the lighter elements or molecules such
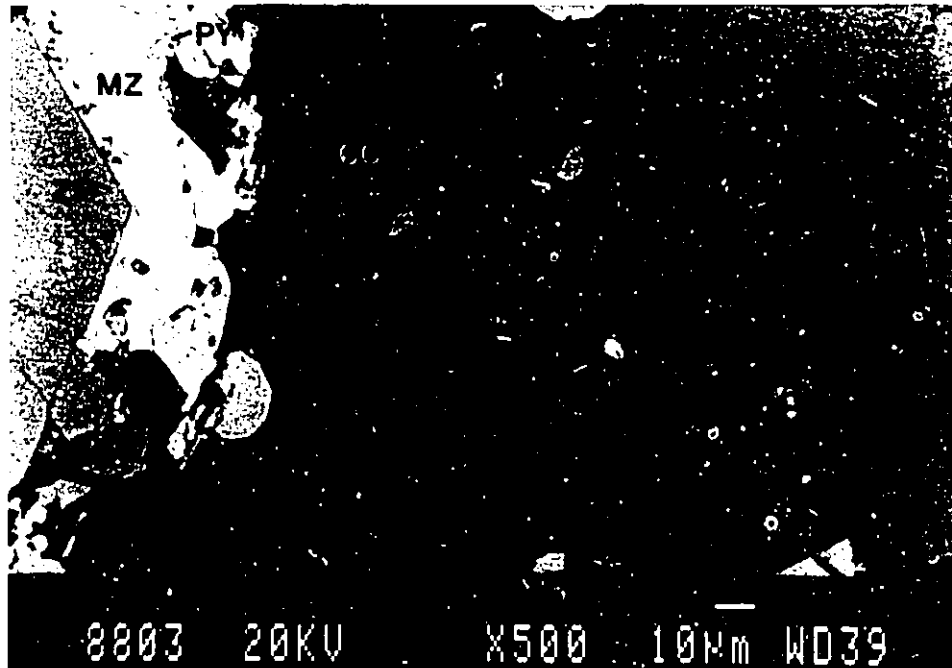
Plate 11. Secondary electron image of euhedral zircon. Note the presence also of monazite-(Ce) and closely associated pyrochlore. Scale bar is 10 μm.
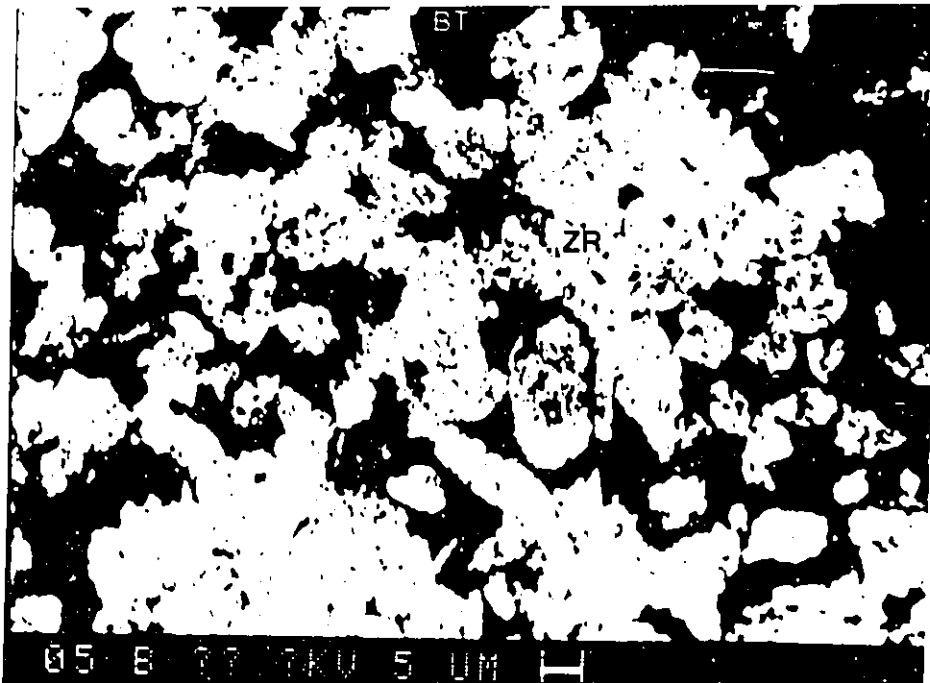
Plate 12. Backscattered electron image of small, anhedral zircons. Scale bar is 5 μm.

as water may become liberated. The release of such light elements increases the average atomic number of the remaining material and thus creates the lighter area. According to Caruba et al. (1975) these bipyramidal zircons are common in agpaitic melts and are indicative of low temperatures of formation (500-550°C). Also, the incorporation of U, Th, REEs, P and H_2O are believed to favour bipyramids (confirmed by microbeam analyses as discussed later) where.s Hf tends to promote prismatic crystals (Speer, 1982). The bipyramidal form results from the suppression of (100) and (110) face development.

In addition, many very small (2-5 μm), anhedral grains of zircon are found (plate 12). These crystals tend to be found, along with quartz, biotite, carbonate and allanite-(Ce), replacing original, euhedral grains. Also within the rock, thin laminations of tan coloured zircon are found to invade a matrix of quartz, biotite and magnetite. In this situation, a third type of zircon may be defined. It is relatively rare but is unique in that it is anhedral (plate 13) and may form hydrothermally as suggested by Rubin et al. (1988).

All second stage or type 2 zircons are found to be heavily metamictised as opposed to the zonally metamictised or type 1 zircons which are only mildly metamict in certain zones. The metamict nature of type 2 zircons is a result of formation within a hydrous fluorinated environment rich in radioactive elements and associated REEs at low (400-500°C)
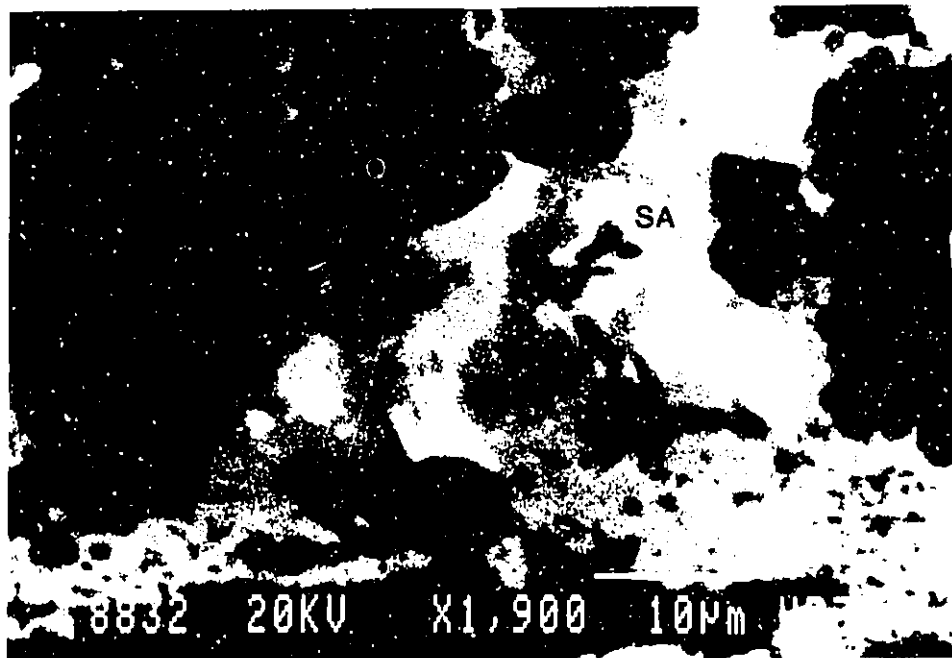
Plate 13. Secondary electron image of 'hydro-
thermal' zircon and samarskite-(Y).
Scale bar is 10 μm.

temperatures (Caruba et al., 1985). The addition of weakly bonded H_2O (favoured at low temperature) into the zircon structure weakens the crystal lattice thus facilitating the destruction of the zircon by metamictisation. This is contrary to previous ideas of initial metamictisation followed by hydroxyl group incorporation. Caruba et al. (1985) have determined that $(OH,F)_4$ groups substitute for SiO_4 tetrahedra under the above mentioned conditions, therefore, such zircons can have the following general formula: $[Zr(SiO_4)_{1-x}(OH,F)_{4x}, x=0.2-0.8]$.

Chemically, the zircons contain various amounts of Y and REEs in addition to minor Al, Fe, Ca, etc. (see appendix 1, analyses 64-66). Both type 1 and type 2 zircons are enriched in Nb and the REEs (anal. 64 and 65). Note that they generally display a REE maximum at Nd followed closely by substantial Sm, Gd and Ce. None of the HREEs were detected even though approximately 1 wt% Y_2O_3 exists in most grains. Another important chemical feature is the existence of both F and presumably, because of the low totals, hydroxl ions. This confirms the existence of a hydrous fluorinated REE-rich environment necessary for the formation of these small, bipyramidal zircons. Analysis 66 was performed on the rarer type 3 zircons. In these grains, no REEs, Nb or F were detected as these recrystallised zircons apparently did not scavenge any elements from the parent zircons or if they did, migrated elsewhere. Finally, it may be noted that the Hf values are lower than average. Ahrens and Erlank (1969)

compiled 463 zircon analyses for which HfO_2 was reported and found the average HfO_2 value to be 1.71 wt% with a Zr:Hf ratio of 40:1. In the Lake zone, the average HfO_2 value is 1.09 wt% and Zr:Hf is about 50:1. The relatively low Hf values here are indicative of a lack of chemical differentiation especially compared to highly evolved rare metal-bearing granitic pegmatites which are known to contain hafnian zircon and hafnon.

NIOBIUM AND TANTALUM

Of all the economically important elements, Nb mineralisation is the most diverse, encompassing ferrocolumbite, fersmite(?), fergusonite-(Y), samarskite-(Y)(?), aeschynite-(Nd), nioboaeschynite-(Ce) and nioboaeschynite-(Nd), pyrochlore, uranpyrochlore, betafite and ceriopyrochlore. Ta, closely associated with Nb because of its similar charge and size (Nb^{5+}=0.069 nm, Ta^{5+}=0.068 nm), is present in most Nb-bearing phases, although in minor quantities and never as discrete minerals.

In these rocks, the Ta/(Ta+Nb) ratios are very low indicating little in the way of incompatible element fractionation. This correlates with the low Hf/(Hf+Zr) ratios seen in zircon, thus there is an enrichment of Zr and Nb over Hf and Ta. In granitic pegmatites high degrees of fractionation yield, in addition to Li-, Cs- and Be-bearing minerals, high Ta/(Ta+Nb) and Zr minerals which contain greater amounts of Hf (Cerny, 1982). The Lake zone does not

exhibit any of these characteristics. Cerny (1986) summarised the abundance of Nb and Ta in alkaline rocks and made the following generalisations: deposits of alkaline anorogenic affiliations (Blachford Lake) produce exclusively Nb (with associated Ti, Zr, Y and REE); calc-alkaline or peraluminous late-tectonic to post-tectonic granites yield both Nb and Ta (with associated Li, Sn and W) and orogenic granitic pegmatites produce only significant Ta (with associated Li, Rb, Cs, Be, Sn and B). Thus the Lake zone can not be expected to contain significant Ta mineralisation.

In terms of Nb, the mineral of prime importance is ferrocolumbite ($Fe^{2+}Nb_2O_6$). Structurally, ferrocolumbite is a disordered Fe-niobate, the equivalent ordered mineral being ixiolite (T.S. Ercit, pers. comm.). No structural work was performed on this mineral so the globally more common ferrocolumbite is assumed.

Ferrocolumbite is orthorhombic and is a member of the columbite group which is defined as follows. From ferrocolumbite, Mn substitution for Fe^{2+} leads to manganocolumbite while Ta substitution for Nb and Mn substitution for Fe gives manganotantalite. The Fe-Ta member, separated from the others by a miscibility gap, is actually tetragonal and belongs to the tapiolite series. Lake zone material corresponds very closely to end-member ferrocolumbite as indicated by chemical analyses given in appendix 1, analyses 40-45.

Like the zircons, ferrocolumbite is found in a number of habits. Earlier formed grains are always as small (30-40 μm), acicular crystals with very high length to width ratios. Measured ratios are generally on the order of 11-13:1. These crystals commonly aggregate as 'pinwheel' clusters (plate 14) and are found to form relatively early (table 3). In this situation, fluorite or quartz acts as host material to either intact 'pinwheel' clusters or to individual needles.

The more bladed, later-forming crystals are on the order of 20-50 μm and have length to width ratios varying from 4-7:1. Generally, they are found in the melanocratic zircon-rich zones mentioned earlier, interstitial to type 2 zircons, or in Wall zone rocks associated with, and armoured by, later-forming hematite (plate 15). Finally, ferrocolumbite crystals may be found as complex masses intergrown with magnetite, galena, ilmenite, ishikawaite (see later), allanite-(Ce) and calcite (plate 16). Note in this situation the lack of crystal habit.

In all cases, Ta_2O_5 is no greater than 5 wt% (maximum in anal. 41), MnO 7 wt% (maximum in anal. 45) and TiO_2 4 wt% (maximum in anal. 45). Small concentrations of U (anal. 42 and 43) and Sn (anal. 45) were found. Although the association with hematite rarely occurs, it can develop and have the affect of producing a ferrocolumbite rich in Fe^{3+} as shown in analyis 45. In this case, ferric iron is more abundant than ferrous iron meaning a significant emplacement
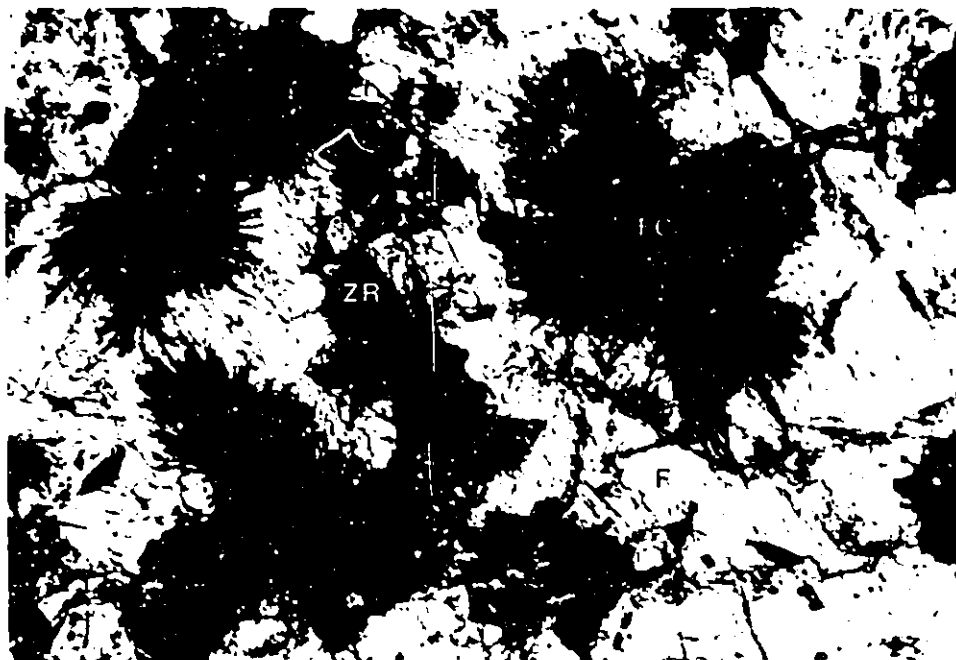
Plate 14. Photograph displaying 'pinwheel' aggregates of ferrocolumbite in a matrix of fluorite. Magnification X185, PPL
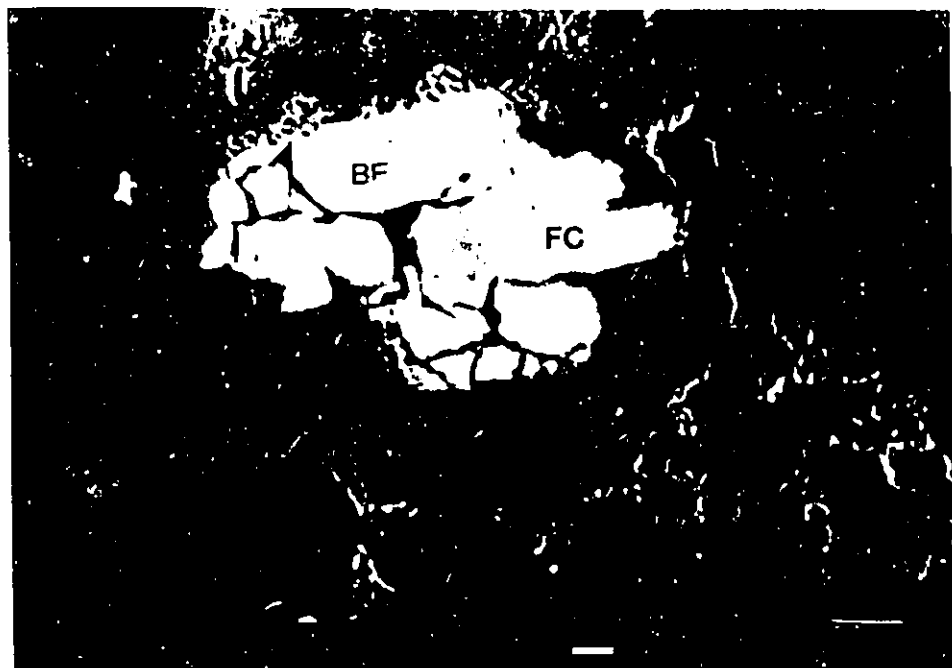
Plate 15. Backscattered electron image of betafite and the bladed variety of ferrocolumbite armoured by hematite. Scale bar is 5 μm.

of Fe^{3+} into the Nb^{5+} sites. Some samples contain minor U which manifests itself in the purple colouration of, when present, nearby fluorite. Although difficult to detect optically, Ewing (1976) has suggested that metamict ferrocolumbite is rather common.

Cerny and Ercit (1986) have summarised the various alteration products of ferrocolumbite. One such reaction occurs during albitisation when pyrochlore forms at the expense of ferrocolumbite. Although uncommon, pyrochlore group minerals (see later) have been detected in the Lake zone possibly indicating an interaction of some earlier-formed ferrocolumbite with subsequent albitisation. The more acicular ferrocolumbite crystals are found, in rare instances, to overgrow a Ca-rich niobate which is probably identified, though energy dispersive microprobe analysis, as fersmite [$(Ca,Ce)(Nb,Ta,Ti)_2(O,OH,F)_6$]. This mineral occurs as very small (2-5 μm), poorly formed crystals and hence was not suitable for quantitative analysis.

Another important group of Nb-bearing minerals is the pyrochlore group. The group is complex, comprising at least 20 recognised species. The general formula of $A_{1-2}B_2O_6$ $(O,OH,F):nH_2O$ means numerous chemical substitutions in both A and B sites and various degrees of hydration are possible. In the Lake zone, at least three members of this group have been identified in accordance to the nomenclature outlined by Hogarth (1977): pyrochlore [$(Ca,Na)_2Nb_2O_6(OH,F)$], ceriopyrochlore [$(Ce,Ca,Y)_2(Nb,Ta)_2O_6(OH,F)$], uranpyrochlore

[(U,Ca,Ce)$_2$(Nb,Ta)$_2$O$_6$(OH,F)] and betafite

[(Ca,Na,U)$_2$(Ti,Nb)$_2$O$_6$(OH)]. These pyrochlore group minerals are usually found in the albite-rich rocks of the Lake zone typically as very fine-grained crystals intimately associated with other phases. They are found as: i) very small, poorly defined grains clustering near zircon and monazite-(Ce)-rich regions and ii) associated with ferrocolumbite and rimmed by hematite in fine grained albite-rich rocks.

The small (2-5 μm), anhedral crystals in case one cluster near earlier-formed zircon and monazite-(Ce) crystals as typified in plate 11. More common though are the grains typified in case two. In those circumstances, the pyrochlore contains more Ti (betafite) or REEs (ceriopyrochlore), is larger in size (10-15 μm), subhedral and appears to have formed at the same time as the closely associated ferrocolumbite (plate 15). Note from plate 15 that it is impossible to distinguish between ferrocolumbite and betafite on the basis of backscattered electron images because both have approximately the same average atomic number. Rimming most of these composite grains is hematite.

Chemically, these minerals are represented in appendix 1 by analyses 61-63. Assuming various amounts of structurally bound OH, the analytical totals come reasonably close to 100 wt% in all cases. Note the various concentrations of Fe, Si and Th and the lack of any HREEs. Again, as in the ferrocolumbite, Ta values are very low,

never greater than 2 wt%. U contents are elevated but not enough to make any one of these minerals a uranpyrochlore.

A very U-rich niobate, believed to be uranpyrochlore, was found intimately associated with ferrocolumbite, magnetite and allanite-(Ce) (see plate 16). It is on the scale of 5-15 μm and may include small (<5 μm) recrystallised grains of galena. Microprobe analyses of the material (anal. 54 and 55) indicates it has a (Nb+Ti):O ratio of about 1:3 with variable Si, Fe, REEs and Pb (contamination?). Application of MinIdent (Smith and Leibovitz, 1986) gives only a limited number of possibilities. The most likely include: petscheckite [$U^{4+}Fe^{2+}(Nb,Ta)_2O_8$], a mineral found in the complex pegmatites of Madagascar (Mucke and Strunz, 1978); ishikawaite [$(U,Fe,Y,Ca)(Nb,Ta)O_4(?)$], a mineral of questionable structure but believed to be a U-rich samarskite (Cerny, 1986); ashanite [$(Nb,Ta,U,Fe,Mn)_4O_8$], a mineral believed to be a U-rich ixiolite (T.S. Ercit, pers. comm.) or uranpyrochlore. There is not enough U and Fe in this mineral to be petscheckite, therefore, the best possibilities are either a hydrated ishikawaite or uranpyrochlore. MinIdent prefers uranpyrochlore and because of the association of other pyrochlore group minerals nearby, this identification does not seem unlikely. These grains are extremely small and therefore it is very difficult to obtain reliable chemical information because of the inadvertent excitation of elements in nearby minerals.

Plate 16. Secondary electron image of uranpyro-
chlore (labelled IS) enclosed in ferro-
columbite. Note the galena and al-
lanite-(Ce). Scale bar is 10 μm.
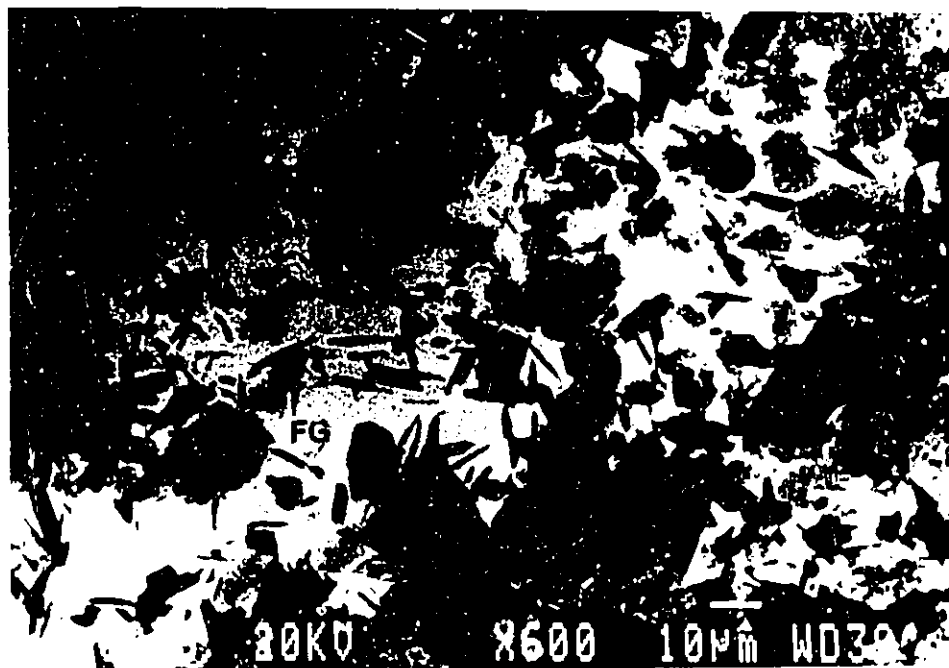
Plate 17. Secondary electron image of anhedral
fergusonite-(Y) and zircon. Note the
enclosed flakes of biotite in the fer-
gusonite-(Y). Scale bar is 10 μm.

Associated with type 2 zircons is an Y-niobate identified here as fergusonite-(Y) [$YNbO_4$]. The mineral is noticeably common in the zircon-rich zones thereby suggesting fergusonite-(Y) as a major source of Y in the Lake zone. The mineral is found as later-forming grains associated with type 2 zircons (plate 17) or with aeschynite group minerals. Typically, the fergusonite-(Y) ranges from 10-100 μm and may enclose biotite flakes. Optically, the mineral has high positive relief, is colourless (non metamict) to clear yellow-brown, displays low birefringence, possibly of the order of 0.025-0.030, and is optically negative with a small 2V. The colourless characteristic in these grains is very rare for fergusonite group minerals (T.S. Ercit, pers. comm.) mainly because they generally contain U and Th (metamict crystals). These particular samples have virtually none of these elements (anal. 46-51).

Chemically, the fergusonite-(Y) grains are simple with little in the way of minor element substitutions. In the Y sites are found the REEs while in the Nb sites is found minor Ta. Analyses 52 and 53 are chemically similar to the fergusonites except that significant Ca, Fe and Si are found. Also in these two analyses, because of the excess cations and low analytical totals, 2-3 wt% water is inferred. These last two analyses likely represent samarskite-(Y) as the Nb:O ratio is still 1:4 but some replacement of Y by Fe (approximately 5 wt% Fe is characteristic of samarskite-(Y)) has occurred.

Alternatively, all other aspects of this mineral, including close chemical and physical associations, are similar to fergusonite-(Y) and, additionally, MinIdent prefers fergusonite-(Y) in its identification. Plate 13 displays the fine-grained, anhedral nature of the samarskite-(Y) in association with type 3 zircon. The REE patterns within fergusonite-(Y) grains display maxima in the MREEs, either at Nd (anal. 46-48), Gd (anal. 49,51) or Dy (anal. 50) while in samarskite-(Y), the maximum is at Gd. Cerny (1986) notes that the whole range of REE cations may be found, therefore the composition of both fergusonite-(Y) and samarskite-(Y) does not depend upon the crystal structure but on the geochemistry of the parental environment. Both minerals are commonly found in anorogenic, peralkaline granites and metasomatic deposits.

The aeschynite group has an ideal formula of $AMM'O_6$ where A = Y, Ce, Nd; M = Nb, Ta and M' = Ti. Various chemical substitutions especially in the A and M sites can lead to a number of species (at least 7) therefore chemical variability and overlap within species is inevitable. Species identified in the Lake zone include: aeschynite-(Nd) $[(Nd,Ce,Ca)(Ti,Nb)_2(O,OH)_6]$, nioboaeschynite-(Ce) $[(Ce,Nd,Ca)(Nb,Ti)_2(O,OH)_6]$ and nioboaeschynite-(Nd) $[(Nd,Ce,Ca)(Nb,Ti)_2(O,OH)_6]$. The minerals are found as anhedral grains closely associated with fergusonite-(Y) or zircons. Optically, these particular aeschynite group minerals are virtually impossible to distinguish from

allanite-(Ce) as both are very pleochroic in shades of blood-red to brownish-red (plate 18 for nioboaeschynite-(Nd) and plate 19 for allanite-(Ce)). Note in plate 18, the primary growth bands. This feature resulted from the changing availability of Ti and Nb at the time of growth. In this case, atomic proportions of both Ti and Nb were near 50% so that this grain represents the primary crystallisation of both aeschynite-(Nd) and nioboaeschynite-(Nd). Like the allanite, both minerals have high positive relief and because of the heavily pleochroic nature, their biaxial interference figures are well masked. Again because of the paucity of Th and U in the aeschynite minerals, these grains are uniquely non-metamict.

Analyses 56-60 in appendix 1 represent the various aeschynite minerals. Analysis 56 is a nioboaeschynite-(Ce), analyses 57 and 58 are nioboaeschynite-(Nd) (note the high Ca content of anal. 57 almost making it a vigezzite $[(Ca,Ce)(Nb,Ti)_2O_6])$ while analyses 59 and 60 are aeschynite-(Nd). Note that most grains contain a maximum at Nd with secondary Ce and Sm. Even analysis 56, which indicates Ce to be the most common REE, has an overall REE pattern similar to the Nd varieties. No HREEs were found in any aeschynite group mineral. The aeschynite group is common to rare-element granites of anorogenic affiliation and is found to form at low temperatures (Cerny, 1986).
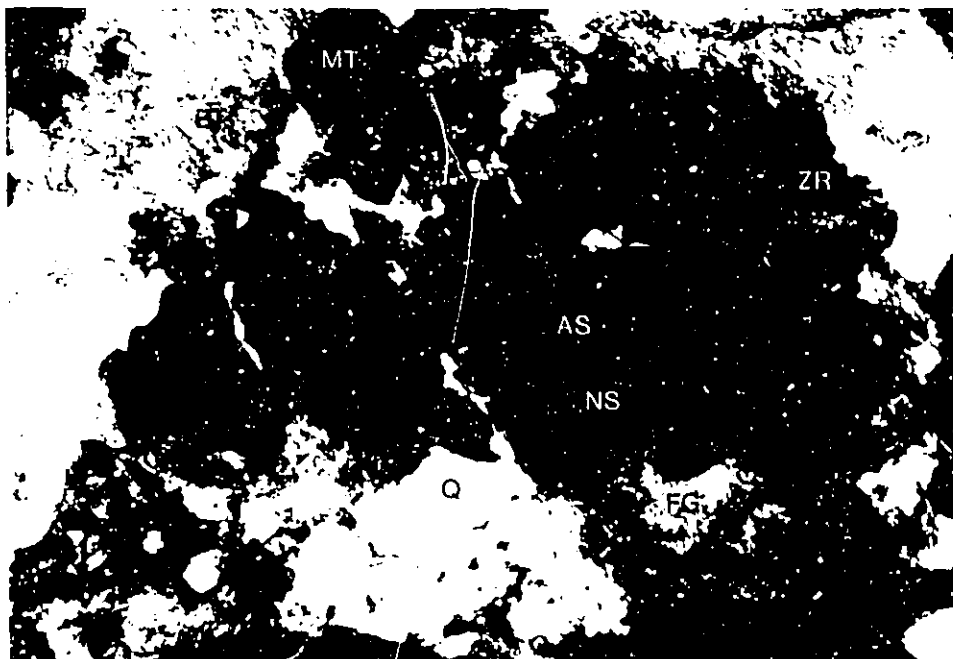
Plate 18. Photograph of a nioboaeschynite-(Nd) and
aeschynite-(Nd) intergrowth. Note the
adjacent fergusonite-(Y). Magnification
X185, PPL
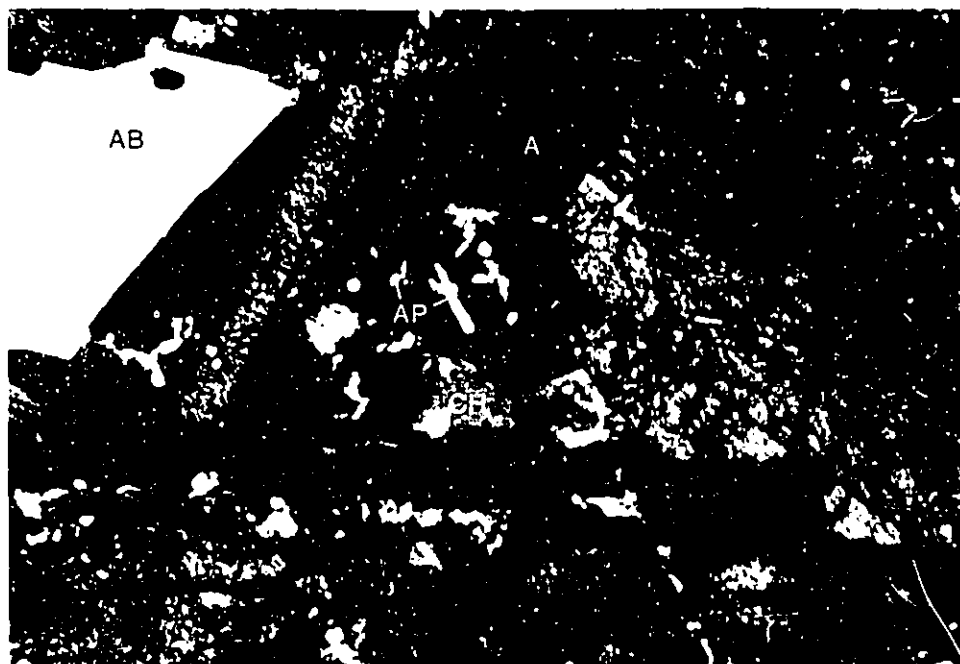
Plate 19. Photograph displaying twinned allanite-
(Ce) enclosing small apatite crystals and
chamosite. Magnification X62, PPL

RARE EARTH ELEMENTS

Three important mineral groups have been noted:
allanite-(Ce), the bastnäsite group and monazite-(Ce) all of
which are enriched in the LREEs hence the (Ce) suffix. Like
the zircon, all REE-bearing phases are found as early, well-
formed crystals and as later generation xenomorphic crystals
associated with type 2 zircons (table 3). Of the three REE-
bearing minerals, allanite-(Ce) is most common whereas in
the T zone, the bastnäsite group minerals prevail.
Allanite-(Ce) has also been found within the nepheline
syenite but is somewhat different in composition (to be
discussed later).

Allanite-(Ce), a REE-rich epidote-group mineral is
typically found in low temperature metamorphic or
hydrothermal deposits rich in rare earths. It is, because
of high relief and a distinctive pleochroic scheme, very
conspicuous in thin section. The pleochroism of Lake zone
allanite-(Ce) generally varies as follows: n_a=orange red or
blood red, n_b=reddish orange, n_c=green, rather typical of
other occurrences (Deer et al., 1982).

Early or type 1 allanite-(Ce) is subhedral to anhedral
and somewhat brecciated by late-stage green biotite. Most
grains when left sequestered reached sizes up to 5-6 mm and
formed large crystal masses. In this situation the crystals
appear tabular, are commonly twinned by simple (100) twins
and contain numerous inclusions of apatite (plate 19).
Later-forming or type 2 allanite is always associated with

type 2 zircons. It forms interstitially to zircon, feldspars and quartz or may be found replacing pre-existing minerals in the form of overgrowths and cleavage plane infiltration. It has also been found intimately associated with ferrocolumbite, magnetite, fergusonite-(Y) and calcite. In this situation, allanite-(Ce) is overgrowing these small opaque masses.

A common feature is the deuteric alteration of allanite-(Ce) to bastnäsite-(Ce). This particular replacement feature has been described in several localities (Deer et al., 1982). Alteration is simply accomplished by the interaction of F- and CO_2-bearing fluids with the allanite-(Ce). As determined by Mineyev et al. (1973), the F and CO_2 pervade the rock, allanite-(Ce) breaks down and forms a number of secondary minerals as shown in the following general reaction:

$$(Ca,REE)_2(Al_2Fe)_3Si_3O_{12}(OH) + F,CO_2 \rightarrow REECO_3F + CaF_2 + Al_4Si_4O_{10}(OH)_8 + Fe_3O_4$$
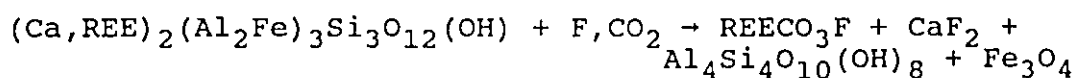
In the Lake zone, only the allanite-(Ce) and bastnäsite-(Ce) are noted in intimate association with each other, presumably the fluorite, magnetite and kaolinite group mineral have formed but migrated elsewhere. Of these minerals, only the kaolinite group mineral has not been identified within the Lake zone. Plate 20 illustrates an example of bastnäsite-(Ce) invading allanite-(Ce).

Unlike the manganoan allanite-(Ce) detected within the nepheline syenite, these particular grains contain less than 1 wt% Mn which, along with negligible Zn, likely accounts
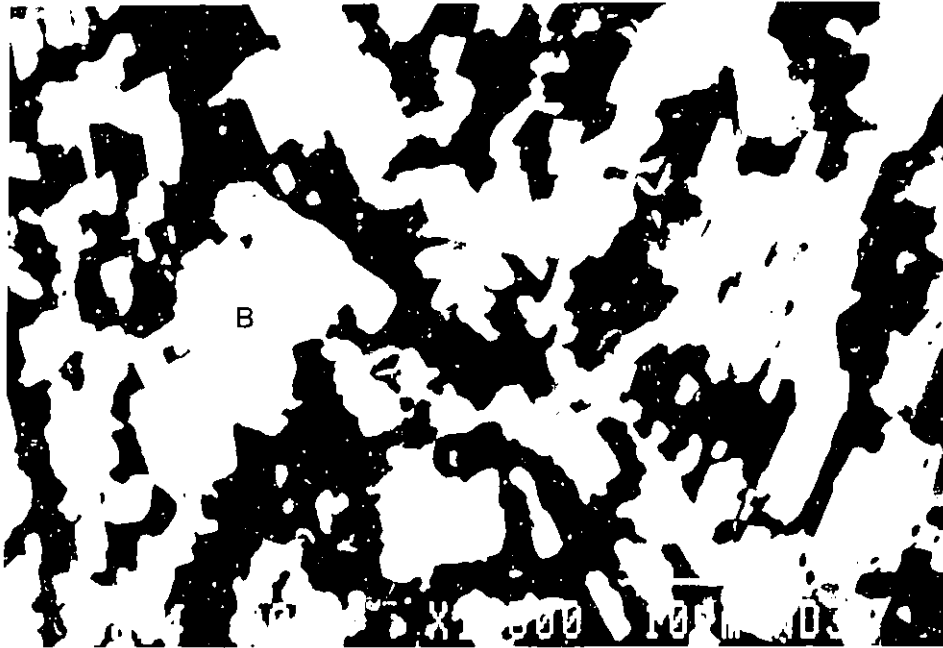
Plate 20. Secondary electron image of bastnäsite-
(Ce) replacing allanite-(Ce). Scale bar
is 10 μm.

for the slightly different pleochroic scheme in the Mn-rich

varieties. According to Deer et al., (1986), Mn^{2+} should

substitute in the irregularly-shaped 8-fold Ca sites and

because of that, the sum of Ca plus Mn should be constant.

But in Lake zone grains, low Ca seems to correspond to low

Mn while the Mn-rich varieties in the silica-undersaturated

rocks contain high Ca. Therefore, Mn must not be

substituting in the larger Ca sites but in the Al sites

(i.e., Al^{VI}) independent of the chains of Al octahedra

(i.e., Al^{IV}) probably as Mn^{3+} cations. This appears to be

the case as Al is low in all examples (see anal. 70 and

71).

The next most common REE-bearing mineral belongs to the

bastnäsite group. The group consists of: bastnäsite (La, Ce

or Y varieties), hydroxylbastnäsite-(Ce), parisite (Ce or

Nd), röntgenite-(Ce) and synchysite (Ce, Nd or Y). In the

Lake zone only bastnäsite-(Ce), parisite-(Ce) and

synchisite-(Ce) have been identified with certainty. Like

allanite-(Ce), this group is also found as two distinct

crystal types. In the first, bastnäsite-(Ce) appears as

blocky, hexagonal crystals either as homogeneous grains or

as polycrystals intergrown with parisite-(Ce) whilst

parisite-(Ce) tends to form bladed or acicular crystals and

is more commonly Fe stained or inclusion-rich. The second

type is found interstitially to type 2 zircon, in-filling

the voids left by the earlier forming zircon and

fergusonite-(Y). It is mostly Ca-poor (parisite-(Ce)) with minor intergrowths of bastnäsite-(Ce).

A third mineral in the bastnäsite group has been detected. It contains more Ca than either bastnäsite-(Ce) or parisite-(Ce) and its identity is likely synchisite-(Ce). Like the bastnäsite-(Ce), it is found to replace allanite-(Ce) in small quantities along cracks and cleavage planes (plate 21). Such a reaction has been described by Deer et al., (1986).

Chemically, the group is enriched in the LREEs with Ce and La comprising about 90% of the total REE values (EDA data). In addition to Ca, the only other cation of note is Fe which is usually found along the edges of crystal boundaries and is a result of weathering or alteration. Generally, the compositions, distribution and modes of occurrence of this group are similar to those found in T zone rocks. The reader is therefore referred to the work completed by de St. Jorre (1986) for more information.

The final mineral of importance is monazite-(Ce). Although not as common as allanite-(Ce) or the bastnäsite-(Ce) group minerals, it does constitute a major source of REEs within the Lake zone. The mineral is generally found as i) euhedral, acicular crystals scattered throughout the Lake zone on the order of 200-500 μm or more commonly ii) as subhedral to anhedral, blocky crystals generally associated with fergusonite-(Y) and zircon (plate 22). The grains are optically similar to bastnäsite-(Ce) having high positive
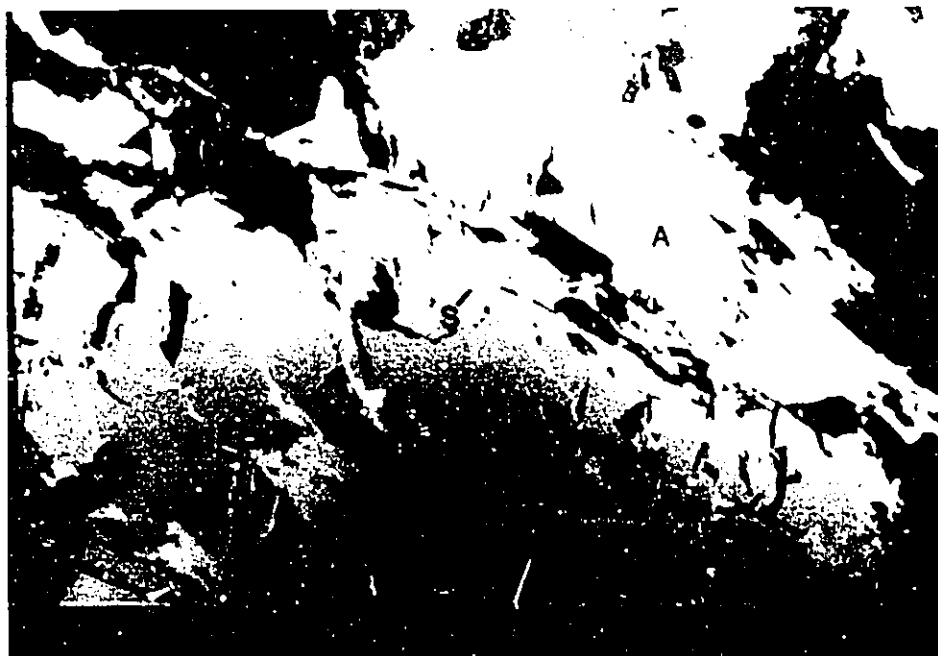
Plate 21. Backscattered electron image of synchisite-(Ce) invading allanite-(Ce). Scale bar is 20 μm.
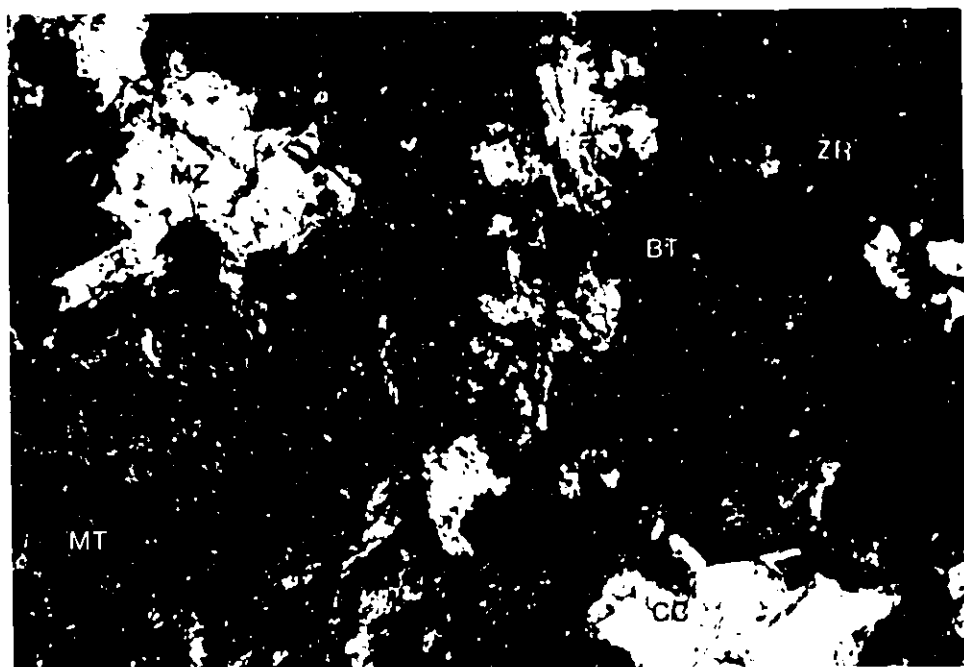
Plate 22. Photograph of monazite-(Ce) in a matrix of carbonate and biotite. Note the metamict zircon. Magnification X185, XPL

relief, clear, subhedral grains and a nearly uniaxial positive interference figure. Generally, monazite-(Ce) lacks any replacement or alteration features although some replacement of bastnäsite-(Ce) by monazite-(Ce) was noted (plate 23). For such a replacement to occur, an influx of phosphorus would be needed as indicated in the following general reaction:

$$PO_4^{3-} + Ce(CO_3)F \rightarrow CePO_4 + CO_3^{2-} + F^-$$
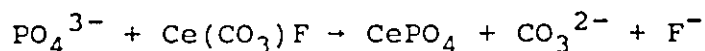
In the presence of apatite, bastnäsite-(Ce) may possibly be resorbed, resulting in monazite-(Ce), calcite and fluorite crystallisation.

Isolated cases of monazite-(Ce) in fluorite-rich albitic rocks and as small-scale veins have also been found. In the albitic rocks, fluorite is intergrown with monazite-(Ce) as blebs or stringers on the scale of 5-10 μm while monazite-(Ce)-rich veins on the scale of 50-100 μm have been noted to cross-cut the same rock-types. The veins contain bent, elongate, cigar-shaped monazite-(Ce) crystals together with biotite and minor calcite. Analyses 77 and 78 shows the monazite-(Ce) to be rich in Ce, La and Nd with minor Pr and Sm.

YTTRIUM

Probably the most economically important element is Y and hence an extensive search for this element was made. As discussed in the Nb section, fergusonite-(Y) (and possibly zircon) are the minerals principally responsible for overall
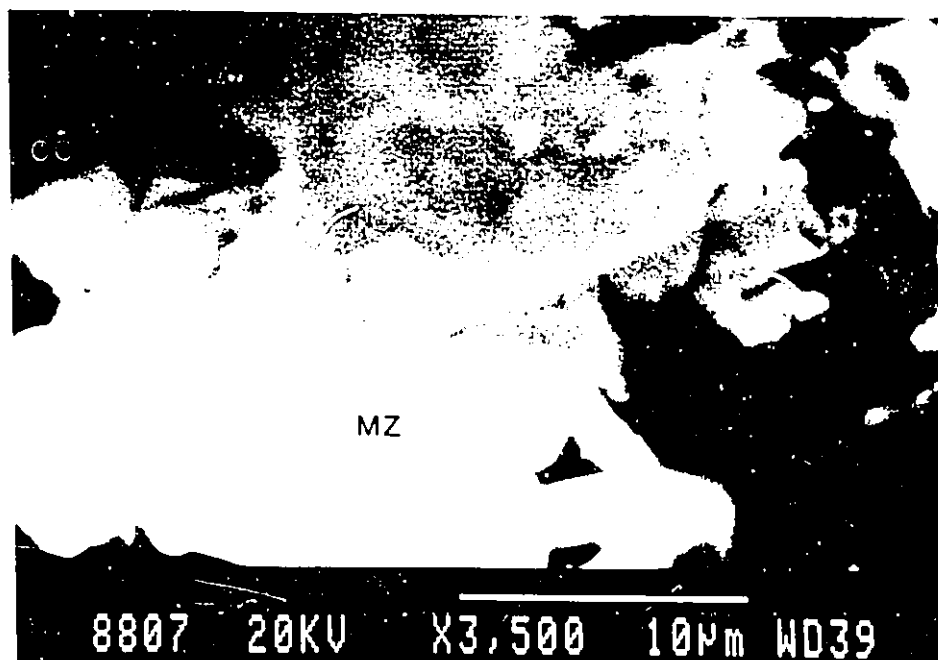
Plate 23. Secondary electron image of monazite-
(Ce) replacing bastnäsite-(Ce). Scale
bar is 10 μm.
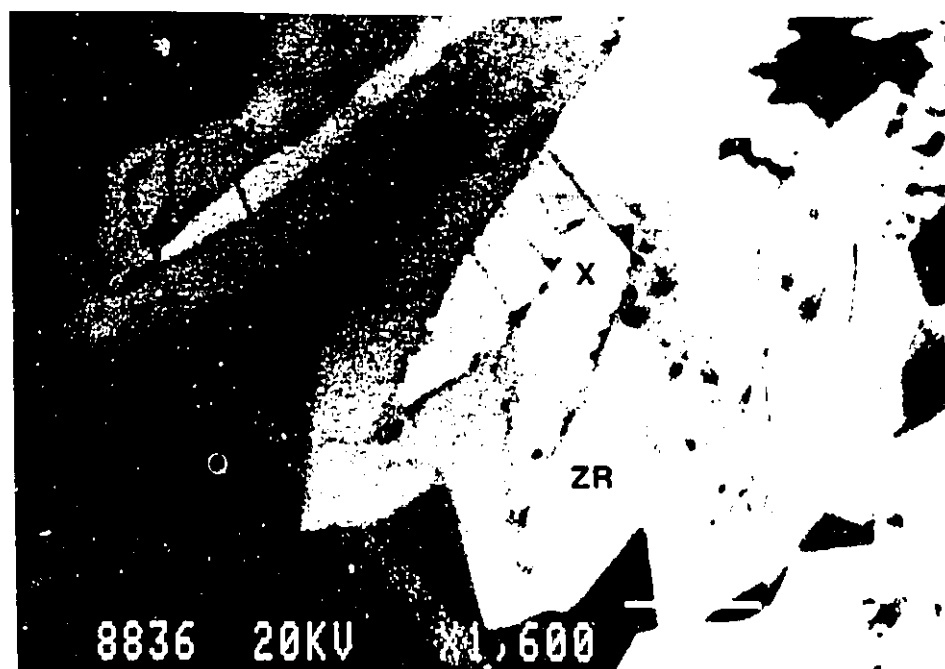
Plate 24. Secondary electron image of zircon over-
growths on xenotime-(Y). Scale bar is 10 μm.

Y values. The fergusonite-(Y) contains upwards of 25 wt%
Y_2O_3 whilst the zircons have, as noted earlier, Y_2O_3 values
up to 2.5 wt%. These two minerals must therefore account
for the majority of Y within the Lake zone.

However, not all Y resides in the above mentioned
minerals. Xenotime-(Y) [YPO_4] is not common but has been
found scattered throughout the Lake zone as small (20-50
μm), euhedral crystals. All grains are overgrown by a rim
of zircon 5-10 μm thick (plate 24). This close association
of xenotime-(Y) with zircon is not unusual as both are
isostructural and have similar cell dimensions (zircon:
a=0.659 nm, c=0.599 nm; xenotime: a=0.689 nm, c=0.604nm).
In the photo, note the well-developed cleavage in xenotime-
(Y), a property useful in identifying xenotime-(Y) from
zircon. The crystals generally are found in a matrix of
quartz and tend to grow as small clusters. Chemically,
minor Gd, Dy and possibly Er has been detected (EDA data).

V SILICA-UNDERSATURATED ROCKS

INTRODUCTION

An important part of the Blachford Lake intrusive complex is a substantial body of nepheline syenite (plate 25) found at depth. It was discovered in the winter of 1986/87 and at the time, was thought to be of minor importance. However with time, its importance was realised as at least 200 m of the rock was discovered to exist immediately beneath the Lake zone on the north shore of Long Lake. Subsequent inspection of other drill cores delineated minor amounts of nepheline-bearing rock in holes along the eastern margin of Thor Lake and of altered material in at least 9 other drill holes. In view of these occurrences, new ideas about the deposit's origins, and indeed of the complex in general, must be considered.

PHYSICAL EXTENT

The discovery hole, 85L-6, was drilled to a depth of 401 m and contains the greatest variety of silica-undersaturated rocks. The uppermost 200 m of the hole contains mineral and alteration assemblages typical of Lake zone material, that is, abundant quartz-ankerite-hematite-replaced pyroxene and amphibole crystals, an albitised groundmass, some large, and in most cases, recrystallised K-feldspar crystals, large scale hematisation and late-stage carbonate and fluoride minerals. Economically, this hole contains important minerals, such as zircon, bastnäsite-

74

75

Plate 25. Photograph of typical nepheline syenite
drill core. Tan-coloured mineral is neph-
eline, green mineral is aegirine and white
mineral is feldspar. Pencil is 14 cm.
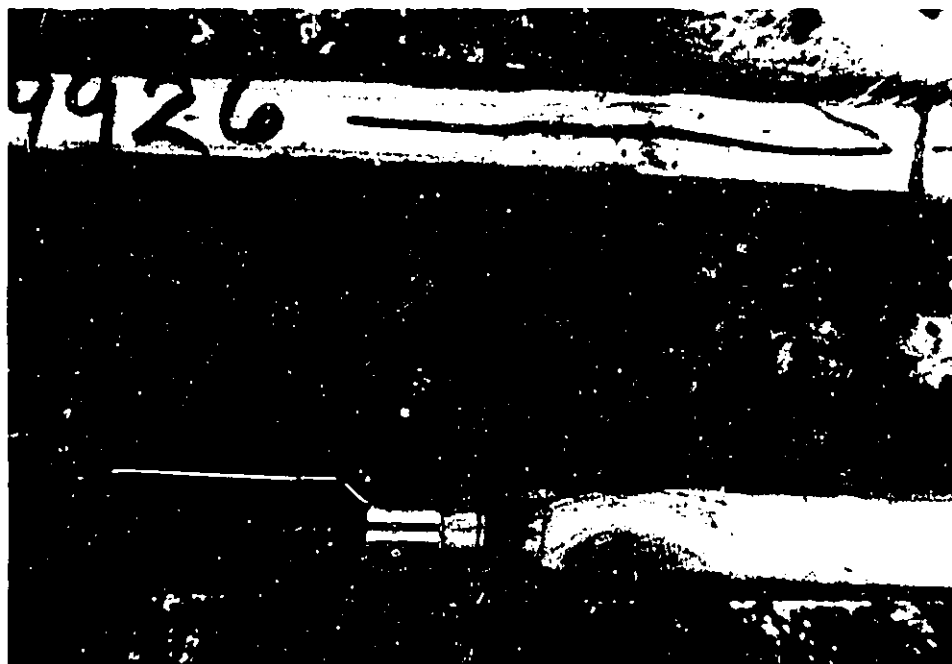
Plate 26. Photograph illustrating the 'spotted'
syenite. Clear material is feldspar and
green mineral is aegirine.

(Ce), ferrocolumbite and allanite-(Ce), which are also found in other holes, but not in significant quantities.

At about the 150 m level relatively fresh aegirine crystals first appear followed closely by the appearance of a 'spotted' syenite (plate 26). The spots are generally 0.5-1 cm in size and were most likely nepheline crystals. This porphyritic rock continues until, at about 235 m, relatively fresh nepheline phenocrysts can be identified with certainty. The nepheline has altered to a fine grained mineral mass whose colour varies from pinkish-red to green. The unique appearance of such grains makes the tracing of original nepheline grains back to the 200 m level possible. In any case, pervasive hematisation and albitisation obscures the contact between nepheline syenite and overlying Lake zone material.

In addition to drill hole 85L-6, numerous other holes were found to contain nepheline, albeit in minor amounts and in rather altered states. Table 4 lists all the holes in which altered nepheline syenite has been found plus the depths at which these rocks were first encountered. In the

TABLE 4
NEPHELINE SYENITE OCCURRENCES

Hole #	vertical depths (metres) from	to		Hole #	vertical depths (metres) from	to
80-7	137	152 (EOH) *		85L-6	128	402 (EOH)
80-8	140	152 "		88L-8	158	305 (diabase)
80-10	91	152 "		88L-11	137	152 (EOH)
80-11	137	152 "		88L-25	168	180 "
84L-5	119	213 "		88L-26	110	152 "

* end of hole

only other hole in which fresh nepheline is found, 84L-5,
fresh aegirine begins at approximately 170 m while the
altered nepheline, now as reddish spots, appears near the
bottom of the hole at about 180 m and continues as the
'spotted' syenite to the end of the hole. Intermittent
fresh material occurs but for no great lengths. In 85L-6,
the same porphyritic textures are seen in the 170 to 200 m
interval and not until about the 245 m mark do large volumes
of fresh nepheline syenite begin to appear. Hole 84L-5 is
over 1000 m from 85L-6 and yet the extent of nepheline
syenite in both corresponds very well. Table 4 shows most
holes are remarkably consistent in terms of depths in which
silica undersaturated rocks are first encountered.

It is thought that nepheline syenite would be found
beneath all holes drilled within the Lake zone and probably
even outside the mineralised area. It should be noted that
these nepheline-bearing rocks are located almost directly in
the centre of the circular Grace Lake granite-Thor Lake
syenite system. Figure 6 displays the subsurface extent of
the nepheline syenite as it is presently known. Holes
drilled outside this area are either too shallow or do not
appear to contain any silica-undersaturated rocks.

ROCK TYPES AND DESCRIPTIONS

Drill hole ⌐L-6 is of primary concern here and in it,
the bottom 215 m display a complex region of variable
textures and lithologies. From 162 to 238 m, the rock

Figure 6   Spatial relationship between zones of mineralisation and silica-
undersaturated rocks

changes from a spotted aegirine syenite to horizons that are heavily hematised with zones of what appear to be, but is unlikely, serpentine. Certain areas also contain abundant albite surrounding phenocrysts of reddish nepheline. Fresh nepheline first appears at 236 m amongst a matrix of well formed aegirine and albite. Specular hematite and altered nepheline still appear after this point but only intermittently. Pristine rock is, for the most part, composed of nepheline, aegirine, albite, K-feldspar and analcime (plate 25). Other minerals found include: pectolite, natrolite, mesolite, apatite, fluorite, sodalite, hydrohetaerolite, a Ca,Zr-silicate, britholite-(Ce) and cerianite-(Ce). Found within the silica-undersaturated rocks are, in places, extensive areas of interstitial material containing, among other minerals: andradite, zircon, manganoan allanite-(Ce), willemite, calcite and manganoan pectolite. The tan coloured region of plate 27 is one such area.

Nepheline, as mentioned earlier, appears as anything from unaltered, steely-grey crystals to a green, powdery material, to any shade of flesh, pink or red depending on the severity of mica and clay mineral replacement. The nepheline is subhedral to euhedral and commonly 0.5-1 cm in size although sometimes reaching 5 cm in length. A common feature noted both microscopically and megascopically is a rim of translucent analcime formed as a result of nepheline
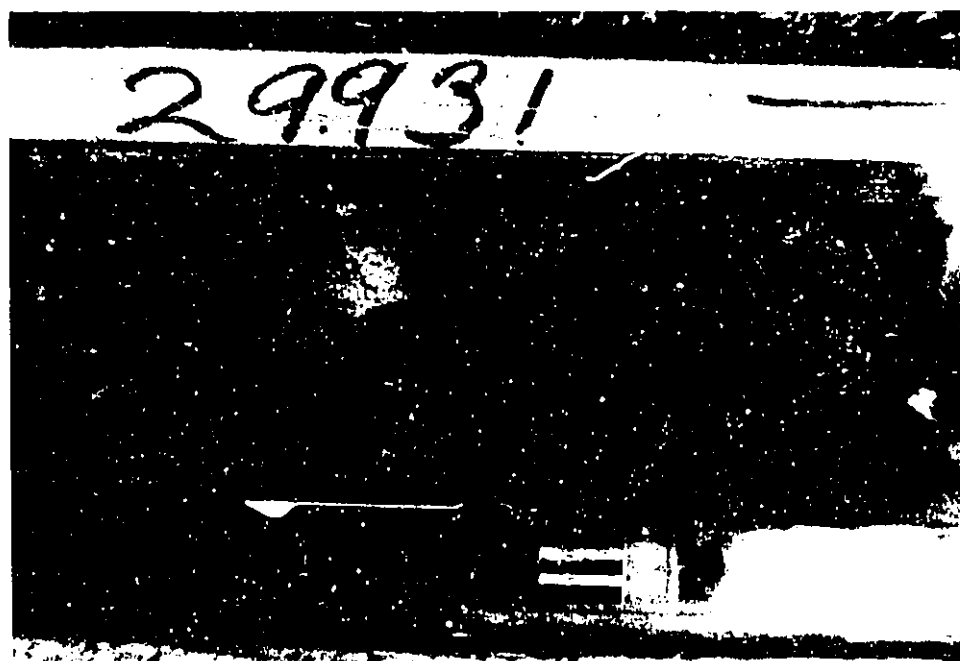
Plate 27. Photograph showing the tan-coloured
regions (interstitial to white nepheline
crystals in this photo) rich in andradite,
allanite-(Ce) and zircon.

reacting with quartz and albite in the presence of water as illustrated in the following reaction:

$$NaAlSiO_4 + NaAlSi_2O_6 + SiO_2 + 2H_2O \rightarrow 2NaAlSi_2O_6:H_2O$$
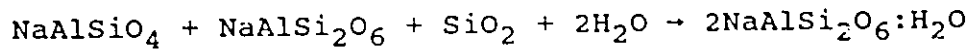
Saha (1961) emulated this reaction in the laboratory and calculated a temperature regime of approximately 550-600°C for the co-existence of nepheline and analcime. Not all nepheline is found to be rimmed with analcime, as zones with well lineated aegirine and albite crystals contain unaltered and unrimmed nepheline grains. These particular rocks are believed to be late stage dykes and/or sills that cross-cut previously emplaced nepheline syenite. Well defined contacts, extreme lineation of both feldspar and pyroxene crystals and the lack of hematisation and albitisation all suggest these rocks to be late stage dykes. At least four such dykes or sills are found. Other areas contain pegmatitic pods of aegirine and nepheline. These areas have aegirine crystals of 3-5 cm in size and massive areas of translucent, smokey grey nepheline 10-15 cm in length.

Most of the silica-undersaturated rocks may simply be termed nepheline syenite or nepheline monzosyenite (IUGS classification) but in some cases the nepheline and pyroxene contents are high enough to use the term ijolite or feldspathic ijolite (LeBas, 1977). Other rock types found include pectolite-bearing syenite where pectolite comprises upwards of 15 modal % of the rock and a sodalite syenite with enough feldspathoid minerals to be termed an urtite.

ROCK FORMING MINERALS

Four minerals have been considered as being rock forming: albite, K-feldspar, aegirine and nepheline. Others such as sodalite and analcime are common in specific areas but are not considered important to the overall composition of the nepheline syenite. Table 5 is a generalised paragenetic scheme for these and other minerals found in the silica-undersaturated rocks. What follows is a physical and chemical description of these minerals.

Unaltered nepheline, as mentioned earlier, is found as sub-translucent greyish crystals. Slightly altered grains have a fleshy coloured appearance and if alteration is more severe, red or green colours predominate. Generally, the blocky nepheline crystals vary in size from 0.5 to 2 cm, do not display cleavage and if fresh, exhibit a greasy lustre. In thin section, the larger crystals display poikilitic textures, enclosing small grains of aegirine and albite.

Nepheline generally does not cathodoluminesce but it does, in areas, display blue colours especially in thin rims at the interface between analcime and nepheline (plate 28). By analogy with blue cathodoluminescence of albite rims in T zone rocks, it was suspected that these blue rims might result from minor amounts of Ga (de. St. Jorre and Smith 1988). Subsequent work found neither Ga nor any other activator element. As an alternative, Mariano (pers. comm.) has suggested the existence of a thin rim of leucite

TABLE 5
PARAGENESIS OF THE MINERALS WITHIN THE
SILICA-UNDERSATURATED ROCKS

```
nepheline                   -----
microcline          ----
albite              ----
analcime                        ------
aegirine            ----
arfvedsonite        ----
sodalite                    ----                        --
pectolite                       ----              ---
wollastonite            ?--?
zeolites                                --
muscovite                               --
andradite                                     ----
allanite-(Ce)                               ----
zircon                                  ?----
calcite                                     -------------
fluorite                                    -------------
ferrobustamite      --
Ca,Nb silicate      ---
willemite                               ?--
thorite             --
cerianite-(Ce)                          ?--
hydrohetaerolite                        ?--
Ca,Zr silicate                          --
britholite-(La)                         ?--
britholite-(Ce)     ---
apatite                                 ?--
```

TIME ---------->

Plate 28. Blue cathodoluminescent rims separating nepheline from analcime. Note the calcite (red), feldspar (yellow), pectolite (bright yellow) and willemite (g---en). Magnification X50

(luminesces a blue colour) separating the nepheline from the analcime. Close inspection of the regions of blue cathodoluminescence reveals that only the areas of incipient nepheline alteration to analcime luminesce, implying a possible structural effect analogous to the generation of colours due to a colour centre.

Microprobe analyses of fresh nepheline (appendix 1 anal. 5 and 6) show it to be typical of many nephelines found in silica-undersaturated rocks. Conversely, altered grains show varying amounts of hydration and alkali element depletion (anal. 7-10). A slightly altered nepheline (anal. 7), as indicated by creamy brown or pinkish colouration in hand specimen, yielded slightly lower Na_2O and K_2O values, similar SiO_2 and Al_2O_3 values and a higher degree of hydration (low total). More altered grains tend to be red in hand specimen and are characterised by substantial Na_2O and minor K_2O depletion plus moderate to intense hydration (anal. 8 and 9). Severely altered grains (anal. 10) are dark green in colour and no longer contain any Na. FeO and MgO contents are up at the expense of Al and there is significant K enrichment.

Aegirine occurs as dark green, elongate or acicular crystals throughout the nepheline syenite. Grain size is highly variable but generally on the scale of 0.5 to 1 cm. In some instances, aegirine occurs as minute, acicular crystals (25-40 μm) included within K-feldspar or as vein material adjacent to K-feldspar or albite. Almost all

aegirine is unaltered, as shown by the chemical analyses in appendix 1 (anal. 11 and 12). In pristine samples, Al_2O_3 is usually less than 2 wt% as is CaO and MgO. Interesting to note are the unusual ZrO_2 values (anal. 11). All aegirines examined contain, on average, 4000 ppm ZrO_2 which probably accounts for most of the known Zr within the nepheline syenite (Ca-Zr silicates are rare). In the aegirine crystal structure, Zr resides in the 4-fold Fe^{3+} sites as a result of coupled substitution with Fe^{2+}, Mn and Mg. Duggan (1988) found that with small amounts of late-stage pyroxene formation, high magma peralkalinity and low oxygen fugacity, aegirine can accomodate up to 14.5 wt% ZrO_2. Even though aegirine is very common in the Lake zone, ZrO_2 values are relatively low, therefore, economic concentrations of Zr do not appear to exist.

Plagioclase is very albitic (appendix 1, anal. 2) and similar in appearance to Lake zone albite. However, this albite tends to be more acicular and is found in various colours including yellow, red and light green. Albite in the nepheline syenite tends to be colourless or sometimes creamy-white due to incipient alteration to fine grained micaceous material. Cathodoluminescence in albite is shown by dark red colours probably due to minor concentrations of Fe^{3+} activators. Multiple twinning is common whereas in the mineralised zones, albite is rarely twinned. This feature likely reflects the absence of Na metasomatism in the

undersaturated rocks and may point to slightly higher temperatures of crystallisation.

Petrographically, K-feldspar is difficult to distinguish from albite. It is always untwinned therefore differentiation of the two is based on differences in grain size and shape. K-feldspar is generally larger, on the order of 0.5 to 2 mm, and blockier than the co-existing albite. Optically, the alkali feldspar displays neither twinning (simple or multiple) nor unmixing in the form of perthites. Therefore, this rock is, as also noted within the Lake zone, a subsolvus (wet magma) syenite which contrasts with the neighbouring perthite-rich hypersolvus Thor Lake syenite and Grace Lake granite. The K-feldspar is probably microcline as 2V(gamma) is nearly 90°.

ACCESSORY MINERALS

Many accessory minerals have been found and the following account describes the more significant or unusual ones. Many of these minerals are found forming small, brownish regions disseminated throughout the core as previously outlined in plate 27. These areas contain significant concentrations of rare-metal-bearing minerals.

Analcime is found almost exclusively to rim nepheline although occasionally it occurs as independent blocky, white crystals. Commonly, anomalous first order grey birefringence is displayed, due to what Coombs (1955) has described as distortion in the lattice from Si-Al

disordering. This anomalous birefringence is especially noticeable in material not associated with nepheline and in those grains which display well developed 'tartan' twinning (twinned on {001} and {110}) (plate 29). Several analyses have been performed on the analcime (appendix 1, anal. 25 and 26) and all appear to conform to analyses in the literature.

Another common accessory mineral is pectolite. Megascopically, it appears as large, creamy white material usually lacking any discernible crystal shape. It is a late-forming mineral and generally occurs interstitially to aegirine and nepheline. Some samples, such as at 340 m, contain upward of 15-20 modal % pectolite. In thin section the mineral is commonly found to have formed in the voids between aegirine and nepheline (plate 30), however, in one instance it occurs as blocky, euhedral grains with subsequent replacement by fluorite, natrolite and mesolite. Pectolite was also found within the nepheline syenite dykes or sills but only as an accessory mineral (3-5 modal %). The mineral cathodoluminesces a brilliant yellow which is believed to be due to Mn^{2+} activators.

Microprobe analyses performed on pectolite showed that certain grains have significantly different quantities of Mn and Ca. This is because Mn substitutes freely for Ca in 6-fold sites in the pectolite $[NaCa_2Si_3O_8OH]$-serandite $[Na(Mn,Ca)_2Si_3O_8OH]$ series. Most pectolite grains have MnO_2 values less than 5 wt% whereas manganoan pectolite is
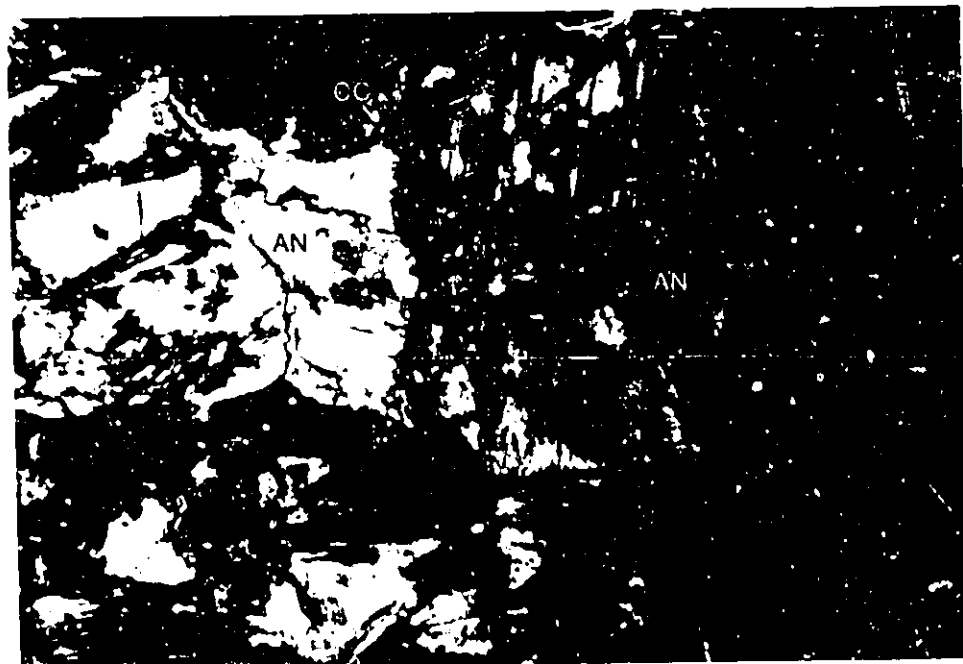
Plate 29. Photograph displaying complex twin-
ning in analcime. Magnification X62,
XPL

Plate 30. Interstitially forming pectolite
commonly surrounds aegirine and feld-
spars. Magnification X62, XPL

defined as those grains with significant Mn replacement of
Ca but at values less than 50 mol. % Mn/[Mn+Ca]
(Schaller,1955). When this ratio is greater than 50 mol. %
the mineral is called serandite. Generally, grains with
high Mn contents (appendix 1, anal. 31) are found associated
with REE-bearing minerals such as britholite-(Ce) whereas
the majority of grains are typified by analyses 29 and 30.
All grains appear to be homogeneous with no evidence of Mn
zonation.

A mineral commonly found in alkaline igneous rocks
especially as a result of metasomatic alteration or
fenitisation is andradite and the Ti-rich variety, melanite.
Most classic fenite localities, such as Fen, Norway, Alno,
Sweden and Usaki, Kenya, contain some andradite and/or
melanite. The Blachford Lake intrusive complex can now be
added to such a list.

In these rocks, andradite has been found in at least 10
locations. In every case, it is associated with a variety
of other minerals in the previously mentioned brown clots or
'pockets' interstitial to aegirine and nepheline. The
andradite is euhedral (dodecahedral), blocky in nature,
shows anomalous first order grey or in some instances yellow
birefringence and commonly displays sector zoning (plate
31). According to Deer et al., (1982), anomalous
birefringence and sector twinning are relatively common in
the grandite series of garnets (grossular-andradite) of
which there is plenty in these rocks (appendix 1, anal. 21-
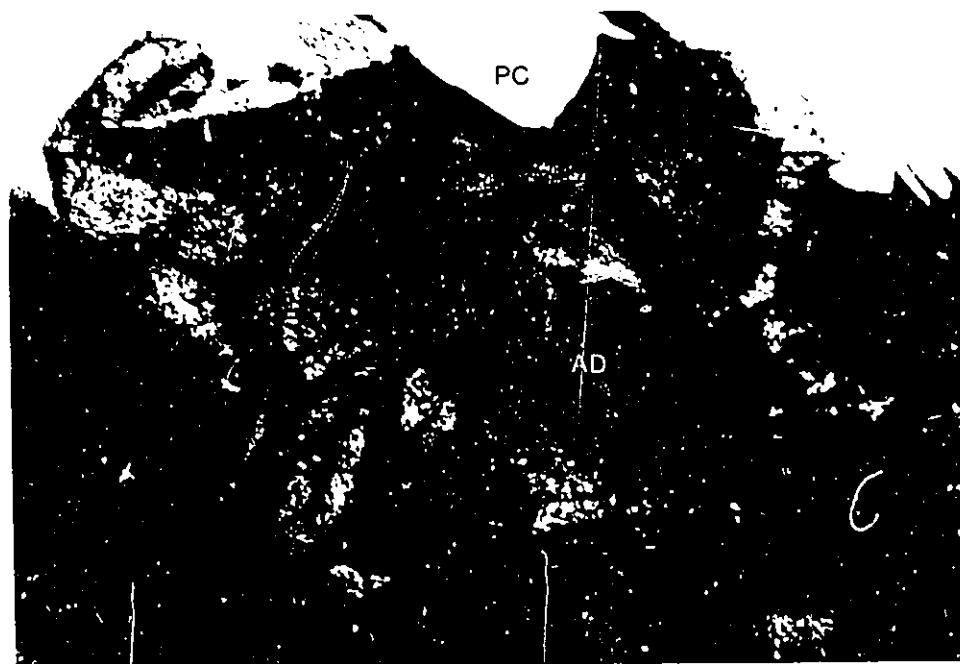
Plate 31. Andradite displaying anomalous birefrin-
gence and sector twinning. These grains
are found lining a partially replaced
wollastonite grain. Magnification X185,XPL

Plate 32. Grandite garnet in a matrix of calcite and
fluorite. Magnification X185, PPL

24). The sector twins are a response to internal growth strain but the birefringence is more problematic. A number of ideas have been proposed but the most recent (and most likely) was given by both Takeuchi (1986) and Hirai and Nakazawa (1986). Because the grandite garnets consist of alternating Fe^{3+} and Al octahedra stacked into 'rods', order-disorder between these two nonequivalent sites may ensue. In this manner, the ordering of Fe^{3+} and Al, analogous to the ordering of Si and Al in alkali feldspars, will cause distortion of the cubic lattice especially if the garnet contains approximately equal molecular proportions of Fe^{3+} and Al. The more complete the ordering, the more the deviation from cubic symmetry. Upon cooling, the following sequence may result: cubic ($I4_1/a32/d$) → orthorhombic (Fddd) → monoclinic (I2/c) or triclinic (I1). Takeuchi (1986) determined that a temperature of $750^{\circ}C$ and a pressure of 1 kb was needed for the inversion of cubic to non-cubic grandite.

In plate 31 note that the andradite is replacing a pre-existing mineral, probably wollastonite, which is in turn being replaced by pectolite. Gustafson (1974) described the replacement of wollastonite by andradite as follows:

$$9CaSiO_3 + 2Fe_3O_4 + 1/2O_2 \rightarrow 3Ca_3Fe_2Si_3O_{12}$$
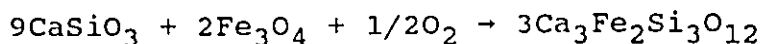
This reaction was found to occur at approximately $750^{\circ}-800^{\circ}C$ with a pressure of 2 kbars.

In some areas, nucleation sites are plentiful enough to cause the andradite to mesh together into large masses. In

this situation the crystals tend to be isotropic reflecting a low grossular component (appendix 1, anal. 21 and 22). Analyses have shown that very little Ti is found in any of the grains (anal. 23 and 24). WDS crystal scans using the electron microprobe for the HREEs and Y did not detect any of these elements even though they commonly substitute into the garnet structure.

Closely associated with the blocky andradite is an acicular, Al-rich andradite(?) (appendix 1, anal. 23 and 24). It displays similar colour, relief and birefringence to the blockier andradite yet has an entirely different crystal habit (plate 32). It is elongate to acicular, averages 50-100 μm in size, contains numerous feather-like inclusions and, like the andradite, tends to form as crystal masses. Either this material is not andradite and is, in fact, an unidentified Ca-Fe silicate with a composition similar to garnet, or alternatively the material is andradite that has pseudomorphed a pre-existing acicular mineral. The second possibility seems more likely as sector zoning is found to exist within the mineral. Also, the structural formula of the acicular andradite conforms very well with an Al-rich andradite. To identify this Al-rich garnet with certainty an X-ray diffraction pattern should be obtained, but due to the mineral's small size and intimately associated neighbours such tests would be very difficult.

Two other minerals are found to be closely associated with the andradite: zircon and manganoan allanite-(Ce).

Zircon, the first of these three minerals to form, is found as euhedral, partially metamict crystals, 50-100 μm in size or as larger (150-500 μm), subhedral to anhedral, entirely metamict crystals. The smaller grains have metamict cores and are surrounded by andradite while the larger ones are not associated with any particular mineral and are randomly oriented throughout the 'pockets'. The surrounding minerals, mostly andradite, sodalite and manganoan allanite-(Ce), contain no evidence of radiation damage even though darkened lines perpendicular to the crystal faces of the zircon are found. Bromley (1964) has suggested that these lines indicate the tracks of alpha particles ejected during the decay of U. The Mn and Zn contents of a few zircon grains were investigated and some grains were found to contain upwards of 2000 ppm Zn and 1500 ppm Mn.

Neighbouring manganoan allanite-(Ce) appears to have been partially replaced by andradite and to have formed around pre-existing zircons. The allanite is typically tabular, sometimes anhedral and has a pleochroic scheme different to that seen in Lake zone material: N_a= blood red, N_b= brownish red and N_c= light green. The intense green colour seen in Lake zone material is not present. This is probably due either to the fact that these grains contain more Mn than Fe (appendix 1, anal. 70) or else that, in most cases, the presence of significant quantities of ZnO; upwards of 6 wt% (anal. 71) have been found. These particular examples are the most Mn- and Zn-rich allanites

found anywhere. It is known that the variation of Mn and Fe in mafic minerals of alkaline complexes are sensitive indicators of oxidation-reduction conditions (Bonin and Giret, 1985). In this case allanite-(Ce), present in both the Lake zone and nepheline syenite, can be used as an indicator mineral in the same manner as olivines and clinopyroxenes. Bonin and Giret (1985) found that Mn-rich olivines tend to crystallise in silica-undersaturated rocks and that in an oxidising environment, Mn-rich minerals were more stable than their Fe-rich equivalents. The fact that allanite-(Ce) in these rocks contain more Mn than those in the Lake zone indicates that these incompatible-element-rich regions have formed under more oxidising conditions (see the hydrohetaerolite analysis) and that Fe^{2+} = Mn is sensitive to the silica activity.

Commonly, manganoan allanite-(Ce) is replaced by andradite (plate 33) and if calcite and fluorite are added to the system, the following reaction may result:

$$CaF_2 + 2CaCO_3 + (Ca,Ce)_2(Al,Fe)_3Si_3O_{12}(OH) \rightarrow 2CeCO_3F + H_2O$$
$$Ca_3Fe_2(Si,Al)_3O_{12}$$
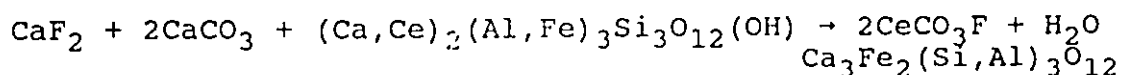
As a result of such a reaction, bastnäsite-(Ce) (±parisite-(Ce)) may form. Reactions similar to this are common when metasomatic fluids, such as those found in skarns, are involved. The T-Xco_2 conditions of these and other reactions involving andradite and epidote have been investigated by Taylor and Liou (1978). One such reaction involving epidote (allanite-(Ce)) plus CO_2 to give grandite,
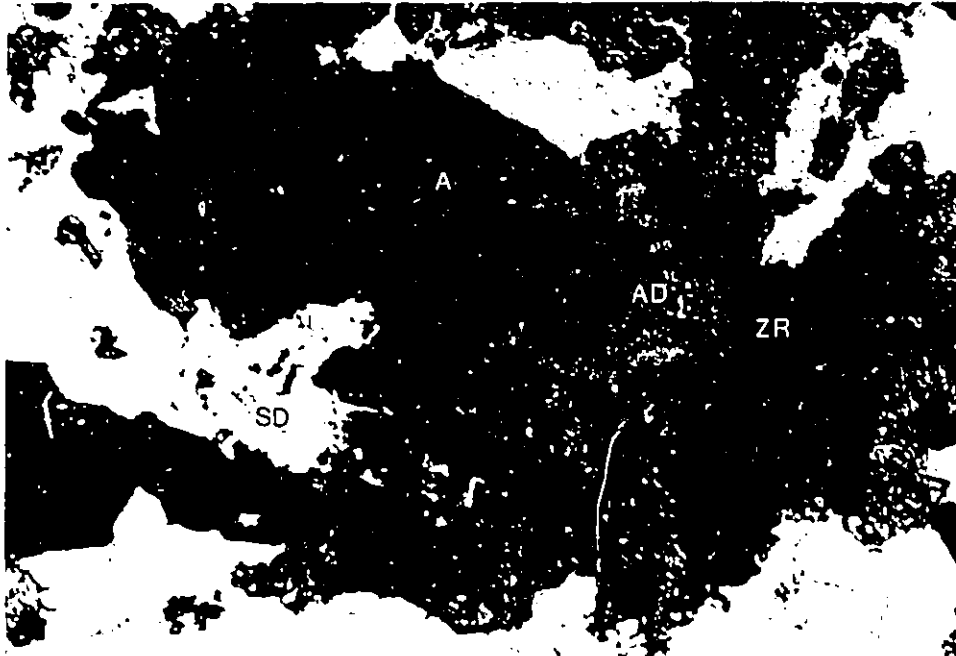
Plate 33. An example of andradite replacing mangan-
oan allanite-(Ce). Note the zonally meta-
mict zircon in the upper left. Magnifi-
cation X75, PPL
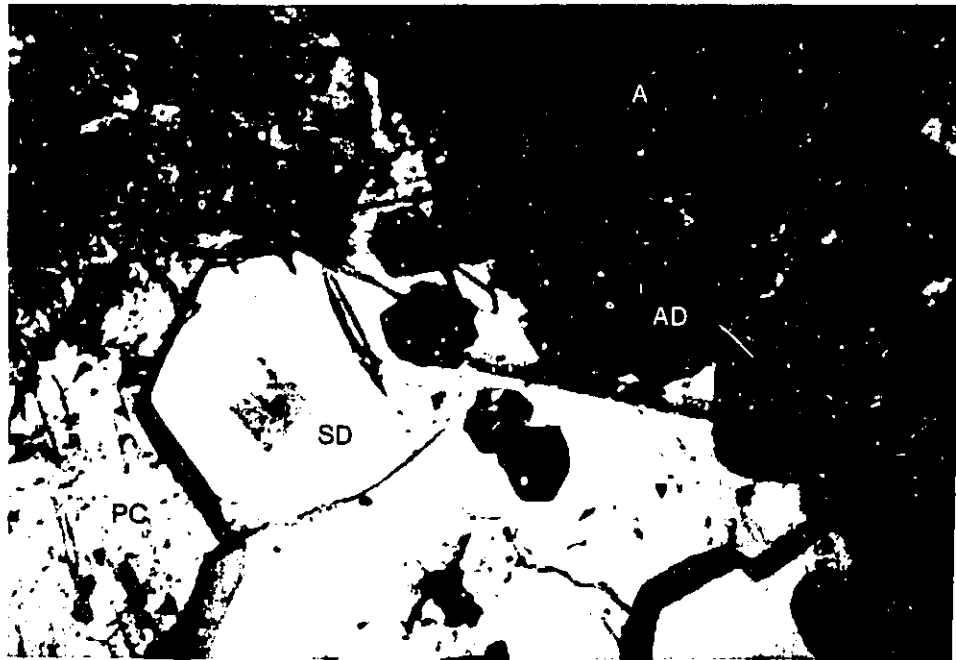
Plate 34. Pink colouration in sodalite resulting
from electron beam damage. Magnifi-
cation X300, PPL

calcite and water, similar to the above reaction, occurred at 400-500°C.

Subsequent to the crystallisation of these minerals is late-stage infilling by pectolite followed by sodalite, analcime, fluorite and calcite. The pectolite in these particular samples is very fibrous and appears only in vugs or replacing grains of what is probably wollastonite. The fluorite appears as small (5-20 μm), sub-spherical, purple grains set in a calcite matrix (see plate 31) possibly indicative of immisicibility between CO_2- and F-rich solutions. Minor amounts of willemite were found as clusters of small crystals near the andradite-rich clots. Their appearance is not that surprising as elevated Zn values have been found in the nearby manganoan allanite-(Ce) and in co-existing hydrohetaerolite.

At this point a few general observations may be made about these patches of exotica. First, all minerals in these clots are, with the exception of zircon, of low to moderately low temperature origins. Second, these regions are rich in incompatible elements such as Mn, Zn, Th, LREEs and Zr. Third, relatively high oxygen fugacities must have existed. And fourth, numerous low temperature metasomatic reactions, due in part to the high concentrations of H_2O-, CO_2-, Cl- (sodalite) and F-bearing fluids, have occurred. All these factors suggest that late-stage enrichment of incompatible elements and subsequent subsolidus mineral reactions or metasomatism was prevalent within the nepheline

syenite. Therefore, in addition to the host peralkaline granite-syenite system, these silica-undersaturated rocks may have also contributed to rare-metal enrichment within the Lake zone. Furthermore, other accessory and rare-metal-bearing minerals exist independently of these clots and remain to be discussed.

Sodalite is, in places, a very common constituent. First, it occurs frequently within the andradite-rich regions and second, at certain depths (i.e., at 319 m in hole 85L-6), it is abundant enough to be a rock-forming mineral, comprising up to 40 modal % of the rock. In hand specimen, it appears similar to fluorite although its orange fluorescence and greyish colour are characteristic. Under the electron beam, the sodalite was noted to turn pink in colour (plate 34). Waychumas (1988) desribes the phenomenon as resulting from the change of S_2^{2-} ions to S_2^- ions and subsequent trapping of the excited electron by a Cl^- vacancy site. The two ensuing absorption bands, centred at 400 and 530 nm respectively, give the pink-purple colour observed. At lower energy levels (i.e., exposure to visible light) the process reverses and the mineral heals itself (reverse photosensitivity). Healing in Thor Lake samples under partial exposure to fluorescent lights occurred within two weeks.

In the sodalite syenite, sodalite occurs as moderately sized (1-2 mm), blocky crystals that are dark grey in colour. The crystals are bigger than co-existing feldspar

and aegirine and are late-forming as they tend to push these crystals aside. In comparison, late-forming nepheline incorporates the feldspar and aegirine thus forming the commonly seen poikilitic textures. At 348 m, in hole 85L-6, sodalite appears as large (up to 5 cm), ill-defined crystals definitely forming as a late-stage mineral. Very little, if any, alteration is noted within the sodalite. Typical microprobe analyses are found in appendix 1, analyses 27 and 28.

Filling in the voids of a number of minerals are two types of zeolites: natrolite and mesolite(?). Natrolite was found amongst the voids left by muscovite bundles in a pectolite-rich rock. The muscovite crystals (anal. 20) are oriented in two directions approximately 70° from each other and have probably epitaxially replaced a pre-existing mineral. Both natrolite and mesolite along with fluorite were noted to replace pectolite. Chemical analyses were performed on both zeolites (anal. 32 and 33).

A volumetrically minor yet significant mineral is a Ca,Nb-silicate found deep within the nepheline syenite. The material is easily observed by the naked eye (3 cm in size) and displays well formed, brownish-yellow, tabular crystals. Physically, cleavage is well developed, perfect in one direction but poor in another (approximately perpendicular to each other), hardness is about 5 while the lustre is vitreous.

Optically, the material shows dull bluish-grey, first order birefringence although around the edges it changes to first order white, indicative of chemical zoning or overgrowths (plate 35). Refractive indices were measured and found to be as follows: $n_a=1.656-1.658$, $n_b=1.660$ and $n_c=1.672-1.676$ while the 2V(gamma) was found to be $65^0\pm5^0$ (Kamb's method). The mineral is colourless in thin section and contains no discernible pleochroism.

Chemically, the mineral displays two distinct varieties. One, as typified by the central portions of the mineral, is rich in Ti (see anal. 75) while the other, typified by the thin rimmed overgrowths, is much poorer in Ti (anal. 76). The mineral contains abundant F and, presumably because of the low analytical totals, OH groups. Note also the abundant LREEs, especially Ce which is found substituting for the Ca and Na. The chemical information seems to indicate this mineral to be a hydrated niocalite $[Ca_{14}Nb_2(Si_2O_7)_4O_6F_2]$, a mineral only found in Quebec at the Oka carbonatite (Nickel, 1956). Based on analysis 75, the atomic proportions of the various cations comes to the following: $(Ca,Na,REE)_{6.55}(Nb,Ti)_{1.03}Si_{4.20}O_{15.88}F_{2.12}$, which is close to niocalite whereas in the Ti-poor rims (anal. 76), the proportions are rather different, likely indicating another mineral. Note that the Si:(Nb+Ti) ratio of this mineral (3.5-4:1) precludes all other known niobosilicates including another likely candidate, mosandrite $[(Na,Ca,Ce)_3Ti(SiO_4)_2F]$.
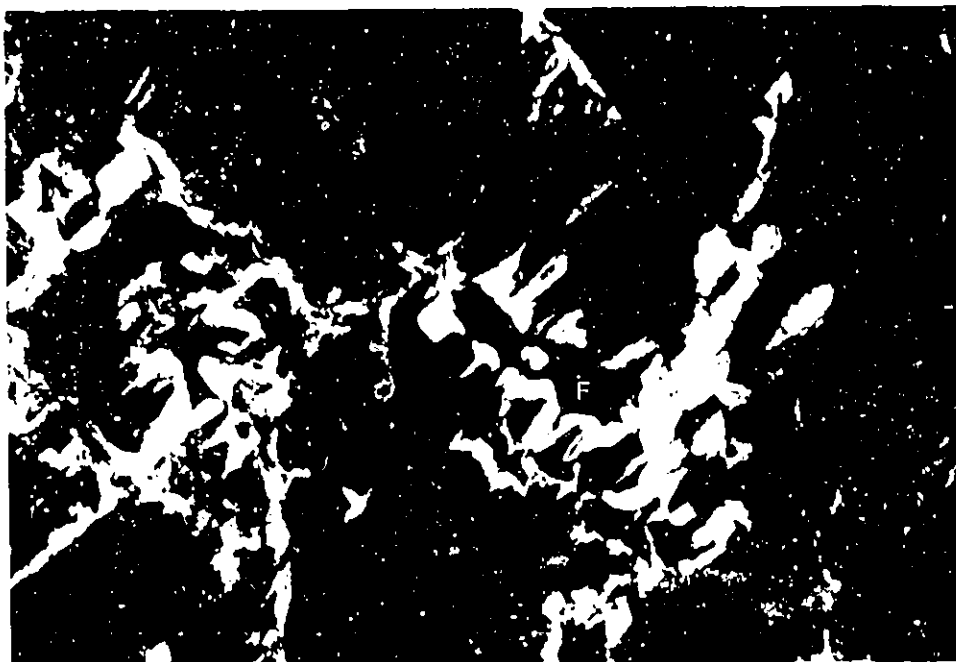
Plate 35. Ca,Nb,Ti-silicate rimmed by a Ca,Nb-
          silicate (white colour). Note the
          pockets of fluorite. Magnification
          X62, XPL
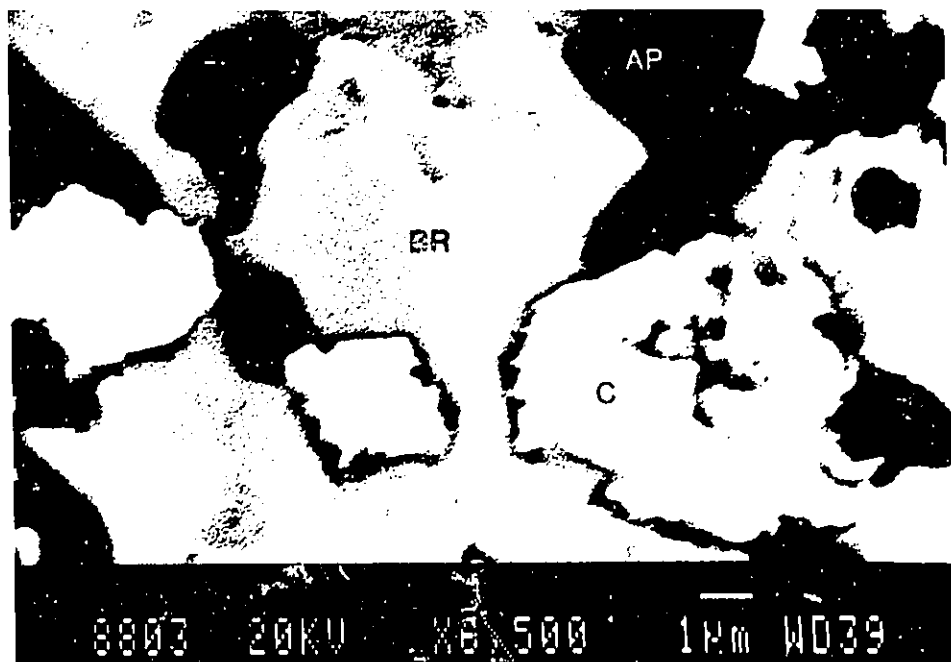
Plate 36. Secondary electron image of cerianite-
          (Ce) grains in a matrix of britholite-
          (La). Scale bar is 1 μm.

D-values were obtained in the hope of determining unequivocably the identification of this mineral. Unfortunately, the d-values seem to suggest mosandrite whereas the chemical information points to niocalite. To obtain these values, small amounts of the material were crushed, placed on a glass slide in an acetone slurry and then analysed using a Rigaku automated X-ray diffractometer. CoK_{α} radiation was used with a scan speed of 2° 2θ/min ranging from between 20° to 80°. Table 6 displays the resulting 10 most intense lines, their corresponding intensities, 2θ values and, as a comparison, the same data given by JCPDS files for mosandrite and niocalite.

TABLE 6
D-VALUES FOR THE UNKNOWN, MOSANDRITE AND NIOCALITE

unknown			mosandrite			niocalite		
D-values	I/I_1	2θ	D-values	I/I_1	2θ	D-values	I/I_1	2θ
3.575	25	29.1	3.581	25	29.0	7.31	30	14.0
3.062	100	34.0	3.071	100	33.9	3.240	50	32.1
2.944	30	35.4	2.945	40	35.4	3.012	100	34.6
2.792	25	37.4	2.798	40	37.3	2.891	60	36.1
2.695	35	38.8	2.702	70	38.7	2.852	60	36.6
2.305	15	45.7	2.577	20	40.6	2.557	30	41.0
2.020	20	52.6	2.024	25	52.5	2.433	30	43.2
1.852	20	57.8	1.853	30	57.8	2.292	20	46.0
1.815	15	59.1	1.817	20	59.0	2.031	30	52.3
1.677	15	64.5	1.682	25	64.3	1.844	40	58.1

The match for mosandrite is nearly perfect (MinIdent gave a total match of 98.5) but for niocalite it differs substantially. Since both the d-values and the refractive indices do not match for niocalite, it is thought that the unknown is a new mineral.

Intimately associated with the above mentioned mineral
are small 'pockets' filled with unusual minerals, among them
cerianite-(Ce), britholite-(La), a Ca-Zr silicate plus
apatite, fluorite, hydrohetaerolite and recrystallised K-
feldspar. The cerianite-(Ce) occurs as very small (5-10
μm), yellowish-brown cubes usually embedded in a fluorite
and apatite matrix (see plate 36). Cerianite-(Ce) can
accomodate variable amounts of Th and U simply because two
other oxides, uraninite and thorianite, form solid solution
series with this mineral. At Thor Lake, these particular
crystals contain upwards of 20 wt% ThO_2 but only minor UO_2
(appendix 1, anal. 68 and 69). Because cerianite-(Ce)
contains quadrivalent Ce, very little La, Nd or other REEs
were detected. Most neighbouring fluorite has turned purple
in response to structural damage due to the radioactive Th
in cerianite-(Ce).

The existence of Ce^{4+} indicates a highly oxidising
environment (note the Fe^{3+} in allanite and the Mn^{3+} in
hydrohetaerolite) as discussed earlier. This means that any
co-existing REE-bearing mineral must not contain any
significant Ce as only Ce^{4+} ions are available. One other
REE-bearing mineral was found and has been identified as
britholite-(La), which would make it the first La-dominant
mineral found at Thor Lake (plate 36). Britholite-(La) is
small (5-50 μm), poorly defined and is only found only in
the rare-metal-bearing pockets associated with analcime,
fluorite and cerianite-(Ce). Analysis 74 in appendix 1

indicates the La-rich nature of these crystals which, if it has been correctly analysed and identified, would represent a new mineral within the britholite group. Chemically, the mineral is slightly hydrated, contains minor F but has over 50 wt% REEs.

Similar to britholite-(La) is the mineral represented by analysis 73, which typifies another member of the britholite group found elsewhere in the nepheline syenite. That mineral, britholite-(Ce), is typically large (1-3mm), euhedral, and severly metamict (plate 37). Because these large grains are not found within the 'pockets', Ce occurs in the trivalent state and hence dominates over La in the crystal structure. Severe metamictisation resulted because of internally high Th values and of its association with thorite. Plate 36 displays a mottled texture common to metamict minerals. The various shades of grey delineate different concentrations of La, Ce and Th and various degrees of hydration. Note the dark overgrowths (more La-rich), the interspersed thorite grains and the hexagonal outline of the britholite-(Ce) crystal. The thorite was analysed (anal. 67) and found to have substantial Ce and to be hydrated (low analytical total).

Because of the high activities of both Na and K in most undersaturated agpaitic rocks, complex Ca,Na,Zr-silicates preferentially crystallise over zircon. These rocks do contain some complex zirconosilicates albeit in small quantities. One example is a small (50-100 μm), colourless,
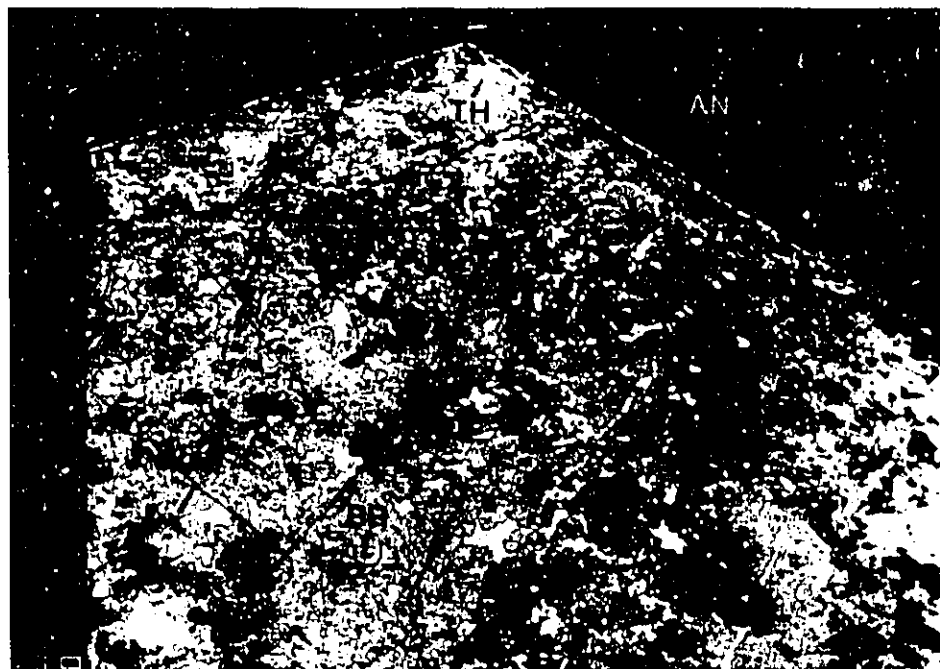
Plate 37. Backscattered electron image of a large britholite-(Ce) crystal with interstitial thorite. Note the mottled texture. Scale bar is 100 μm.

anhedral mineral found associated with the previously mentioned minerals. Microprobe analysis of this mineral (anal. 72) shows it to be very hydrated and devoid of REEs or other incompatible elements. Assuming two H_2O molecules are attached to the mineral, the following general chemical formula results: $(Ca,Na)_{0.48}(Si,Al)_{3.14}(Zr,Hf)_{1.13}O_9:2H_2O$. This formula correlates with Ca-catapleiite except that only one half the required alkalies are present. No other known Ca,Zr-silicate appears to be similar enough, therefore this phase might be considered previously undescribed.

Another brownish-yellow mineral found has been tentatively identified, based on X-ray diffraction, as ferrobustamite. It appears somewhat acicular and colour zoned from a dark brown to a light brownish yellow. It is a euhedral, wedge-shaped crystal with a vitreous lustre and has a hardness of about 5.5-6. Cleavage is hard to distinguish as the crystals are rather splintery in nature, although a good cleavage was noted.

Identification was achieved through X-ray diffraction. Operating conditions used for this mineral were kept the same as those for the Ca,Nb-silicate. Table 7 shows the 10 most intense lines, their corresponding intensities, 2θ values and as a comparison, the same data given by JCPDS files for ferrobustamite.

TABLE 7
D-VALUES FOR THE UNKNOWN AND FERROBUSTAMITE

unknown				JCPDS		
D-values	I/I_1	2θ		D-values	I/I_1	2θ
7.67*	25	13.4*		7.67	25	13.4
3.862	35	26.8		3.84	55	26.9
3.481	50	29.8		3.470	60	29.9
3.267	100	31.8		3.270	100	31.8
3.062	80	34.0		3.049	80	34.1
2.897	20	36.0		2.947	25	35.4
2.708	30	38.6		2.696	30	38.8
2.574	30	40.7		2.563	20	40.9
2.277	55	46.3		2.445	20	43.0
1.738	20	62.0		2.278	65	46.3

*2θ angle too small for
peak to be detected

MinIdent provided a 99.8 total matching index for
ferrobustamite.

At the bottom of hole 85L-6, the rock becomes more
altered; nepheline is replaced by micas and carbonate and
the mafic minerals have altered to fine grained biotite and
magnetite and/or hematite. In some cases, the original
mafic mineral, probably aegirine, has been replaced by
riebeckite. The pleochroism of the riebeckite is very
noticeable, varying from n_a= light yellowish green to n_c=
dark greenish blue. A chemical analysis of the material is
found in appendix 1, analysis 34. The last 10 metres of the
hole contain riebeckite as the sole mafic mineral and is the
only known area in the nepheline syenite to contain an
amphibole.

VI DISCUSSION

RING COMPLEXES

Scattered throughout the continental crust exist bodies
of rocks known, because of their chemical composition,
arcuate shape and ring-like features, as alkaline ring
complexes. They are rare, comprising less than 1% of the
total crustal volume and appear to be strongly controlled by
lithospheric movements in the form of rifts or transform
faults (Black et al., 1985). The lithosphere therefore has
a very active role in determining where emplacement takes
place but only a minimal role in the generation of the
magmas. The origin may be ascribed to the process of mantle
metasomatism whereby localised areas of the mantle may
experience infiltration by incompatible-element-rich fluids
and subsequent partial melting. The resulting magma can
then interact with the crust (crustal metasomatism,
assimilation of wall rocks or magma mixing) to form these
alkaline complexes.

Ring complexes are petrologically variable but are
linked together by the common development of a peralkaline
fluid phase and by shallow level or subvolcanic emplacement
which usually includes the formation of ring dykes or cone
sheets. The Blachford Lake intrusive suite displays these
features and can therefore be included with some of the more
famous complexes such as those found in Nigeria, Saudi
Arabia and Greenland.

Many but not all of the world's alkaline ring complexes are found with enriched levels of Zr, Nb, Y, Th, U and REEs. Alkaline complexes which do not contain any elements of economic interest include the strongly alkaline nephelinites and carbonatites of the Kenya rift province; the Chilwa alkaline province at the southern end of the East Africa rift valley or the Velasco alkaline province of Bolivia. Both the Chilwa and Velasco systems display remarkable similarities to the Blachford Lake Complex in terms of, rock associations (a peralkaline granite-syenite with Si-undersaturated rocks), structure (ring dykes with large oversaturated plutons and small undersaturated plugs) and mineralogy. Other, more economically viable provinces can also show similarities to Blachford Lake. Included are the Gardar alkaline province along the southwest coast of Greenland, the Nigerian alkaline ring complexes, the felsic plutonic rocks of the Arabian Shield and the chemically diverse plutons of the Lovozero massif, USSR.

The A-type granites of the Nigerian Shield are known world-wide for their Sn mineralisation although, in addition, they are known to be rich in F, Nb, Zr, REEs and Y (Bowden, 1985). The style of intrusion and mineralisation in these silica saturated to oversaturated rocks again shows similarities to those at Blachford Lake. First, as discussed by Bowden et al. (1987) there exists in many individual complexes (e.g., Air massif, Niger) an associated outer margin of leucogabbros and anorthosites with an inner

core of granite, syenite and syenite breccia. Second, are the similar structural styles which include the emplacement of simple 'bell-jar' plutons (see later) and of ring dykes or cone sheets. Third, are the comparable types of post-magmatic alteration and subsolidus processes in which sodic and potassic metasomatism is followed by acid metasomatism (greisenisation) either by local scavenging from country rocks or by initiation from subsequent intrusions or by both. As an example, alteration sequences within both the Mada Younger Granite complex (Abba, 1985) and the Kiriwai complex (Kinnaird et al., 1985) both of Nigeria, have successive phases of Na followed by K, H and Si metasomatism. Mineralisation in these complexes tends to favour Sn and sulphide minerals but plenty of ferrocolumbite, pyrochlore and thorite are also found.

In Saudi Arabia, all granite-hosted mineralisation resulted from late-stage hydrothermal alteration through albitisation, microclinisation and greisenisation (see, for example, Ramsay, 1986). Two complexes are worthy of mention; the Jabal Tawlah and Jabal Umm Al Suqian intrusions. The first is a microgranite-hosted Nb, Ta, Sn, Th, Y, REE and Zr deposit believed to be the largest in Saudi Arabia. Drysdall and Douch (1986) have determined that fergusonite-(Y), xenotime-(Y), ferrocolumbite, thorite and abundant, fine-grained, bipyramidal zircons are found within the heavily metasomatised zones. The Jabal Umm Al Suqian intrusion is another microgranite with associated

albitised, microclinised and greisenised country rock.
Mineralisation consists of fluorite-rich zones with
disseminated ferrocolumbite, monazite-(Ce), bastnäsite-(Ce)
and betafite (Bokhari et al., 1986).

The similarities of these alkaline ring complexes to
the Blachford Lake Intrusive Suite and its associated rare-
metal deposits are quite obvious. Keeping the preceeding
examples in mind, what follows is a generalised description
of how mineralisation may have resulted.

ORIGIN OF THE DEPOSIT

The origin of the these extensive deposits has, since
its discovery over 10 years ago, been speculated upon by
many workers. A number of ideas varying from the realistic
(late-stage magmatic or metasomatic alteration) to the
ridiculous (a collision with a neutron star) has been
proposed. Most common is the idea proposed by Davidson
(1978,1981), in which the enrichment of rare elements is
ascribed to the build-up of these elements in residual
fluids. These rare element-rich fluids were generally
exluded from the earlier crystallising Grace Lake granite
(GLG) and Thor Lake syenite (TLS) and hence deposited as the
R,S,T, Lake and Fluorite zones. Hylands and Campbell (1980)
have suggested a similar idea, proposing that volatiles and
incompatible elements from the GLG accumulated at the
central core of the TLS. Hudson (1987) invoked both
magmatic and metasomatic situations for the enrichment of
these incompatible elements.

In all these models, one significant set of rocks, the silica-undersaturated suite, has been omitted either because they were dismissed as being unimportant or because their existence was unknown. The following discussion extends the idea of the peralkaline GLG-TLS system as the major source of K and Na metasomatism (and greisenisation) within the Lake zone but also includes the underlying, agpaitic (in part), silica-undersaturated rocks as being the major source for the rare-metals.

Some time after the emplacement of the simple, circular-shaped GLG into surrounding Archean granitoids was the intrusion of the TLS (figure 7a). The syenitic magma forced its way into one of the many cooling-induced ring fractures within the GLG, eventually causing down-stoping of a block of granite (figure 7b). This process, known as ring-fracture stoping, is the method commonly envisaged for the formation of ring dykes (Bonin, 1986). An influx of magmas (labelled as 2,3 and 4 in figure 7c) would represent different magmatic pulses and provide an explanation for the various TLS rock types mentioned earlier. Figure 7c therefore represents what Pitcher (1978) termed a 'bell-jar' pluton, which has since been modified to a 'complex bell-jar' pluton by Roobol and White (1986) in describing the felsic ring complexes of Saudi Arabia.

Being one of the final magmas in the peralkaline portion of the Blachford Lake complex, the TLS was relatively rich in volatiles and incompatible elements

A

B

C

D

continued...
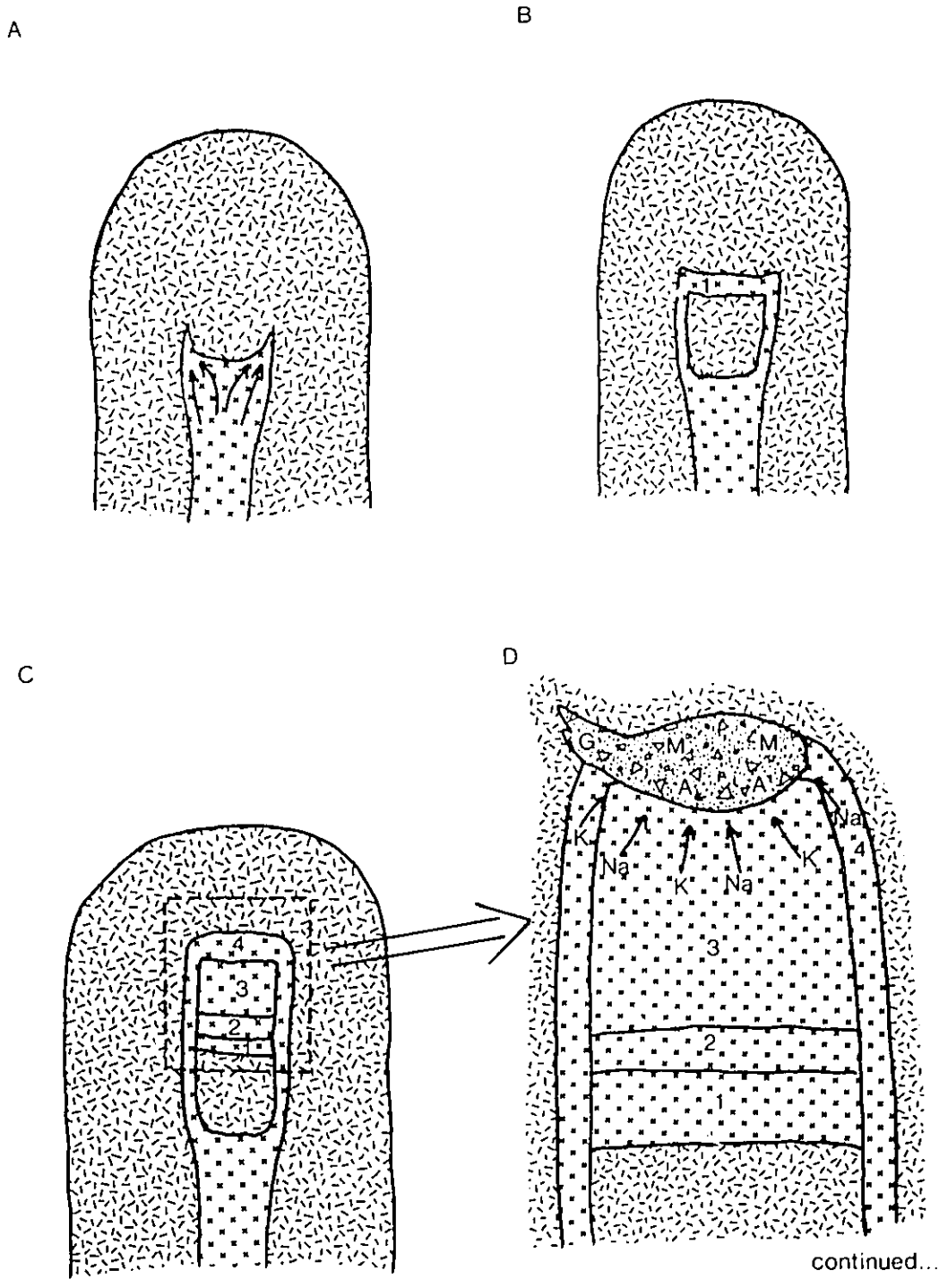
Figure 7   Schematic diagrams of the origin of the Thor Lake Syenite and associated rare-metal deposits.

E

F

T zone   Lake zone   Fluorite zone

Grace Lake Granite

Thor Lake Syenite

Nepheline Syenite

Carbonatite

Region of mineralisation (A = albitisation, G = greisenisation, M = microclinisation)

Region of fenitisation and associated rare-metal enrichment
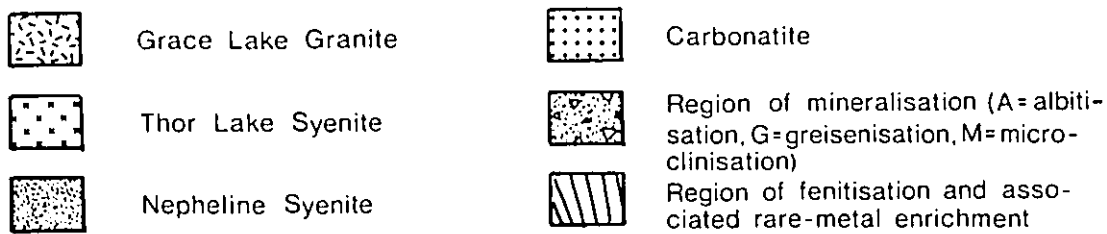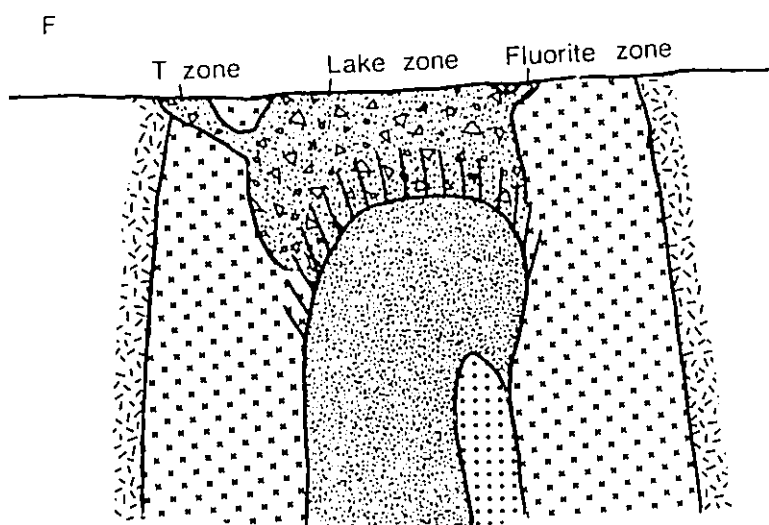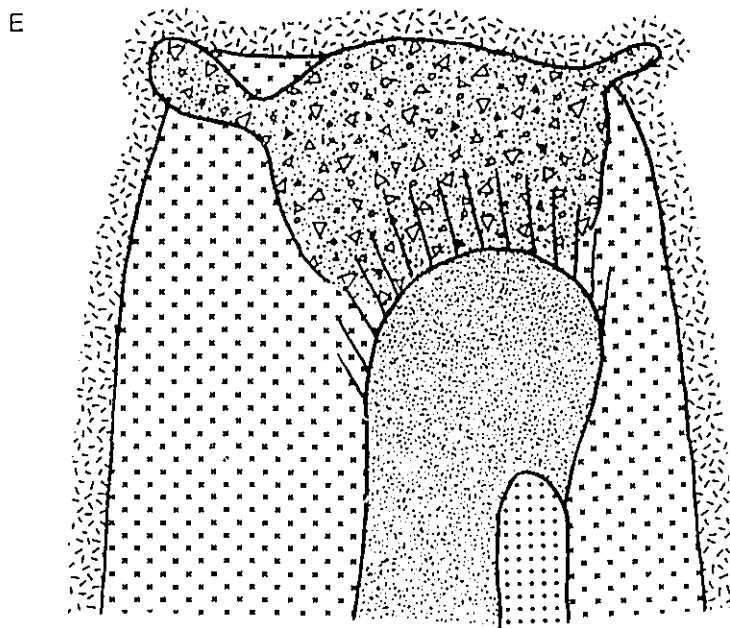
Figure 7   Schematic diagrams of the Thor Lake Syenite and associated
rare-metal deposits.

(Davidson, 1981). As it cooled and solidified many late-stage, subsolidus mineral reactions including albitisation, microclinisation and greisenisation occurred as suggested by Vlasov (1966) and Pollard (1986), amongst others. Figure 7d suggests a general concept for the accumulation of Na and K into specific zones of alteration. Generally, microclinisation occurs first and, in addition to albitisation, typically becomes trapped at the upper levels of the host rock (i.e., Wall zone). If the conditions are right, greisenisation may ensue and indeed did so in some areas (T zone). The T zone therefore represents a more altered appendage to the Lake zone as shown diagramatically in figure 7d.

First stage or type 1 rare-metal-bearing minerals such as the acicular ferrocolumbite and monazite-(Ce) and the zonally metamictised zircon probably formed at this stage. Overall, their relatively low concentrations and moderately well-developed crystal habits seem to suggest an initial accumulation of rare-metals in this 'cap zone' of the TLS. As these changes were occurring, the next important phase was the emplacement of a body of silica-undersaturated rocks directly beneath the Lake zone (figure 7e). At this stage, significant Si remobilisation occurred. As mentioned earlier there exists, for 30-60 m immediately overlying the nepheline syenite, a zone of quartz depletion. Apparently Si was forced upwards out of this 'intermediate' zone and into the overlying Lake zone. The Lake zone does in fact

contain abundant quartz, significantly more than does the GLG. The phenomenon of quartz depletion and redeposition at some distance away from the intruding rock body is common in fenite zones (Saether, 1957).

Consanguineous is a significant rare-metal enrichment feature responsible for the type 2 or second-stage minerals (see table 3). These minerals are rather poorly developed, fine grained and generally found in the previously mentioned 10-20 m thick bands of mafic rock found deep within the Lake zone. Rare-metal enrichment due to the underlying nepheline syenite can be explained by a number of features. First, the peralkalinity, although not explicitly measured, is equally as high as that of the TLS (the TLS has as K- and Na-bearing rock-forming minerals, perthite and arfvedsonite whilst the nepheline syenite has albite, microcline and aegirine). Second, the nepheline syenite contains frequent pockets of volatile- and incompatible-element-rich minerals including britholite-(Ce), allanite-(Ce), Ca,Nb-silicates and Ca,Zr-silicates among others. And third, the occurrences and mineral reactions peculiar to these pockets suggests low temperature, metasomatic conditions necessary for the observed enrichment in the overlying rocks. Also note in figure 7e the emplacement of a small body of carbonatite. This is entirely speculative as no direct evidence for such a body of rocks exists. Nevertheless, the abundance of carbonates in all zones of mineralisation and of minor calcite in the nepheline syenite might indicate the

existence of a carbonatite at depth. Figure 7f illustrates the present-day situation with the erosional surface fortuitously revealing the R,S,T, Lake and Fluorite zone. Other zones may exist at depth or alternatively may have since been eroded.

FUTURE WORK

The complexities of the Thor Lake rare-metal deposits are slowly being solved but at the same time, more questions about these rocks emerge. The problems that should be addressed include the following:

1. Since there is an exceptional diversity of Nb minerals, continued microprobe work in the more mafic Lake zone rocks will probably lead to more mineral discoveries.

2. Structural studies of the non-metamict fergusonite-(Y) and aeschynite group minerals should be undertaken mainly because these non-metamict grains are extremely rare in nature and an investigation of these unperturbed crystals would be invaluable.

3. Stable isotope work on both C and O isotopes to determine whether all the carbonates are reworked crustal material, mantle-derived (carbonatite) or both.

4. Whole rock geochemistry of the nepheline syenite to determine the degree of agpaicity, peralkalinity, etc.

5. Nd-Sm whole rock or mineral isochron work on the nepheline syenite to determine, if possible, the relative ages of all rock types

6. If continued drilling in the Lake zone occurs, an interpretation of the various mineralised and nonmineralised zones including confirmation of the flat-lying mafic, zircon-rich zones found at depth.

VII REFERENCES

Abaa, S.I. (1985) The structure and petrography of alkaline rocks of the Mada Younger Granite complex, Nigeria. Journal of African Earth Sciences, 3, 107-113.

Ahrens, L.H. and Erlank, A.J. (1969) Hafnium, Sections B-O, Handbook of Geochemistry II/5. Springer-Verlag, New York.

Badham, J.P.N. (1978) The early history and tectonic significance of the East Arm graben, Great Slave Lake, Canada. Tectonophysics, 45, 201-215.

Bayliss, P. and Levinson, A.A. (1988) A system of nomenclature for rare-earth mineral species: Revision and extension. American Mineralogist, 73, 422-423.

Best, M. (1982) Igneous and Metamorphic Petrology. W.H. Freeman and Co., San Francisco.

Black, R., Lameyre, J. and Bonin, B. (1985) The structural setting of alkaline complexes. Journal of African Earth Sciences, 3, 5-16.

Bokhari, M.M., Jackson, N.J. and Oweidi, K.A. (1986) Geology and mineralization of the Jabal Umm Al Suqian albitized apogranite, southern Najd region, Kingdom of Saudi Arabia. Journal of African Earth Sciences, 4, 189-198.

Bonin, B. (1986) Ring Complex Granites and Anorogenic Magmatism. Elsevier, New York.

Bonin, B. and Giret, A. (1985) Contrasting roles of rock-forming minerals in alkaline ring complexes. Journal of African Earth Sciences, 3, 41-49.

Bowden, P. (1985) The geochemistry and mineralization of alkaline ring complexes in Africa (a review). Journal of African Earth Sciences, 3, 17-39.

Bowden, P., Black, R.F., Martin, E.C., Ike, J.A., Kinnaird, J.A. and Batchelor, R.A. (1987) Niger-Nigerian alkaline ring complexes: a classic example of African Phanerozoic anorogenic mid-plate magmatism. In Fitton, J.G. and Upton, B.G.J., eds. Alkaline Igneous Rocks, Geological Society Special Publication #30, 357-379.

Bowring, S.A., Van Schmus, W.R. and Hoffman, P.F. (1984) U-Pb zircon ages from Athapuscow aulacogen, East Arm of Great Slave, N.W.T., Canada. Canadian Journal of Earth Sciences, 21, 1315-1324.

Bromley, A.V. (1964) Allanite in the Tan-Y-Grisiau microgranite, Merionethshire, North Wales. American Mineralogist, **49**, 1747-1752.

Burt, D.M. (1981) Acidity-Salinity Diagrams-Application to Griesen and Porphyry Deposits. Economic Geology, **76**, 832-843.

Callegari, E. and De Pieri, R. (1967) Crystallographical observations on some chess-board albites. Schweizerische Mineralogische und Petrographische Mitteilungen, **47**, 99-110.

Caruba, R., Baumer, A., Ganteaume, H. and Iacconi, P. (1985) An experimental study of hydroxyl groups and water in synthetic and natural zircons: a model of the metamict state. American Mineralogist, **70**, 1224-1231.

Caruba, R., Baumer, A. and Turco, G. (1975) Nouvelles syntheses hydrothermales du zircon: substitutions isomorphiques; relation morphologie-milieu de croissance. Geochimica Cosmochimica Acta, **39**, 11-26.

Cerny, P. (1982) Anatomy and classification of granitic pegmatites. In P. Cerny, ed. Mineralogical Association of Canada Short Course in Granitic Pegmatites in Science and Industry, 1-39.

Cerny, P. (1986) Lanthanides, Tantalum and Niobium. Proceedings of the SGA Workshop, Berlin 1986, Springer-Verlag, in press.

Cerny, P. and Ercit, T.S. (1985) Some recent advances in the mineralogy and geochemistry of Nb and Ta in rare-element granitic pegmatites. Bulletin de Mineralogie, **108**, 499-532.

Cerny, P. and Trueman, D.L. (1985) Polylithionite from the rare-metal deposits of the Blachford Lake alkaline complex, N.W.T., Canada. American Mineralogist, **70**, 1127-1134.

Champness, P.E. (1970) Nucleation and growth of iron oxides in olivines, $(Mg,Fe)_2SiO_4$. Mineralogical Magazine, **37**, 790-800.

Coombs, D.S. (1955) X-ray investigations on wairakite and non-cubic analcime. Mineralogical Magazine, **30**, 699-710.

Davidson, A. (1978) The Blachford Lake Intrusive Suite: an Aphebian alkaline, plutonic complex in the Slave Province, Northwest Territories. In Current research, part A. Geological Survey of Canada, Paper 78-1A, 119-127.

Davidson, A. (1981) Petrochemistry of the Blachford Lake complex, District of Mackenzie; Geological Survey of Canada, Open File 764.

Davidson, A. (1982) Petrochemistry of the Blachford Lake complex near Yellowknife, Northwest Territories. In Uranium in granites. ed. Y.T. Maurice, Geological Survey of Canada, Paper 81-63, 71-79.

de St. Jorre, L. (1986) Economic Mineralogy of the T zone, Thor Lake, N.W.T. Unpublished M.Sc. Thesis, University of Alberta.

de St. Jorre, L. and Smith, D.G.W. (1988) Cathodoluminescent gallium-enriched feldspars from the Thor Lake rare-metal deposits, Northwest Territories. Canadian Mineralogist, 26, 301-308.

Deer, W.A., Howie, R.A. and Zussman, J. (1962) Rock-Forming Minerals. vols. 1-5. Longmans, Green & Co. Ltd., London.

Deer, W.A., Howie, R.A. and Zussman, J. (1982) Rock-Forming Minerals. vol. 1A. Longmans, Green & Co. Ltd., London.

Deer, W.A., Howie, R.A. and Zussman, J. (1986) Rock-Forming Minerals. vol. 1B. Longmans, Green & Co. Ltd., London.

Drysdall, A.R. and Douch, C.J. (1986) Nb-Th-Zr mineralization in microgranite-microsyenite at Jabal Tawlah, Midyan region, Kingdom of Saudi Arabia. Journal of African Earth Sciences, 4, 275-288.

Duggan, M.B. (1988) Zirconium-rich sodic pyroxenes in felsic volcanics from the Warrumbungle Volcano, Central New South Wales, Australia. Mineralogical Magazine, 52, 491-496.

Ewing, R.C. (1976) Metamict columbite re-examined. Mineralogical Magazine, 40, 898-899.

Fleischer, M. (1987) Glossary of Mineral Species. Mineralogical Record Inc., Tucson.

Foster, M.D. (1959) Interpretation of the composition of trioctahedral micas. United States Geological Survey Professional Paper 354-E, 115-147.

Gustafson, W.L. (1974) The stability of andradite, heden-
    bergite, and related minerals in the system Ca-Fe-Si-O-
    OH. Journal of Petrology, 15, 455-496.

Henderson, J.B. (1985) Geology of the Yellowknife-Hearne
    Lake Area, District of Mackenzie: A segment across an
    Archean Basin. Geological Survey of Canada Memoir 414.

Hirai, H. and Nakazawa, H. (1986) Visualizing low symmetry
    of a grandite garnet on precession photographs.
    American Mineralogist, 71, 1210-1213.

Hoffman, P.F. (1980) Wopmay Orogen: a Wilson cycle of early
    Proterozoic age in the Northwest of the Canadian
    Shield. In The continental crust and its mineral
    deposits. ed. D.W. Strangway. Geological Association of
    Canada, Special Paper 20, 523-549.

Hoffman, P.F. (1981) Autopsy of Athapuscow aulacogen:
    failed arm affected by three collisions (abstract). In
    Proterozoic basins of Canada. ed. F.H.A. Campbell.
    Geological Survey of Canada, Paper 81-10, 97-102.

Hoffman, P.F. (1987) Is Great Slave Lake Shear Zone a
    Continental Transform Fault? In GAC-MAC Joint Annual
    Meeting, Saskatoon. Program with Abstracts, 56.

Hogarth, D. (1977) Classification and nomenclature of the
    pyrochlore group. American Mineralogist, 62, 403-410.

Hudson, K. (1987) Geology and occurrence gallium in the Lake
    zone of the Thor Lake deposit, N.W.T. Unpublished
    Mineral Exploration Project, Queen's University.

Hylands, J.J. and Campbell, S.W. (1980) Progress report on
    Highwood Resources Thor Lake property. DIAND Cancelled
    Assessment File, 85 I/2.

Jackson, N.J. (1986) Mineralization associated with felsic
    plutonic rocks in the Arabian Shield. Journal of
    African Earth Sciences, 4, 213-227.

Johnson, W. (1977) Internal Report of the Thor Project for
    Highwood Resources Ltd.

Kinnaird, J.A., Bowden, P., Ixer, R.A. and Odling, N.W.A.
    (1985) Mineralogy, geochemistry and mineralization of
    the Ririwai complex, northern Nigeria. Journal of
    African Earth Sciences, 3, 185-222.

LeBas, M.J. (1977) Carbonatite-Nephelenite Volcanism. John
    Wiley and Sons, New York.

Mineyev, D.A., Rozanov, K.I., Smirnova, N.V. and Matrosova, T.I. (1973) Bastnaesitization products of accessory orthite. Akademiia Nauk S.S.S.R. Doklady, Earth Sciences Section, **210**, 149-152.

Miyano, T. and Miyano, S. (1982) Ferri-annite from the Dales Gorge Member iron-formations, Wittenoom area, Western Australia. American Mineralogist, **67**, 1179-1194.

Mucke, A. and Strunz, H. (1978) Petscheckite and liandratite, two new pegmatite minerals from Madagascar. American Mineralogist, **63**, 941-946.

Nickel, E. (1978) The present status of cathode luminescence as a tool in sedimentology. Minerals Science Engineering, **10**, 73-100.

Nickel, E.H. (1956) Niocalite - a new calcium niobium silicate mineral. American Mineralogist, **41**, 785-786.

Nickel, E.H. and Mandarino, J.A. (1987) Procedures involving the IMA Commission on New Minerals and Mineral Names and guidelines on mineral nomenclature. American Mineralogist, **72**, 1031-1042.

Pitcher, W.S. (1978) The anatomy of a batholith. Journal of the Geological Society of London, **135**, 157-182.

Pollard, P.J. (1986) Lanthanides, Tantalum and Niobium. Proceedings of the SGA Workshop, Berlin 1986, Springer-Verlag, in press.

Ramsay, C.R. (1986) Specialized felsic plutonic rocks of the Arabian Shield and their precursors. Journal of African Earth Sciences, **4**, 153-168.

Ribbe, P.H. (1983) Aluminum-silicon order in feldspars; domain textures and diffraction patterns. In P.H. Ribbe, ed., Reviews in Mineralogy, **2**, 21-55.

Roobol, M.J. and White, D.L. (1986) Cauldron-subsidence structures and calderas above Arabian felsic plutons; a preliminary survey. Journal of African Earth Sciences, **4**, 123-134.

Rubin, J.N., Henry, C.D. and Price, J.G. (1988) Hydrothermal zircons and Zr mobility: how unusual? GSA Abstracts with Program, **20**, A397-398.

Saether, E. (1957) The Alkaline Rock Province of the Fen Area in Southern Norway. Det Kongelige Norske Videnskabus Selskabs Skrifter, 1957, #1, 1-148

Saha, P. (1961) The system $NaAlSiO_4$ (nepheline) - $NaAlSi_3O_8$ (albite) - H_2O. American Mineralogist, **46**, 859-868.

Schaller, W.T. (1955) The pectolite-schizolite-serandite series. American Mineralogist, **40**, 1022-1234.

Smith, D.G.W. and Leibovitz, D.P. (1986) MinIdent: A data base for minerals and a computer program for their identification. Canadian Mineralogist, **24**, 695-708.

Smith, J.V. (1974) Feldspar Minerals. Springer-Verlag, New York.

Speer, J.A. (1982) Zircon. In P.H. Ribbe, ed. Reviews in Mineralogy, **5**, 67-112.

Starkey, J. (1959) Chess-board albite from New Brunswick, Canada. Geological Magazine, **96**, 141-145.

Takeuchi, Y. (1986) Deviations of garnets from cubic symmetry. 14th General Meeting of the IMA, Abstracts with Program, 245.

Taylor, B.E. and Liou, J.G. (1978) The low-temperature stability of andradite in C-O-H fluids. American Mineralogist, **63**, 378-393.

Trueman, D.L., Pedersen, J.C., de St. Jorre, L. and Smith, D.G.W. (1988) The Thor Lake rare-metal deposits, Northwest Territories. In R.P. Taylor and D.F. Strong, eds. Canadian Institute of Mining and Metallurgy Special Volume 39, 280-290.

Vlasov, K.A. (1966) Geochemistry and Mineralogy of Rare Elements and Genetic Types of their Deposits, volumes 1 and 2.

Waychumas, G.A. (1988) Luminescence, X-ray emission and new spectroscopies. In F.C. Hawthorne, ed. Reviews in Mineralogy, 18, 640-698.

APPENDIX 1 (ANALYTICAL DATA)

	1	2	3	4
	albite	albite	K-feldspar	K-feldspar
SiO_2	67.39	69.26	65.23	63.43
Al_2O_3	20.06	18.69	17.39	17.64
Fe_2O_3	0.33	0.34	n.d.	0.07
MgO	n.d.	n.d.	n.d.	n.d.
CaO	n.d.	n.d.	0.71	n.d.
Na_2O	11.89	11.67	0.53	0.48
K_2O	0.08	0.10	16.47	16.07
total	99.75	100.06	100.33	97.69

STRUCTURAL FORMULA
BASED ON 8 OXYGENS

	1		2		3		4	
Si	2.959		3.024		3.016		3.004	
Al	1.038		0.962		0.948		0.985	
Fe^{3+}	0.012	1.05	0.012	0.97	0.000	0.95	0.003	0.99
Mg	0.000		0.000		0.000		0.000	
Ca	0.000		0.000		0.035		0.000	
Na	1.012	1.02	0.988	1.00	0.048	1.06	0.044	1.02
K	0.004		0.006		0.972		0.971	

		1	2	3	4
	An	0.0	0.0	3.3	0.2
mol.	Ab	99.6	99.4	4.5	4.3
%	Or	0.4	0.6	92.2	95.5

n.a. = not analysed
n.d. = not detected

125

	5 nepheline	6 nepheline	7 altered nepheline	8 altered nepheline
SiO_2	41.79	45.13	41.96	46.96
Al_2O_3	34.25	31.89	34.77	33.85
Fe_2O_3	0.08	0.69	0.17	0.88
MnO	n.d.	n.d.	0.04	0.05
MgO	n.d.	n.d.	0.04	0.71
CaO	n.d.	0.04	0.04	1.07
Na_2O	15.99	16.14	13.59	6.34
K_2O	7.32	5.88	3.64	4.88
Cl	n.a.	n.d.	n.a.	0.08
total	99.43	99.77	94.25	94.82

STRUCTURAL FORMULA
BASED ON 4 OXYGENS

	5		6	
Si	1.017		1.083	
Al	0.982		0.902	
Fe^{3+}	0.002	0.98	0.014	0.92
Mn	0.000		0.000	
Mg	0.000		0.000	
Ca	0.000		0.001	
Na	0.755	0.98	0.751	0.93
K	0.227		0.180	
Cl	–		0.000	

	9 altered nepheline	10 altered nepheline	11 aegirine	12 aegirine
SiO_2	45.35	44.02	53.27	53.92
TiO_2	n.d.	n.d.	0.04	0.10
Al_2O_3	32.06	22.68	1.21	1.08
FeO	0.81	9.12	n.d.	n.d.
Fe_2O_3	n.a.	n.a.	30.79	30.81
MnO	0.09	n.d.	0.11	0.20
MgO	0.38	7.83	n.d.	n.d.
ZrO_2	n.d.	n.d.	0.76	0.34
CaO	0.45	0.05	1.36	1.91
Na_2O	4.41	0.23	13.09	12.71
K_2O	7.45	10.74	n.d.	n.d.
Cl	0.18	0.09	n.a.	n.a.
total	91.18	94.76	100.63	101.07

STRUCTURAL FORMULA
BASED ON 6 OXYGENS

Si			2.017	2.02	2.028	2.03
Ti			0.001		0.003	
Al			0.054		0.048	
Fe^{2+}			0.000		0.000	
Fe^{3+}			0.877	0.95	0.872	0.93
Mn			0.004		0.006	
Mg			0.000		0.000	
Zr			0.014		0.006	
Ca			0.055		0.077	
Na			0.961	1.02	0.927	1.00
K			0.000		0.000	
Cl			–		–	

	13 green biotite		14 green biotite		15 green biotite		16 annitic(brown) biotite	
SiO_2	35.42		37.81		37.92		35.15	
TiO_2	n.d.		n.a.		n.d.		n.a.	
Al_2O_3	14.63		19.63		12.55		17.88	
FeO	24.14		17.63		20.14		27.22	
MnO	0.16		0.47		0.18		0.48	
MgO	12.59		12.31		13.41		6.27	
CaO	n.d.		n.d.		n.d.		0.04	
Na_2O	0.08		0.38		0.07		1.02	
K_2O	8.55		8.98		9.36		8.37	
H_2O*	3.87		4.00		3.81		3.80	
total	99.44		101.21		97.44		100.23	

STRUCTURAL FORMULA
BASED ON 12 OXYGENS

	13		14		15		16	
Si	2.746	4.00	2.774	4.00	2.957	4.00	2.746	4.00
Al	1.254		1.226		1.043		1.254	
Al	0.083		0.472		0.111		0.392	
Ti	0.000		—		0.000		—	
Fe^{2+}	1.565	3.11	1.082	3.19	1.314	2.99	1.778	2.93
Mn	0.011		0.029		0.012		0.032	
Mg	1.455		1.347		1.559		0.730	
Ca	0.000		0.000		0.000		0.003	
Na	0.012	0.86	0.054	0.90	0.011	0.94	0.155	0.99
K	0.846		0.841		0.931		0.834	
H	2.000		2.000		2.000		2.000	

*determined by stoichiometry

	17	18	19	20
	chamosite	chamosite	muscovite	muscovite
SiO_2	23.47	26.06	50.59	45.51
TiO_2	0.07	n.d.	n.a.	n.d.
Al_2O_3	19.62	16.04	28.14	36.51
FeO	38.25	37.18	3.08	2.17
MnO	0.14	0.07	n.d.	n.d.
MgO	5.70	6.15	2.71	0.04
CaO	n.d.	0.09	n.d.	n.d.
Na_2O	n.d.	n.d.	0.15	0.16
K_2O	n.d.	n.d.	9.49	11.19
H_2O^*	10.46	10.24	4.46	4.49
total	97.71	95.83	98.62	100.07

	STRUCTURAL FORMULA BASED ON 18 OXYGENS		STRUCTURAL FORMULA BASED ON 12 OXYGENS	
Si	2.686 4.00	3.018 4.00	3.399 4.00	3.039 4.00
Al	1.314	0.982	0.601	0.961
Al	1.332	1.207	1.627	1.912
Ti	0.006	0.000	–	0.000
Fe^{2+}	3.661	3.601	0.173 2.07	0.121 2.04
Mn	0.014 5.99	0.007 5.89	0.000	0.000
Mg	0.972	1.062	0.271	0.004
Ca	0.000	0.011	0.000	0.000
Na	0.000	0.000	0.020 0.83	0.021 0.97
K	0.000	0.000	0.813	0.953
H	8.000	8.000	2.000	2.000

*determined by stoichiometry

	21	22	23	24
	andradite	andradite	andradite	andradite
SiO_2	36.34	35.20	36.79	36.96
TiO_2	n.a.	n.a.	n.d.	0.53
Al_2O_3	3.80	4.11	10.74	8.90
Fe_2O_3	25.09	25.82	15.72	17.64
MnO	2.58	2.41	3.44	2.33
MgO	n.d.	0.07	0.05	0.06
CaO	30.41	29.16	30.99	32.56
Na_2O	0.11	0.09	n.d.	0.08
total	98.33	96.86	97.73	99.06

STRUCTURAL FORMULA
BASED ON 12 OXYGENS

	21		22		23		24	
Si	3.058		3.011		3.012		3.009	
Ti	–		–		0.000		0.032	
Al	0.377	1.97	0.414	2.08	1.036	2.01	0.854	1.97
Fe^{3+}	1.589		1.662		0.969		1.081	
Mn	0.184		0.175		0.239		0.161	
Mg	0.000	2.94	0.009	2.87	0.006	2.97	0.007	3.02
Ca	2.742		2.672		2.719		2.840	
Na	0.018		0.015		0.000		0.013	

		21	22	23	24
	gross.	18.0	18.6	47.3	46.1
mol.	pyrope	0.0	0.1	0.1	0.1
%	spess.	1.2	1.2	4.2	4.0
	andra.	80.8	80.1	48.4	49.8

	25	26		27	28
	analcime	analcime		sodalite	sodalite
SiO_2	55.75	54.30		38.56	38.99
Al_2O_3	22.84	23.02		31.02	31.08
FeO	n.d.	0.10		n.d.	0.19
MgO	n.d.	n.d.		0.05	n.d.
CaO	n.d.	n.d.		n.d.	n.d.
Na_2O	12.53	14.17		23.20	23.52
K_2O	0.06	n.d.		n.d.	n.d.
Cl	n.a.	n.a.		7.43	7.38
H_2O*	8.20	8.15		–	–
total	99.38	99.74		100.26	101.16
			O=Cl	-1.68	-1.67
				98.58	99.49

STRUCTURAL FORMULA BASED ON 7 OXYGENS / STRUCTURAL FORMULA BASED ON 13 ANIONS

Si	2.039	1.997		3.117	3.126	
Al	0.984	0.998		2.955	2.937	
Fe^{2+}	0.000 / 0.98	0.003 / 1.00		0.000 / 2.96	0.013 / 2.95	
Mg	0.000	0.000		0.006	0.000	
Ca	0.000	0.000		0.000	0.000	
Na	0.888 0.89	1.011 1.01		3.636 3.64	3.656 3.66	
K	0.003	0.000		0.000	0.000	
Cl	–	–		1.018	1.003	
H	2.000	2.000		11.982	11.997	

*determined by stoichiometry

	29 pectolite	30 pectolite	31 manganoan pectolite	32 natrolite
SiO_2	54.03	53.75	52.38	47.68
Al_2O_3	0.06	0.08	0.08	27.73
FeO	n.d.	n.d.	n.d.	n.d.
MnO	0.44	4.86	10.82	0.08
MgO	n.d.	n.d.	0.05·	n.d.
CaO	31.73	29.39	23.38	n.d.
Na_2O	9.39	9.72	9.60	16.12
K_2O	n.d.	n.d.	n.d.	n.d.
H_2O*	2.67	2.69	2.62	9.58
total	98.32	100.49	98.93	101.19

	STRUCTURAL FORMULA BASED ON 9 OXYGENS			BASED ON 12 OXYGENS

	29		30		31		32	
Si	3.029	3.03	2.993	2.99	2.998	3.00	2.979	
Al	0.004		0.005		0.005		2.042	
Fe^{2+}	0.000		0.000		C.000		0.000	2.05
Mn	0.021	1.93	0.229	1.99	0.525	1.97	0.004	
Mg	0.000		0.000		0.004		0.000	
Ca	1.906		1.753		1.434		0.000	
Na	1.021	1.02	1.049	1.05	1.065	1.07	1.952	1.95
K	0.000		0.000		0.000		0.C00	
H	1.000		1.000		1.000		4.000	

*determined by stoichiometry

	33 mesolite(?)	34 riebeckite	35 willemite	36 hydro-hetaerolite
SiO_2	39.42	52.40	29.53	0.38
TiO_2	n.d.	n.d.	n.d.	n.d.
Al_2O_3	35.34	0.40	0.10	0.27
Fe_2O_3	n.a.	22.28	n.a.	n.a.
FeO	0.03	12.36	0.43	0.19
Mn_2O_3	n.a.	n.a.	n.a.	62.09
MnO	n.d.	0.15	0.58	0.43
ZnO	n.a.	n.a.	71.39	31.39
MgO	0.03	3.55	n.d.	n.a.
CaO	6.20	0.89	n.d.	0.79
Na_2O	9.31	7.47	n.d.	n.d.
K_2O	n.d.	n.d.	n.d.	n.a.
H_2O^*		2.02	–	3.62
total	90.33	101.52	102.03	99.47**

STRUCTURAL FORMULAS BASED ON:

	24 OXYGENS		4 OXYGENS		9 OXYGENS
Si	7.795	7.80	1.047		0.031
Ti	0.000		0.000	1.05	0.000
Al	0.070	2.56	0.004		0.026
Fe^{3+}	2.494		–		–
Fe^{2+}	1.538		0.013		0.013
Mn^{3+}	–		–	1.90	3.911
Mn^{2+}	0.019	2.66	0.017		0.030
Zn	–		1.869		1.918
Mg	0.787		0.000		–
Ca	0.142		0.000		0.070
Na	2.155	2.16	0.000		0.000
K	0.000		0.000		–
H	2.000		–		2.000

*determined by stoichiometry
**includes Ce_2O_3=0.31

	37 hematite	38 magnetite	39 'orange mineral'
SiO_2	3.04	0.35	40.34
TiO_2	0.89	n.d.	n.d.
Al_2O_3	0.49	0.10	0.89
FeO	n.a.	28.50	n.a.
Fe_2O_3	90.72	68.7C	42.97
MnO	n.d.	0.05	n.d.
MgO	0.13	0.09	1.15
CaO	n.d.	0.06	2.30
Nb_2O_5	2.20	n.d.	0.42
Ta_2O_5	n.d.	n.a.	n.d.
Y_2O_3	n.d.	n.a.	0.17
UO_2	n.d.	n.a.	n.a.
total	97.47	97.91	88.24

STRUCTURAL FORMULA BASED ON:
3 OXYGENS   4 OXYGENS

	3 OXYGENS		4 OXYGENS	
Fe^{3+}	1.808		2.017	2.02
Si	0.080		0.014	
Ti	0.018		0.000	
Al	0.015		0.005	
Fe^{2+}	—		0.929	
Mn	0.000	1.95	0.002	0.96
Mg	0.003		0.005	
Ca	0.000		0.003	
Nb	0.026		0.000	
Ta	0.000		—	
Y	0.000		—	
U	0.000		—	

	40 ferro-columbite	41 ferro-columbite	42 ferro-columbite	43 ferro-columbite
SiO_2	0.11	0.12	0.12	0.16
TiO_2	1.36	2.15	3.57	2.80
Al_2O_3	n.d.	0.13	0.12	n.d.
FeO	17.14	16.14	12.20	11.87
Fe_2O_3	3.85	3.76	8.31	7.28
MnO	1.15	1.12	2.61	3.38
MgO	0.22	0.32	0.33	0.28
CaO	n.d.	n.d.	n.d.	0.15
Nb_2O_5	74.90	69.79	70.64	70.61
Ta_2O_5	1.16	4.69	1.01	1.06
Y_2O_3	n.d.	n.d.	n.d.	n.d.
UO_2	n.d.	n.d.	0.46	0.62
ZrO_2	n.a.	n.d.	n.d.	n.d.
total	99.89	98.22	99.37	98.21

STRUCTURAL FORMULA
BASED ON 6 OXYGENS

	40		41		42		43	
Si	0.006		0.007		0.007		0.009	
Al	0.000		0.009		0.008		0.000	
Y	0.000		0.000		0.000		0.000	
U	0.000		0.000		0.006		0.008	
Fe^{3+}	0.162		0.161		0.344		0.307	
Fe^{2+}	0.799		0.771		0.562		0.556	
Mn	0.054	1.04	0.054	1.03	0.122	1.08	0.160	1.07
Mg	0.018		0.027		0.027		0.023	
Ca	0.000		0.000		0.000		0.009	
Ti	0.057		0.092		0.148		0.118	
Nb	1.887	1.96	1.802	1.97	1.759	1.92	1.789	1.93
Ta	0.018		0.073		0.015		0.016	
Zr	–		0.000		0.000		0.000	

	44 ferro- columbite	45 ferro- columbite	46 fergu- sonite-(Y)	47 fergu- sonite-(Y)
CaO	n.d.	0.08	0.05	0.22
MnO	0.83	6.45	0.10	n.d.
FeO	16.80	7.05	n.d.	n.d.
Fe_2O_3	5.43	8.81	n.d.	n.d.
PbO	n.a.	n.d.	n.d.	n.d.
Al_2O_3	n.a.	n.d.	0.06	0.06
Y_2O_3	n.a.	n.d.	10.42	13.89
La_2O_3	n.a.	n.d.	0.36	0.18
Ce_2O_3	n.a.	n.d.	4.16	2.21
Pr_2O_3	n.a.	n.d.	1.51	0.86
Nd_2O_3	n.a.	n.d.	13.90	8.43
Sm_2O_3	n.a.	n.d.	6.38	5.80
Eu_2O_3	n.a.	n.d.	0.88	0.94
Gd_2O_3	n.a.	n.d.	6.85	7.10
Tb_2O_3	n.a.	n.d.	0.73	0.66
Dy_2O_3	n.a.	n.d.	3.16	3.52
Ho_2O_3	n.a.	n.d.	0.52	0.23
Er_2O_3	n.a.	n.d.	1.20	1.99
Tm_2O_3	n.a.	n.d.	0.29	0.59
Yb_2O_3	n.a.	n.d.	2.12	4.72
Lu_2O_3	n.a.	n.d.	0.37	0.65
SiO_2	n.d.	0.40	0.04	0.06
TiO_2	2.42	5.83	n.d.	n.d.
ThO_2	n.a.	n.d.	n.d.	0.35
UO_2	n.a.	n.d.	n.d.	n.d.
Nb_2O_5	73.27	65.69	43.54	45.01
Ta_2O_5	1.73	1.56	2.25	1.40
WO_3	n.a.	n.d.	0.21	0.11
Na_2O	n.a.	n.d.	n.d.	0.09
MgO	n.d.	0.20	n.d.	n.d.
Sc_2O_3	n.a.	n.d.	n.d.	n.d.
ZrO_2	n.a.	n.d.	n.d.	n.d.
SnO_2	n.d.	1.24	n.d.	n.d.
F	n.a.	n.d.	n.d.	0.19
O=F				-0.08
total	100.48	97.31	99.10	99.18

STRUCTURAL FORMULA BASED ON:
6 OXYGENS   4 OXYGENS

Ca	0.000		0.005		0.003		0.011	
Mn	0.039		0.305		0.004		0.000	
Pb	—		0.000		0.000		0.000	
Al	—		0.000		0.003		0.003	
Y	—		0.000		0.272		0.356	
La	—		0.000		0.007		0.003	
Ce	—		0.000		0.075		0.039	
Pr	—		0.000		0.027		0.015	
Nd	—		0.000		0.244		0.145	
Sm	—		0.000		0.108		0.096	
Eu	—		0.000		0.015		0.015	
Gd	—		0.000		0.112		0.113	
Tb	—	1.04	0.000	1.19	0.012	1.00	0.010	0.99
Dy	—		0.000		0.050		0.055	
Ho	—		0.000		0.008		0.004	
Er	—		0.000		0.019		0.030	
Tm	—		0.000		0.004		0.009	
Yb	—		0.000		0.032		0.069	
Lu	—		0.000		0.005		0.009	
Si	0.000		0.022		0.002		0.003	
Th	—		0.000		0.000		0.004	
U	—		0.000		0.000		0.000	
Na	—		0.000		0.000		0.008	
Mg	0.000		0.017		0.000		0.000	
Fe^{2+}	0.777		0.329		0.000		0.000	
Fe^{3+}	0.226		0.370		0.000		0.000	
Ti	0.101		0.245		0.000		0.000	
Nb	1.832		1.657		0.967		0.979	
Ta	0.026		0.024		0.030		0.018	
W	—	1.96	0.000	1.95	0.003	1.00	0.001	1.00
Sc	—		0.000		0.000		0.000	
Zr	—		0.000		0.000		0.000	
Sn	0.000		0.028		0.000		0.000	
F	—		0.000		0.000		0.000	

	48 fergu-sonite-(Y)	49 fergu-sonite-(Y)	50 fergu-sonite-(Y)	51 fergu-sonite-(Y)
CaO	0.07	0.06	0.12	0.18
MnO	n.d.	n.d.	n.d.	n.d.
FeO	n.d.	n.d.	0.10	0.10
PbO	n.d.	n.d.	n.d.	n.d.
Al_2O_3	0.07	n.d.	n.d.	0.18
Y_2O_3	11.85	19.96	22.03	16.75
La_2O_3	0.30	0.09	n.d.	0.15
Ce_2O_3	3.40	0.76	1.14	1.69
Pr_2O_3	1.23	0.44	0.43	0.56
Nd_2O_3	11.38	4.33	4.25	4.69
Sm_2O_3	6.05	4.65	2.86	5.14
Eu_2O_3	1.01	0.49	0.52	1.03
Gd_2O_3	7.29	7.52	4.40	9.23
Tb_2O_3	0.84	0.79	0.81	1.38
Dy_2O_3	3.52	5.02	6.60	7.05
Ho_2O_3	n.d.	0.76	1.22	0.86
Er_2O_3	1.47	2.73	3.02	1.54
Tm_2O_3	0.32	0.44	0.22	0.06
Yb_2O_3	2.83	1.51	1.24	0.55
Lu_2O_3	0.34	0.17	0.29	0.18
SiO_2	0.14	0.14	0.08	0.10
TiO_2	n.d.	0.57	n.d.	n.d.
ThO_2	0.32	n.d.	n.d.	0.37
UO_2	n.d.	n.d.	n.d.	n.d.
Nb_2O_5	43.61	43.06	47.23	45.79
Ta_2O_5	1.87	4.53	2.02	1.73
WO_3	0.13	0.75	0.14	0.16
Na_2O	n.d.	0.12	0.08	0.09
MgO	n.d.	n.d.	n.d.	n.d.
Sc_2O_3	n.d.	n.d.	n.d.	n.d.
ZrO_2	n.d.	n.d.	n.d.	n.d.
SnO_2	n.d.	n.d.	n.d.	n.d.
F	n.d.	n.d.	n.d.	n.d.
total	98.04	98.89	98.80	99.56

STRUCTURAL FORMULA
BASED ON 4 OXYGENS

Ca	0.004		0.003		0.006		0.009
Mn	0.000		0.000		0.000		0.000
Fe	0.000		0.000		0.004		0.004
Pb	0.000		0.000		0.000		0.000
Al	0.004		0.000		0.000		0.010
Y	0.311		0.503		0.543		0.421
La	0.005		0.002		0.000		0.003
Ce	0.061		0.013		0.019		0.029
Pr	0.022		0.008		0.007		0.010
Nd	0.200		0.073		0.070		0.075
Sm	0.103		0.076		0.046		0.084
Eu	0.017		0.008		0.008		0.017
Gd	0.119	1.00	0.118	0.99	0.068	0.98	0.145	1.00
Tb	0.014		0.012		0.012		0.021
Dy	0.056		0.077		0.098		0.107
Ho	0.000		0.011		0.018		0.013
Er	0.023		0.041		0.044		0.023
Tm	0.005		0.006		0.003		0.001
Yb	0.042		0.022		0.018		0.008
Lu	0.005		0.002		0.004		0.003
Si	0.007		0.007		0.004		0.005
Th	0.004		0.000		0.000		0.004
U	0.000		0.000		0.000		0.000
Na	0.000		0.011		0.007		0.008
Mg	0.000		0.000		0.000		0.000
Ti	0.000		0.020		0.000		0.000
Nb	0.971		0.922		0.989		0.978
Ta	0.025		0.058		0.025		0.022
W	0.002	1.00	0.009	1.01	0.002	1.02	0.002	1.00
Sc	0.000		0.000		0.000		0.000
Zr	0.000		0.000		0.000		0.000
Sn	0.000		0.000		0.000		0.000
F	0.000		0.000		0.000		0.000

	52 samar- skite-(Y)?	53 samar- skite-(Y)?	54 uran- pyrochlore	55 uran- pyrochlore
CaO	2.35	1.82	2.27	2.59
MnO	0.24	0.14	0.39	0.14
FeO	3.05	1.98	4.53	2.79
PbO	n.d.	n.d.	2.60	0.47
Al_2O_3	0.15	0.11	0.25	0.06
Y_2O_3	19.18	20.95	n.d.	n.d.
La_2O_3	n.d.	n.d.	0.70	0.67
Ce_2O_3	0.33	0.37	3.24	4.37
Pr_2O_3	n.d.	n.d.	0.38	n.d.
Nd_2O_3	0.82	1.28	1.57	1.29
Sm_2O_3	2.06	2.57	0.35	0.21
Eu_2O_3	0.35	0.50	n.d.	n.d.
Gd_2O_3	5.10	5.90	n.d.	n.d.
Tb_2O_3	0.90	1.06	n.d.	n.d.
Dy_2O_3	4.97	5.72	n.d.	n.d.
Ho_2O_3	0.60	0.94	n.d.	n.d.
Er_2O_3	1.56	1.53	n.d.	n.d.
Tm_2O_3	0.18	0.20	n.d.	n.d.
Yb_2O_3	0.62	0.75	n.d.	n.d.
Lu_2O_3	n.d.	C.15	n.d.	n.d.
SiO_2	3.61	3.12	1.82	5.20
TiO_2	0.17	0.31	2.39	4.55
ThO_2	0.75	0.43	n.d.	n.d.
UO_2	0.14	n.d.	29.06	26.46
Nb_2O_5	44.93	41.68	42.69	39.53
Ta_2O_5	4.38	3.04	0.48	0.60
WO_3	0.31	0.36	n.d.	n.d.
Na_2O	n.d.	n.d.	0.25	n.d.
MgO	0.15	0.10	n.d.	n.d.
Sc_2O_3	n.d.	n.d.	n.d.	n.d.
ZrO_2	n.d.	n.d.	n.d.	n.d.
SnO_2	n.d.	n.d.	0.19	n.d.
F	0.40	0.36	n.d.	n.d.
H_2O*	–	–	5.98	6.05
O=F	-0.17	-0.15		
total	97.13	95.22	99.14	94.98

*determined by stoichiometry

STRUCTURAL FORMULA BASED ON:

	4 OXYGENS			5 OXYGENS	
Ca	0.109		0.089	0.122	0.138
Mn	0.009		0.005	0.017	0.006
Fe	0.111		0.075	0.190	0.116
Pb	0.000		0.000	0.035	0.006
Al	0.008		0.006	0.015	0.004
Y	0.443		0.506	0.000	0.000
La	0.000		0.000	0.013	0.012
Ce	0.005		0.006	0.059	0.079
Pr	0.000		0.000	0.007	0.000
Nd	0.013		0.021	0.028	0.023
Sm	0.031		0.040	0.006	0.004
Eu	0.005		0.008	0.000	0.000
Gd	0.073	1.10	0.089 1.15	0.000 0.94	0.000 0.94
Tb	0.013		0.016	0.000	0.000
Dy	0.069		0.084	0.000	0.000
Ho	0.008		0.014	0.000	0.000
Er	0.021		0.022	0.000	0.000
Tm	0.002		0.003	0.000	0.000
Yb	0.008		0.010	0.000	0.000
Lu	0.000		0.002	0.000	0.000
Si	0.157		0.142	0.091	0.258
Th	0.006		0.004	0.000	0.000
U	0.001		0.000	0.324	0.292
Na	0.000		0.000	0.024	0.000
Mg	0.010		0.007	0.000	0.000
Ti	0.006		0.011	0.090	0.170
Nb	0.881		0.856	0.968	0.886
Ta	0.052		0.038	0.007	0.008
W	0.003	0.94	0.004 0.91	0.000 1.07	0.000 1.06
Sc	0.000		0.000	0.000	0.000
Zr	0.000		0.000	0.000	0.000
Sn	0.000		0.000	0.004	0.000
F	0.055		0.052	0.000	0.000
H	–		–	2.000	2.000

	56 nioboaeschy- nite-(Ce)	57 nioboaeschy- nite-(Nd)	58 nioboaeschy- nite-(Nd)	59 aeschy- nite-(Nd)
CaO	3.54	3.59	2.73	1.47
MnO	n.d.	n.d.	n.d.	n.d.
FeO	0.46	0.33	0.34	0.27
PbO	n.d.	n.d.	n.d.	n.d.
Al_2O_3	n.d.	n.d.	n.d.	n.d.
Y_2O_3	0.59	1.19	0.86	1.01
La_2O_3	1.49	1.04	1.40	1.16
Ce_2O_3	11.48	9.27	12.00	11.65
Pr_2O_3	2.24	2.07	2.49	2.78
Nd_2O_3	11.60	12.35	13.39	16.41
Sm_2O_3	2.64	3.61	3.65	4.10
Eu_2O_3	0.38	0.42	0.45	0.52
Gd_2O_3	1.51	2.19	1.94	2.46
Tb_2O_3	n.d.	n.d.	n.d.	n.d.
Dy_2O_3	0.31	0.51	0.46	0.72
Ho_2O_3	n.d.	n.d.	n.d.	n.d.
Er_2O_3	n.d.	0.14	n.d.	n.d.
Tm_2O_3	n.d.	n.d.	n.d.	n.d.
Yb_2O_3	n.d.	0.15	n.d.	n.d.
Lu_2O_3	n.d.	n.d.	n.d.	n.d.
SiO_2	n.d.	n.d.	n.d.	n.d.
TiO_2	16.59	15.73	17.88	21.35
ThO_2	n.d.	n.d.	n.d.	n.d.
UO_2	n.d.	n.d.	n.d.	n.d.
Nb_2O_5	34.49	39.84	38.49	33.67
Ta_2O_5	10.45	5.20	1.54	0.32
WO_3	0.19	0.13	n.d.	n.d.
Na_2O	n.d.	n.d.	n.d.	n.d.
MgO	n.d.	n.d.	n.d.	n.d.
Sc_2O_3	n.d.	n.d.	n.d.	n.d.
ZrO_2	n.d.	n.d.	n.d.	n.d.
SnO_2	0.20	n.d.	n.d.	n.d.
F	n.d.	n.d.	n.d.	n.d.
O=F				
total	98.16	97.76	97.62	97.89

STRUCTURAL FORMULA
BASED ON 6 OXYGENS

Ca	0.245		0.245		0.186		0.100
Mn	0.000		0.000		0.000		0.000
Fe	0.025		0.018		0.018		0.014
Pb	0.000		0.000		0.000		0.000
Al	0.000		0.000		0.000		0.000
Y	0.020		0.040		0.029		0.034
La	0.035		0.024		0.033		0.027
Ce	0.271		0.216		0.279		0.271
Pr	0.053		0.048		0.058		0.064
Nd	0.267		0.280		0.303		0.373
Sm	0.059		0.079		0.080		0.090
Eu	0.008		0.009		0.010		0.011
Gd	0.032	1.02	0.046	1.05	0.041	1.05	0.052	1.04
Tb	0.000		0.000		0.000		0.000
Dy	0.006		0.010		0.009		0.015
Ho	0.000		0.000		0.000		0.000
Er	0.000		0.003		0.000		0.000
Tm	0.000		0.000		0.000		0.000
Yb	0.000		0.003		0.000		0.000
Lu	0.000		0.000		0.000		0.000
Si	0.000		0.000		0.000		0.000
Th	0.000		0.000		0.000		0.000
U	0.000		0.000		0.000		0.000
Na	0.000		0.000		0.000		0.000
Mg	0.000		0.000		0.000		0.000
Ti	0.805		0.752		0.853		1.022
Nb	1.006		1.145		1.104		0.969
Ta	0.183		0.090		0.027		0.006
W	0.003	1.99	0.002	2.00	0.000	2.01	0.000	1.98
Sc	0.000		0.000		0.000		0.000
Zr	0.000		0.000		0.000		0.000
Sn	0.005		0.000		0.000		0.000
F	0.000		0.000		0.000		0.000

	60 aeschy- nite-(Nd)	61 pyrochlore	62 betafite	63 cerio- pyrochlore
CaO	1.77	3.76	5.13	2.77
MnO	n.d.	0.45	0.18	0.15
FeO	0.31	4.88	8.71	1.65
PbO	n.d.	n.d.	n.d.	0.81
Al_2O_3	n.d.	0.08	0.22	0.26
Y_2O_3	1.63	n.d.	n.d.	n.d.
La_2O_3	1.07	0.47	n.d.	1.06
Ce_2O_3	10.17	3.09	0.73	8.97
Pr_2O_3	2.43	0.24	n.d.	0.74
Nd_2O_3	15.50	0.70	n.d.	2.93
Sm_2O_3	4.39	n.d.	n.d.	0.50
Eu_2O_3	0.53	n.d.	n.d.	n.d.
Gd_2O_3	2.81	n.d.	n.d.	n.d.
Tb_2O_3	0.29	n.d.	n.d.	n.d.
Dy_2O_3	0.67	n.d.	n.d.	n.d.
Ho_2O_3	n.d.	n.d.	n.d.	n.d.
Er_2O_3	0.20	n.d.	n.d.	n.d.
Tm_2O_3	0.26	n.d.	n.d.	n.d.
Yb_2O_3	0.28	n.d.	n.d.	n.d.
Lu_2O_3	n.d.	n.d.	n.d.	n.d.
SiO_2	n.d.	4.70	1.62	2.85
TiO_2	22.30	5.60	17.87	9.21
ThO_2	n.d.	1.39	n.d.	n.d.
UO_2	n.d.	6.35	2.82	8.85
Nb_2O_5	33.29	52.54	52.83	46.55
Ta_2O_5	0.30	1.62	0.35	0.37
WO_3	n.d.	n.d.	n.d.	0.16
Na_2O	n.d.	0.31	0.47	n.d.
MgO	n.d.	n.d.	0.88	n.d.
Sc_2O_3	n.d.	n.d.	n.d.	n.d.
ZrO_2	n.d.	n.d.	n.d.	n.d.
SnO_2	0.19	n.d.	n.d.	0.27
F	n.d.	n.d.	n.d.	n.d.
H_2O*	−	10.74	7.39	10.33
O=F				
total	98.39	96.92	99.20	98.43

*determined by stoichiometry

STRUCTURAL FORMULA BASED ON:

	6 OXYGENS		9 OXYGENS	
Ca	0.119	0.281	0.334	0.215
Mn	0.000	0.027	0.009	0.009
Fe	0.016	0.285	0.443	0.100
Pb	0.000	0.000	0.000	0.016
Al	0.000	0.007	0.016	0.022
Y	0.054	0.000	0.000	0.000
La	0.025	0.012	0.000	0.028
Ce	0.234	0.079	0.016	0.238
Pr	0.056	0.006	0.000	0.020
Nd	0.348	0.017	0.000	0.076
Sm	0.095	0.000	0.000	0.012
Eu	0.011	0.000	0.000	0.000
Gd	0.059 1.05	0.000 1.21	0.000 1.09	0.000 1.10
Tb	0.006	0.000	0.000	0.000
Dy	0.014	0.000	0.000	0.000
Ho	0.000	0.000	0.000	0.000
Er	0.004	0.000	0.000	0.000
Tm	0.005	0.000	0.000	0.000
Yb	0.005	0.000	0.000	0.000
Lu	0.000	0.000	0.000	0.000
Si	0.000	0.328	0.099	0.207
Th	0.000	0.022	0.000	0.000
U	0.000	0.099	0.038	0.143
Na	0.000	0.042	0.055	0.000
Mg	0.000	0.000	0.000	0.000
Ti	1.053	0.294	0.818	0.502
Nb	0.945	1.657	1.453	1.527
Ta	0.005	0.031	0.006	0.007
W	0.000 2.01	0.000 1.98	0.000 2.28	0.003 2.04
Sc	0.000	0.000	0.000	0.000
Zr	0.000	0.000	0.000	0.000
Sn	0.005	0.000	0.000	0.008
F	0.000	0.000	0.000	0.000
H	-	5.000	3.000	5.000

	64	65	66	67
	zircon	zircon	zircon	thorite
Na_2O	n.d.	n.d.	n.d.	0.22
CaO	0.13	0.15	n.d.	2.96
MgO	n.d.	n.d.	n.d.	n.d.
MnO	n.d.	n.d.	n.d.	n.d.
FeO	0.25	0.27	0.11	0.48
ZnO	n.d.	n.d.	n.d.	0.80
PbO	n.d.	n.d.	n.d.	n.d.
Al_2O_3	0.12	0.12	n.d.	0.24
Y_2O_3	0.53	1.13	0.99	1.36
La_2O_3	n.d.	n.d.	n.d.	0.33
Ce_2O_3	0.31	0.33	n.d.	6.65
Pr_2O_3	n.d.	n.d.	n.d.	0.78
Nd_2O_3	1.25	0.90	n.d.	4.28
Sm_2O_3	0.78	0.89	n.d.	0.84
Gd_2O_3	0.71	0.75	n.d.	0.84
Dy_2O_3	n.d.	n.d.	n.d.	n.d.
Er_2O_3	n.d.	n.d.	n.d.	n.d.
Yb_2O_3	n.d.	n.d.	n.d.	n.d.
P_2O_5	0.50	0.61	0.17	0.48
SiO_2	28.22	28.38	32.13	17.82
TiO_2	0.31	0.21	n.d.	n.d.
ZrO_2	59.76	59.90	63.83	n.d.
ThO_2	n.d.	0.32	n.d.	53.19
UO_2	n.d.	n.d.	n.d.	1.59
HfO_2	1.16	1.06	1.21	n.d.
Nb_2O_5	1.70	1.67	n.d.	n.d.
Ta_2O_5	n.d.	n.d.	n.d.	n.d.
F	0.38	0.35	n.d.	n.d.
$O=F$	-0.16	-0.35		
total	95.95	96.69	98.44	92.86

STRUCTURAL FORMULA
BASED ON 4 OXYGENS

Na	0.000		0.000		0.000		0.023	
Ca	0.005		0.005		0.000		0.169	
Mg	0.000		0.000		0.000		0.000	
Mn	0.000		0.000		0.000		0.000	
Fe^{2+}	0.007		0.007		0.003		0.021	
Zn	0.000		0.000		0.000		0.032	
Pb	0.000		0.000		0.000		0.000	
Y	0.009		0.020		0.016		0.039	
La	0.000		0.000		0.000		0.007	
Ce	0.004		0.004		0.000		0.130	
Pr	0.000		0.000		0.000		0.015	
Nd	0.015	1.06	0.010	1.06	0.000	1.00	0.082	1.21
Sm	0.009		0.010		0.000		0.015	
Gd	0.008		0.008		0.000		0.015	
Dy	0.000		0.000		0.000		0.000	
Er	0.000		0.000		0.000		0.000	
Yb	0.000		0.000		0.000		0.000	
Ti	0.008		0.005		0.000		0.000	
Zr	0.955		0.950		0.969		0.000	
Th	0.000		0.002		0.000		0.647	
U	0.000		0.000		0.000		0.019	
Hf	0.011		0.010		0.011		0.000	
Nb	0.025		0.025		0.000		0.000	
Ta	0.000		0.000		0.000		0.000	
Al	0.005		0.005		0.000		0.015	
P	0.014	0.94	0.017	0.95	0.004	1.00	0.022	0.99
Si	0.925		0.923		1.001		0.952	
F	0.039		0.036		0.000		0.000	
O	3.961		3.964		4.000		4.000	

	68 cerianite-(Ce)	69 cerianite-(Ce)	70 manganoan allanite-(Ce)	71 zincian allanite-(Ce)
Na_2O	n.a.	n.a.	0.07	0.09
CaO	0.37	0.96	9.97	10.52
MgO	n.a.	n.a.	n.d.	n.d.
MnO	n.a.	n.a.	10.14	4.18
FeO	n.a.	n.a.	n.d.	0.73
Fe_2O_3	n.a.	n.a.	6.98	10.07
ZnO	n.a.	n.a.	0.75	5.60
PbO	n.d.	2.45	n.d.	n.d.
Al_2O_3	n.a.	n.a.	13.93	11.89
Y_2O_3	n.a.	n.a.	n.d.	n.d.
La_2O_3	0.73	1.18	4.27	5.90
Ce_2O_3	n.d.	n.d.	12.59	13.26
CeO_2	89.14	74.15	n.d.	n.d.
Pr_2O_3	n.d.	n.d.	1.25	0.94
Nd_2O_3	2.91	0.87	5.70	3.47
Sm_2O_3	n.a.	n.a.	0.84	0.20
Gd_2O_3	n.a.	n.a.	n.d.	n.d.
P_2O_5	n.a.	n.a.	n.d.	0.08
SiO_2	0.41	0.13	29.40	29.50
TiO_2	n.a.	n.a.	0.07	n.d.
ThO_2	6.47	19.82	n.d.	n.d.
UO_2	n.d.	2.10	n.d.	n.d.
ZrO_2	n.a.	n.a.	n.d.	0.51
H_2O^*	–	–	1.50	1.51
total	100.03	101.66	97.46	98.45

*determined by stoichiometry

STRUCTURAL FORMULA BASED ON:

	2 OXYGENS				13 OXYGENS			
Na	–		–		0.014		0.017	
Ca	0.012		0.032		1.068		1.130	
Mg	–		–		0.000		0.000	
Pb	0.000		0.020		0.000		0.000	
Y	–		–		0.000		0.000	
La	0.008		0.013		0.158		0.218	
Ce^{3+}	0.000		0.000		0.461	1.98	0.487	2.08
Ce^{4+}	0.910		0.799		–		–	
Pr	0.000		0.000		0.046		0.034	
Nd	0.030		0.010		0.204		0.124	
Sm	–		–		0.029		0.007	
Gd	–	1.02	–	1.03	0.000		0.000	
Fe^{2+}	–		–		0.000		0.061	
Fe^{3+}	–		–		0.525		0.759	
Mn^{3+}	–		–		0.859	3.08	0.355	2.93
Zn	–		–		0.055		0.414	
Al	–		–		1.642		1.405	
P	–		–		0.000		0.007	
Si	0.012		0.004		2.940	2.94	2.957	2.97
Ti	–		–		0.005		0.000	
Zr	–		–		0.000		0.025	
U	0.000		0.014		0.000		0.000	
Th	0.043		0.139		0.000		0.000	
H	–		–		1.000		1.000	

	72 Ca,Zr silicate	73 'ritho- lite-(Ce)	74 britho- lite-(La)
Na_2O	0.32	1.06	0.51
CaO	6.08	6.70	10.68
PbO	n.d.	n.d.	5.05
Al_2O_3	0.11	n.d.	n.d.
La_2O_3	n.d.	19.40	33.05
Ce_2O_3	n.d.	36.81	3.55
Pr_2O_3	n.d.	1.67	3.01
Nd_2O_3	n.d.	7.46	13.67
Sm_2O_3	n.d.	0.65	1.06
Gd_2O_3	n.d.	0.32	0.21
P_2O_5	n.d.	0.69	3.17
SiO_2	46.55	18.88	16.87
TiO_2	0.10	n.d.	n.d.
ZrO_2	33.15	n.d.	n.d.
ThO_2	n.d.	1.75	n.d.
HfO_2	1.09	n.d.	n.d.
Nb_2O_5	0.58	n.d.	n.d.
F	n.d.	2.06	0.74
O=F	–	-0.87	-0.31
H_2O^*	8.92	0.04	0.65
total	96.90	96.62	91.91

STRUCTURAL FORMULA BASED ON:
11 OXYGENS   13 ANIONS

Na	0.042	0.48	0.304	0.148	
Ca	0.438		1.061	1.711	
Pb	0.000		0.000	0.203	
La	0.000		1.058	1.823	
Ce	0.000		1.992 5.01	0.194	5.04
Pr	0.000		0.090	0.164	
Nd	0.000		0.394	0.730	
Sm	0.000		0.033	0.055	
Gd	0.000		0.016	0.010	
Th	0.000		0.059	0.000	
P	0.000		0.086	0.401	
Al	0.009	3.14	0.000 2.88	0.000	2.92
Si	3.129		2.790	2.522	
Zr	1.087		0.000	0.000	
Hf	0.021	1.13	0.000	0.000	
Nb	0.018		0.000	0.000	
Ti	0.005		0.000	0.000	
F	0.000		0.963	0.350	
H	4.000		0.037	0.650	

*determined by stoichiometry

	75 Ca,Nb silicate	76 Ca,Nb silicate	77 mona- zite-(Ce)	78 mona- zite-(Ce)
Na_2O	6.68	1.94	n.d.	n.d.
CaO	22.45	19.58	0.06	0.09
Y_2O_3	0.17	n.d.	n.d.	n.d.
La_2O_3	2.76	4.08	13.88	14.14
Ce_2O_3	9.84	13.53	38.51	38.35
Pr_2O_3	0.99	1.22	3.05	3.04
Nd_2O_3	4.74	5.23	12.65	12.34
Sm_2O_3	0.76	0.79	1.16	1.04
Gd_2O_3	0.31	n.d.	n.d.	n.d.
Dy_2O_3	n.d.	n.d.	n.d.	n.d.
P_2O_5	0.11	n.d.	29.40	29.37
SiO_2	28.22	27.10	n.d.	n.d.
TiO_2	2.64	0.59	n.d.	n.d.
ZrO_2	0.77	n.d.	n.d.	n.d.
ThO_2	n.d.	0.27	n.d.	n.d.
Nb_2O_5	10.03	16.48	n.d.	n.d.
Ta_2O_5	0.23	0.17	n.d.	n.d.
F	4.52	3.73	0.38	0.45
O=F	-1.90	-1.57	-0.16	-0.19
total	93.32	93.14	98.93	98.63

STRUCTURAL FORMULA BASED ON:
18 ANIONS   4 ANIONS

	75		76		77		78	
Na	1.923		0.582		0.000		0.000	
Ca	3.571		3.248		0.003		0.004	
Y	0.013		0.000		0.000		0.000	
La	0.151		0.233		0.203		0.207	
Ce	0.535	6.55	0.767	5.23	0.560	1.01	0.558	1.00
Pr	0.054		0.069		0.044		0.044	
Nd	0.251		0.289		0.179		0.175	
Sm	0.039		0.042		0.016		0.014	
Gd	0.015		0.000		0.000		0.000	
Dy	0.000		0.000		0.000		0.000	
P	0.014	4.20	0.000	4.20	0.988	0.99	0.988	0.99
Si	4.189		4.195		0.000		0.000	
Ti	0.295		0.069		0.000		0.000	
Zr	0.056		0.000		0.000		0.000	
Th	0.000	1.03	0.010	1.24	0.000		0.000	
Nb	0.673		1.153		0.000		0.000	
Ta	0.009		0.007		0.000		0.000	
F	2.122		1.826		0.048		0.057	

APPENDIX 2 (MICROPROBE PROCEDURES)

In general, microprobe data for the more common minerals were obtained using wavelength dispersive analysis (WDA) whereas lesser known or unusual mineral data were obtained in a two stage process involving both energy dispersive analysis (EDA) and WDA. In the second situation, a mineral that was too small to identify optically was taken to an electron microprobe or secondary electron microscope with an attached EDA system. This enables one to obtain a semi-quantitative analysis of the material in question, then, with the appropriate standards, an accurate (quantitative) analysis using WDA may be acquired.

EDA was done on a number of instruments including: a CAMECA from the Department of Geology at the University of British Columbia, Vancouver; a JEOL at the Alberta Research Council, Edmonton; and an ISI (International Scientific Instrument) in the Department of Mineral Engineering at the University of Alberta, Edmonton. In all cases, ZAF corrected, standardless analyses normalised to 100% were acquired. The operating conditions varied from instrument to instrument but generally an accelerating voltage of 15-20 kV, a probe current of the order of 1×10^{-11} A and a counting time usually of 100 seconds were used.

Quantitative data were obtained in two places; the Department of Geology at the University of Alberta and at the National Museum of Natural Science, Mineral Sciences Division, Ottawa. The instrument used at the University of

Alberta was an ARL SEMQ with four wavelength spectrometres (LIF, TAP and 2 PET crystals). Operating conditions were as follows: an accelerating voltage of 15 kV, an average probe current of 0.079×10^{-7} A and a counting time of 100 seconds per peak and 40 seconds on each of two background measurements. Data processing was done with ZAF corrections using the MAGIC IV program. MAGIC IV is a simple data processing package that corrects the raw counts for deadtime losses, background, absorption, fluorescence and backscatter losses but ignores elements too light to be detected (H,C,O,etc.). Elements analysed and their appropriate emmission lines are listed, in increasing atomic number as follows:

LIF(200) $TiK_\alpha, MnK_\alpha, FeK_\alpha, LaL_\alpha, CeL_\alpha, HfL_\alpha, TaL_\alpha$

TAP $NaK_\alpha, MgK_\alpha, AlK_\alpha, ZnL_\alpha$

PET $SiK_\alpha, PK_\alpha, ClK_\alpha, KK_\alpha, CaK_\alpha, YL_\alpha, ZrL_\alpha, NbL_\alpha, PbM_\alpha, ThM_\alpha, UM_\alpha$

Since a large number of analyses were perfomed on a variety of minerals, a rather large set of standards were used. The following list displays all elements sought in each standard. Note that some elements are found in more than one standard simply because, depending on the material being analysed, one particular standard may be more appropriate over another. For example, Al in the garnet standard is more appropriate for allanite whilst Al in the kyanite standard is better for nepheline.

A LIST OF ALL STANDARDS USED IN THIS STUDY

U. of Alberta		Ottawa	
standard	elements	standard	elements
albite	Si,Na,Al	albite	Na
$CeAl_2$	Ce	almandine	Fe,Al,Si
diopside	Ca,Mg,Si	brannerite	U
fluorapatite	Ca,P	crocidolite	Pb
garnet	Al	diopside	Ca,Mg
hematite	Fe	fersmite	Ca
Hf metal	Hf	$GdDy(MoO_4)_3$	Gd,Dy
$KTaO_3$	Ta	$MgNb_2O_6$	Mg
kyanite	Al	microlite	Na,Ca,F
lanthanum		$MnNb_2O_6$	Nb,Mn
standard 1	La	monazite	La,Ce,Nd,P
Mn oxide	Mn	$NiTa_2O_6$	Ta
Nb metal	Nb	$NiWO_4$	W
Pb metal	Pb	$Pr_2(WO_4)_3$	Pr
rutile	Ti	REE glass	Eu,Tb,Ho,Er,Tm,
sanidine	Si,K		Lu,Sc
tugtupite	Na,Cl	rutile	Ti
U metal	U	$Sm_2(WO_4)_3$	Sm
willemite	Zn	SnO_2	Sn
YAl_3O_{12}	Y	ThO_2	Th
zircon	Zr	willemite	Zn
		YAl_3O_{12}	Y
		YbF_3	Yb
		ZrO_2	Zr,Hf

In Ottawa, a JEOL 733 microprobe with four crystal
spectrometres (LIF, PET and 2 TAP crystals) and an attached
Tracor Northern EDS were employed. Operating conditions
were as follows: an accelerating voltage of 15 kV, an
average probe current of 25 nA and a maximum counting time
of 40 sec per peak or until a certain level of precision
(0.5% standard deviation) is reached. Two background
measurements were made (25 sec. each), one on either side of
the peak in question. Since the ZAF correction method in
the software could not handle more than 15 elements at one
time, a Bence-Albee procedure was used. The particular

program used is a Bence-Albee routine within a package of programs called 'task' written for the Tracor Northern 5500. It is worth noting that a direct comparison of a simple material corrected with ZAF corrections and the same sample corrected using Bence-Albee yielded very similar results. Alternatively, other more complex minerals might not show the same degrees of similarity. Standards used are listed on the previous page in conjuction with those from the University of Alberta while elements analysed and their appropriate crystals are as follows:

TAP $FK_\alpha, NaK_\alpha, MgK_\alpha, AlK_\alpha, SiK_\alpha, PK_\alpha, ZnL_\alpha, YL_\alpha, ZrL_\alpha, NbL_\alpha, HfL_\alpha, TaL_\alpha, WL_\alpha$

LIF $MnK_\alpha, FeK_\alpha, NdL_\alpha, SmL_\alpha, EuL_\alpha, GdL_\alpha, TbL_\alpha, DyL_\alpha, HoL_\alpha, ErL_\alpha, TmL_\alpha, YbL_\alpha, LuL_\alpha$

PET $CaK_\alpha, ScK_\alpha, TiK_\alpha, SnL_\alpha, LaL_\alpha, CeL_\alpha, PrL_\alpha, PbM_\alpha, ThM_\alpha, UM_\alpha$

All analyses given in appendix 1 are quantitative and hence originate from either the Department of Geology microprobe in Edmonton or from the microprobe lab in Ottawa. Elements are included as detected if they are significant at the 3σ or 99.7% confidence limit otherwise the designation of n.d. (not detected) is applied.